Application of Liposomes for Antimicrobial Photodynamic Therapy

Dissertation

zur Erlangung des akademischen Grades doctor rerum naturalium

(Dr. rer. nat.)

vorgelegt dem Rat der Biologisch-Pharmazeutischen Fakultät
der Friedrich-Schiller-Universität Jena

von Kewei Yang

Master of Science in Pharmazie (M.Sc)

geboren am 28.10.1982, in Heilongjiang, P.R.China

Application of Liposomes for Antimicrobial Photodynamic Therapy

Dissertation

For the obtainment of the academic degree of Doctor rerum naturalium

(Dr. rer. nat.)

Presented to the Council of the Faculty of Biology and Pharmacy,

Friedrich-Schiller-University Jena

Submitted by

Kewei Yang

Master of Science in Pharmaceutics (M.Sc.)

Born on 28.10.1982, in Heilongjiang, P.R.China

Reviewers

Reviewer 1: Professor Dr. Alfred Fahr, Friedrich-Schiller-University Jena

Reviewer 2: Professor Dr. Volker Albrecht, biolitec AG, Jena

Reviewer 3: Professor Dr. Rolf Schubert, Albert-Ludwigs-University Freiburg

Date of Defense: 8.11.2011

Contents

1 Introduction

This present dissertation explores the application of liposomes for antimicrobial photodynamic therapy (APDT). The work includes two parts: the development of bacteria-targeting liposomes for improvement of APDT, and the development of a novel strategy for high-throughput screening of liposomal formulations loading lipophilic photosensitizers.

1.1 Microbial infections and antibiotic-resistance

Microbial infections have threatened the human health since the origin of human beings and people have fought with infectious diseases for thousands of years. In the 20th century, human fight with microbial infections was revolutionized by the discovery and development of antibiotics. Following the first widely applied antibiotic, penicillin, a number of antibiotics of different classes were developed in the last seventy years, as shown in Fig. 1-1, and ushered in the beginning of "antibiotic era". Many life-threatening diseases are readily treated, and surgery and transplantation medicine have also been rendered very much safer procedures (Finch, 2007).

However, the development of new antibiotics peaked after fertile years in the 1960's and has dramatically waned since then, as a result of a deteriorating crisis of antibiotic-resistance. Only three new antibiotics were cleared by the FDA since 2006. One important reason is that more and more antibiotic-resistant organisms are

emerging in both hospital and community settings, due to the decades of antibiotic use and especially antibiotic abuse. Bacteria have developed resistance to all different classes of antibiotics discovered to date (Alanis, 2005).
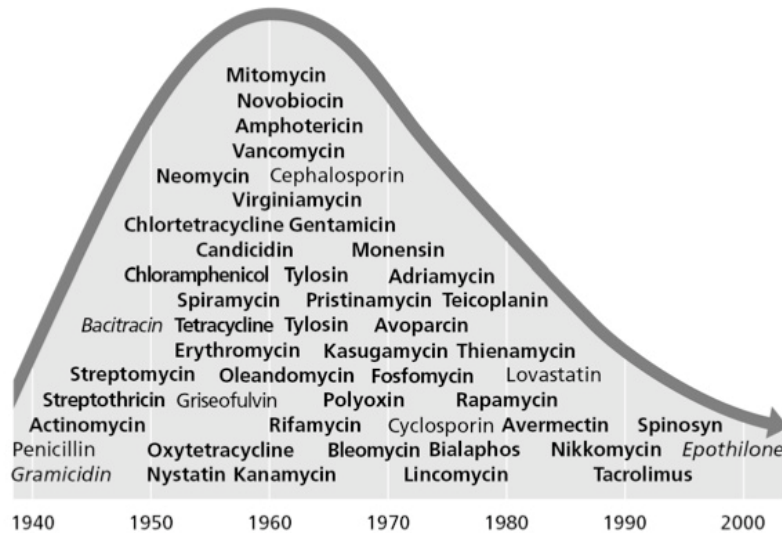
Figure 1-1 Discovery of major antibiotics during the past 70 years. This figure is adopted from Jason Sello Group at Brown University (Bailey and Sello, 2011).

The rapid development of antibiotic-resistance is well illustrated by what is happening in *Staphylococcus aureus (S. aureus),* as shown in Fig.1-2. *S. aureus* is the most prevalent cause of hospital-acquired infections, accounting for about 40% of all such infections. Its methicillin-resistant species, *i.e.* methicillin-resistant *S. aureus* (MRSA), is particularly threatening in hospitals, being the most common identifiable cause of skin and soft-tissue infections among patients presenting to emergency departments (Moran et al., 2006). As shown in Fig. 1-2, although new antibiotics are being continuously introduced, *S. aureus* developed the resistance to these antibiotics quickly. Vancomycin is normally used as the golden standard against MRSA.

Unfortunately, in the last decade Vancomycin-resistant *S. aureus* (VRSA) were identified, too **(Ohlsen, 2009)**. Today, about half of the *S. aureus* strains isolated in hospitals are resistant to multiple antibiotics, rendering the disease management difficult.
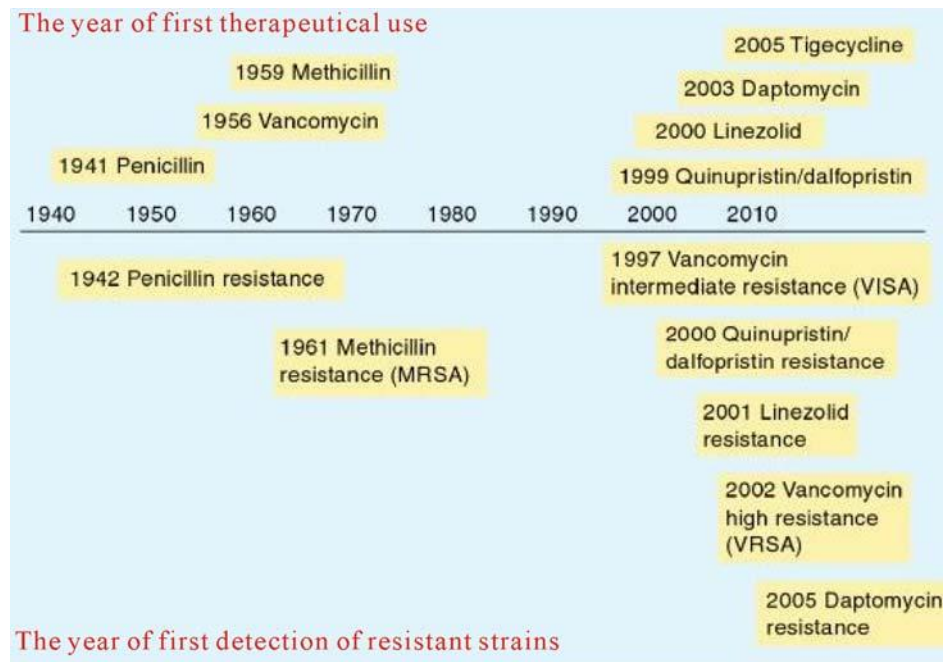
Figure 1-2 History of antibiotic-resistance development in *S. aureus*: modified from (Ohlsen, 2009). MRSA: Methicillin-resistant *S. aureus*; VRSA: Vancomycin-resistant *S. aureus*; VISA: Vancomycin-intermediate resistant *S. aureus*.

The recently isolated *Enterobateriaceae* carrying New Delhi metallo-β-lactamases 1 (NDM-1) are a new culprit in the crisis of antibiotic-resistance. The NDM-1 enzyme is able to hydrolyze β-lactams including carbapenems, the most powerful penicillin-related antibiotics against multi-drug resistant bacteria. The isolated NMD-1 carrying *Escherichia coli* and *Klebsiella pneumonia* were highly resistant to

1 Introduction

all antibiotics except tigecycline and colistinb. Since the first report in 2010, the bacteria carrying NDM-1 have rapidly spread from India and Pakistan to worldwide. By considering the other gram-negative bacteria carrying various extended-spectrum β-lactamases, now clinical microbiologists increasingly agree that multidrug resistant gram-negative bacteria pose the biggest risk to public health (Kumarasamy et al., 2010; Livermore et al., 2011; Poirel et al., 2010).

In summary, the deteriorating crisis of antibiotic-resistance demonstrates clearly that there is urgent need for novel antibacterial drugs without cross-resistance to antibiotics in use (Singh and Pandeya, 2011). By now, several alternative options have been proposed, such as bacteriophages (Coates and Hu, 2007), antimicrobial peptides (Hancock, 2001), and photodynamic therapy (Dai et al., 2009; Maisch, 2009; Maisch et al., 2011; Wainwright, 2010; Wainwright et al., 2007). Among them, photodynamic therapy is especially promising, and will be mainly discussed in this dissertation.

1.2 Antimicrobial Photodynamic Therapy

1.2.1 Photodynamic Therapy (PDT)

Photodynamic therapy is the treatment which uses photosensitizers (PSs), after illumination by a particular type of light, to treat diseases ranging from cancer to age-related macular degeneration and infections (Wilson and Patterson, 2008). This therapy requires the delivery of PSs and light to patients, and oxygen is also involved in most cases. In the first step, a PS is either locally or systemically administered to patients, followed by biodistribution to the site of therapeutic interest. Then the treatment site is irradiated with the light of a particular wavelength, to activate the PSs. The activated PSs further generate cytotoxic products, *e.g.* reactive oxygen species (ROS), resulting in the desired therapeutic effect.

The concept of PDT dated back to the beginning of 1900s. In 1900, Oscar Raab found that the paramecia in the petri dish with a given acridine concentration survived longer in the dark than in the light. Rather than ignoring this tiny difference, this observant student started to investigate the relationship between the light and killing efficiency, and systematically proved that acridine and some other colorful dyes, which had no effect in the dark, sensitized the rapid inactivation of paramecia in the presence of light (Moan and Peng, 2003; Raab, 1900). Continued work discovered that the presence of oxygen was essential for photoinactivation. In 1904, von Tappeiner and Jodlbauer coined the term "photodynamische Wirkung", photodynamic action in English, for the oxygen-requiring photosensitized reactions in biological

systems (Spikes, 1997; von Tappeiner and Jodlbauer, 1904).
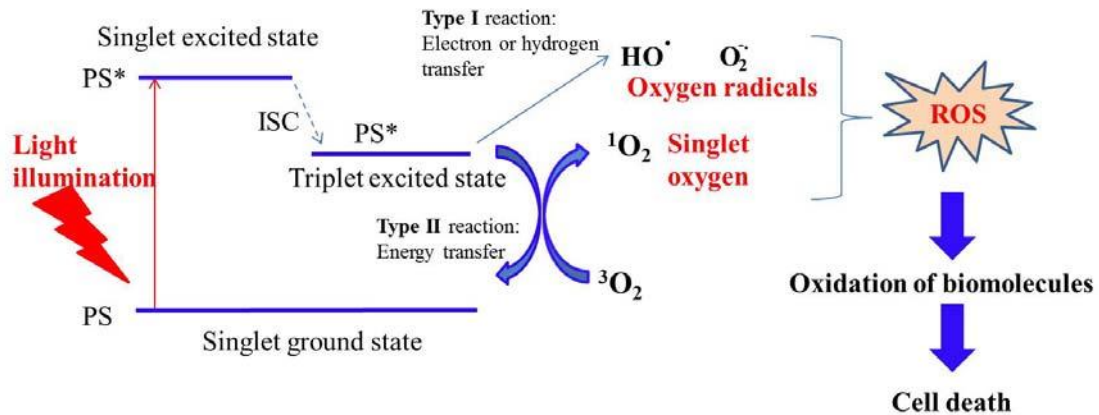
Figure 1-3 The mechanism of photodynamic therapy. PS: photosensitizer; ISC: intersystem crossing; ROS: reactive oxygen species.

Now the mechanism of PDT is better understood, as illustrated in Fig. 1-3. When the PS is illuminated by light with a suitable wavelength, the PS is promoted from its singlet ground state to singlet excited state. Then the activated PS converts to triplet excited state via intersystem crossing (ISC). The triplet activated PS is relatively long-lived and can interact with surrounding molecules via two types of reactions. The type I reaction involves the electron or hydrogen transfer with a substrate, which further reacts with oxygen to generate oxygen radicals, *e.g.* hydroxyl radical, superoxide, peroxide; in the type II reaction the triplet activated PS transfers energy to oxygen, generating singlet oxygen ($^1O_2$). Both the oxygen radicals and singlet oxygen are extremely reactive and thus are termed as reactive oxygen species (ROS). ROS can oxidize a variety of biomolecules, including lipids, amino acids, nucleic bases, causing irreversible damage to membranes, proteins/enzymes and DNA,

consequently leading to cell death (Baglo et al., 2011; Maisch et al., 2011; Moan and Peng, 2003). Type I and Type II reactions can happen simultaneously and the ratio between them depends on the PS, oxygen concentration, substrate and the distance between PS and substrate. Currently, singlet oxygen is widely believed to play the major role in PDT, and thus is the most important index to evaluate a PS (Donnelly et al., 2008).

The most successful application of PDT lies in the treatment of cancers. In the last two decades, PDT has emerged as a potential novel treatment for certain types of cancer and premalignant lesions, demonstrated by the commercial drugs listed in Table 1-1.

Table 1-1. Currently available PDT products in the market and in the ongoing clinical trials.

Drug Name	Photosensitizer (PS)	Type of PS	Application/ Indication	Manufacturer	Formulation
Anticancer					
Visudyne®	Verteporfin	Benzoporphyrin	Age-related macular degeneration (AMD)	Novartis International AG	Lyophilized liposomes
Photofrin®	Porfimer Sodium	Porphyrin	Esophageal cancer; non-small-cell lung cancer	Aptalis Pharma Inc.	Aqueous solution
Foscan®	Temoporfin	Chlorin	Head and neck squamous cell carcinoma	Biolitec AG	Ethanol/Propylene glycol
Aptocine™ Laserphyrin®	Talaporfin sodium	Chlorin	Solid tumor cancers; Hepatocellular carcinoma; Metastatic colorectal cancer	Light Sciences Oncology, Inc.	Aqueous solution
Photochlor®	2-(1-Hexyloxyethyl)-2-devinyl pyropheophorbide-a (HPPH)	Chlorin	Microinvasive (early) endobronchial non-small cell lung cancer; esophageal cancer	Roswell Park Cancer Institute	Infusion solution
Radachlorin®	Bremachlorin	Chlorin	Basal cell carcinoma	Rada-Pharma, Russia	Aqueous solution/gel
Fotoditazin®	Chlorine E6	Chlorophyll	Diagnostics and PDT of skin and lung cancers	Veta Grand Corp., Russia	Infusion solution/gel
Hexvix® /Cysview™	Hexaminolevulinate	Precursor of porphyrin	Detection of bladder cancer	Photocure ASA	Aqueous solution
Metvix™	Methyl aminolevulinate	Precursor of porphyrin	Thin solar keratosis; Superficial and/or thin nodular basal cell carcinomas; Acne vulgaris (Visonic™ Phase II); cervical dysplasia and human papilloma virus (HPV) infection (Cevira™, Phase II)	Photocure ASA	Cream
Antimicrobial					
Levulan® Kerastick®	5-aminolevulinic acid	Precursor of Porphyrin	Actinic keratosis of the face or scalp; Acne vulgaris	DUSA Pharmaceuticals, Inc.	On-site prepared Solution
Periowave™	Methylene blue	Phenothiazine	Chronic Periodontitis; Endodontics; Peri-Implant Disease; Gingivitis	Periowave Corp., Canada	solution
PAD™	Toluidine blue	Phenothiazine	Periodontitis; Endodontics; Caries	Denfotex Ltd.	Solution
Photopharmica	3,7-bis(din-butylamino)phenothiazin-5-ium bromide (PPA904)	Phenothiazinium	Wound therapy: Infected leg ulcers, Diabetic foot; Antifungal application; Acne; Cutaneous Leshmaniasis (Pre-clinical to Phase IIB)	Photopharmica	Cream

1.2.2 Antimicrobial Photodynamic Therapy (APDT)

Although PDT was discovered during the inactivation of microorganisms, *e.g.* paramecia, the potential of PDT against microbial diseases was exploited relatively slowly, compared to its fast development in the treatment of cancers. This was due to the discovery of antibiotics, its rapid development and wide application in the 20th century. But recently, due to the fast developing antibiotic-resistance, PDT is attracting more and more attention as an effective modality to inactivate microbes, and this specific application to microbial infections is termed as antimicrobial Photodynamic Therapy (**APDT**). Some researchers are used to call it photodynamic antimicrobial therapy (**PACT**), or photodynamic inactivation (**PDI**) of bacteria. In this cumulative dissertation, **PACT** was mainly used in Publication 1, while **PDI** was mainly used in Publication 2, due to some demands during the submission process. Nevertheless, all these three abbreviations refer to the same meaning, *i.e.* the application of PSs, after illumination by a particular type of light, for the inactivation of pathogenic microorganisms, such as bacteria, fungi and virus (Garcia et al., 2010; Maisch et al., 2011; Smijs and Pavel, 2011; Wainwright, 2010).

1.2.2.1 Mechanism

The activation of PSs in APDT is the same as discussed in section 1.2.1 and Fig. 1-3, *i.e.* type I and type II reactions. As to the lethal damage to bacteria caused by APDT, two basic mechanisms have been put forward: damage to the cytoplasmic membrane and damage to DNA (Hamblin and Hasan, 2004).

The damage to cytoplasmic membrane is generally believed to be the prime cause of bacterial cell death (Hamblin and Hasan, 2004). The cytoplasmic membrane is

9

mainly composed of phospholipids and proteins, *e.g.* enzymes and specific transporters, which are vital to bacterial survival. These phospholipids and proteins are susceptible to the oxidation caused by ROS, leading to both functional and morphological damages and ultimately cell death (Jori, 2006; Pudziuvyte et al., 2011). For example, the cationic meso-tetra (4 *N*-methyl-pyridyl)-porphine impaired some enzymic and transport functions at the level of both the outer and cytoplasmic membrane, and the activity loss of NADH, lactic and succinic dehydrogenase correlated with drop in survival (Valduga et al., 1999).

The DNA damage also plays a role in the inactivation of bacteria. After photodynamic inactivation, various DNA damages have been detected in bacteria, such as breaks in both single- and double-stranded DNA, the disappearance of the plasmid supercoiled fraction (Capella et al., 1996; Hamblin and Hasan, 2004). However, this DNA damage is not the prime cause of bacterial cell death, as *Deinococcus radiodurans*, which owns a very effective DNA repair system, is also sensitive to APDT (Schafer et al., 1998).

For both mechanisms, sufficient ROS are required around the biomolecules. For type I reaction of PS (oxygen radicals), the PSs must be delivered to the target sites in order to interact with the substrate to generate oxygen radicals. For type II reaction of PS, the generated singlet oxygen has a short life time and thus is estimated to diffuse 20~50 nm (Moan and Berg, 1991; Ochsner, 1997), therefore, the PS may be delivered to the target sites or at least close to the target sites, so that the generated $^1O_2$ can immediately or after diffusion oxidize the nearby biomolecules effectively. Obviously, the PSs being able to penetrate cell walls and generate ROS at the target sites are more efficient in APDT than the PSs outside of the cell walls. The pathways involved in the process of APDT are summarized in Fig. 1-4.
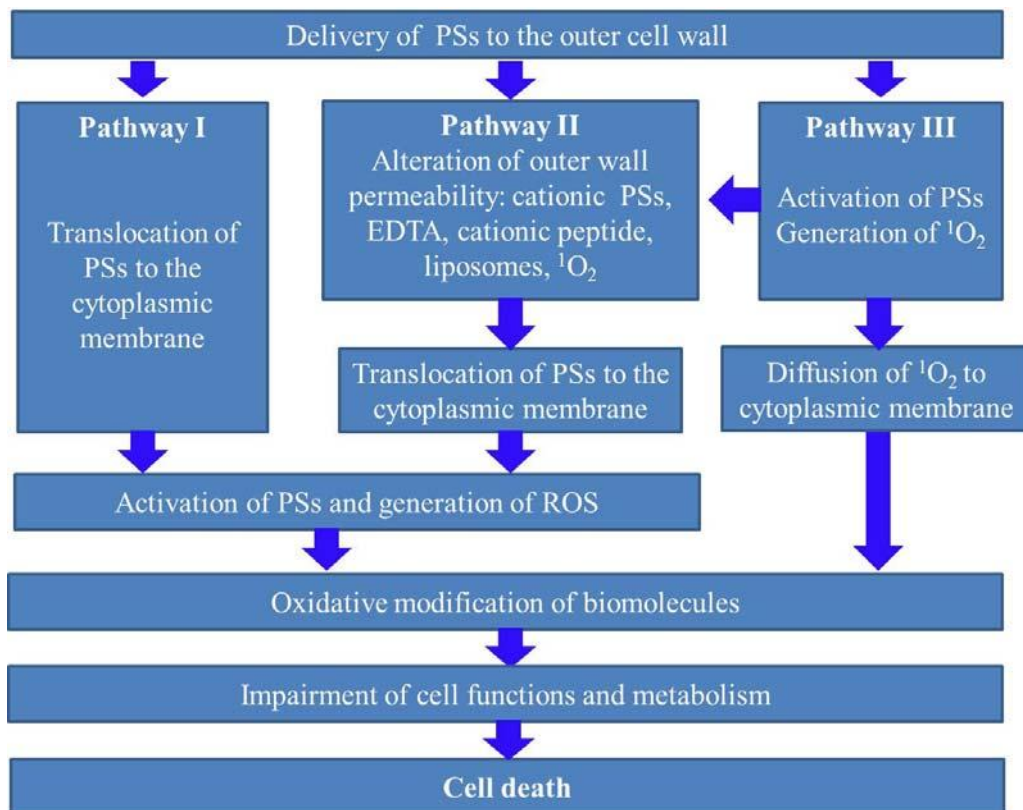
Figure 1-4 Scheme illustrating the essential steps involved in the process of APDT. Pathway I is operative for gram-positive bacteria and protozoa in the trophozoitic stage; pathway II is operative for gram-negative bacteria, yeasts and protozoa in the cystic stage; pathway III is an supplement to the former two pathways. Based on (Jori et al., 2006).

It was observed in the 1990s that gram-negative bacteria were less susceptible to APDT as compared to gram-positive bacteria. The susceptibility difference is because of the difference between the cell walls of the bacteria.

As shown in Fig.1-5, the cell wall of gram-positive bacteria is mainly composed of peptidoglycan, which is made up by chains of the amino sugar backbone glycan (N-acetylglcosamine and N-acetylmuranic acid) connected by peptide bridges. Teichonic acids and lipoteichoic acids are inserted into the peptidoglycan, endowing

the bacterial cell wall negative charge. The peptidoglycan layer is a porous structure, allowing PSs penetrate the cell wall easily and reach the cytoplasmic membrane. Therefore, gram-positive bacteria are susceptible to APDT (Dai et al., 2009; Jori et al., 2006).
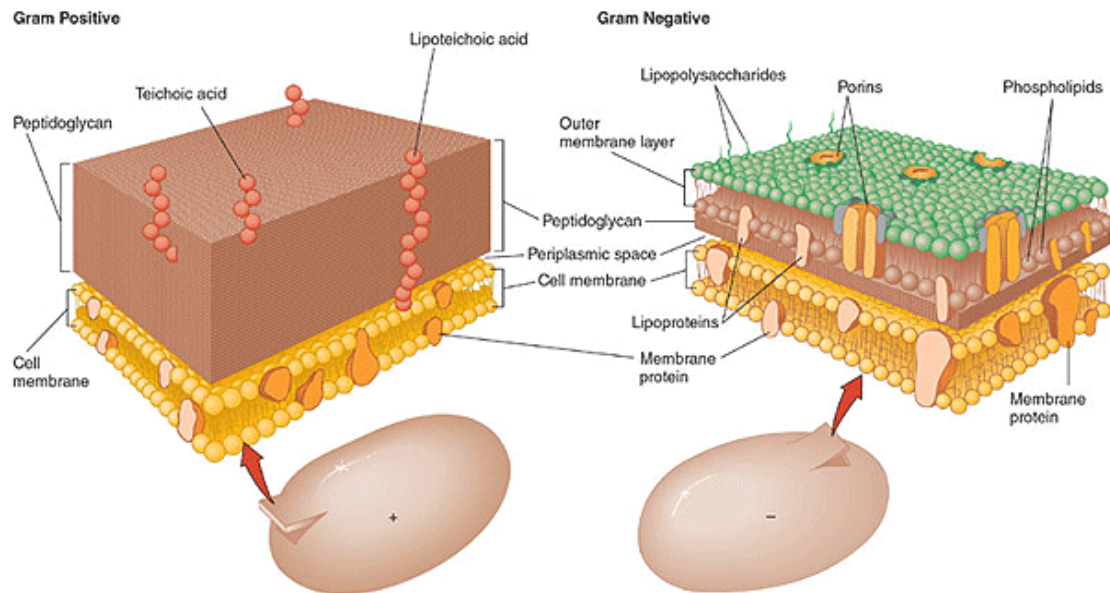
Figure 1-5 Representative structure and major components of the cell wall and cytoplasmic membrane in gram-positive and gram-negative bacteria. Cited from (Amalrich, 2010).

In contrast, gram-negative bacteria contain a quite tightly organized cell wall (Fig. 1-5 right). Particularly the peptidoglycan layer is covered by an outer membrane, whose outer leaflet is composed of lipopolysaccharides (LPS) and porins. LPS are strongly negatively charged macromolecules, comprising lipid A in the membrane and polysaccharide facing toward the aqueous environment. The polyanionic external polysaccharides are partially neutralized by divalent cations, such as Mg^{2+} and Ca^{2+}, thus forming a quasi-continuum of densely packed negative charges (Jori et al., 2006; Malik et al., 1992). The porins form water filled channels for the general or

substrate-specific transport of small water soluble substances. This highly organized system forms a physical and functional barrier between the cell and its environment, and thus limits the permeation of big PSs or lipophilic PSs into cells. Consequently, gram-negative bacteria are less susceptible to APDT (Huang et al., 2010; Malik et al., 1992).

To overcome the barrier of outer membrane, several strategies are devised according to the structure of the outer membrane. Ethylenediaminetetraacetic-acid (EDTA) was used to remove divalent cations (Mg^{2+} and Ca^{2+}), destroy the linkage between LPS and increase the permeability of the outer membrane. A polycationic peptide, poylmyxin B, was employed to disturb the lipid membrane, thus also increasing the permeability of outer membrane (Malik et al., 1992). Cationic PSs are particular effective against gram-negative bacteria, because they gain access across the outer membrane via the "self-promoted uptake pathway", *i.e.* cationic PSs bind to the negatively charged LPS, cause alterations in the outer membrane permeability, and thereby render hydrophobic PSs deep penetration inside bacterial cells, where the generated ROSs execute fatal damage (Merchat et al., 1996; Minnock et al., 2000). In addition, liposomes also have the function to disturb the outer membrane, since some liposomal formulations were able to fuse with bacteria effectively and disturb their cell walls (Jia et al., 2010; Mugabe et al., 2006).

1.2.2.2 Advantages of APDT

APDT exhibits several advantages over the traditional antibiotics therapy:

1) **Broad spectrum of action:** as ROS is toxic to all cells, APDT can act on bacteria, fungi, yeasts, parasitic protozoa and so on.

2) **Efficacy on antibiotic-resistant species**: Even antibiotic-resistant microbes

can be inactivated by APDT, such as multidrug-resistant *Acinetobacter baumannii* (Ragas et al., 2010) and MRSA (Schastak et al., 2010; Zolfaghari et al., 2009).

3) **Safety to the host tissue**: the antimicrobial PDI is more phototoxic to bacteria than to mammalian cells. It has been shown that human cells (keratinocytes and fibroblasts) could survive the antimicrobial PDI in certain conditions which were lethal to microorganisms; thus the bacteria were selectively removed (Cassidy et al., 2009; Hamblin and Hasan, 2004; Zeina et al., 2003; Zolfaghari et al., 2009). In another treatment of epidemic MRSA infected wounds, histological examination of the wounds revealed no difference between the APDT-treated wounds and the untreated wounds (Maisch et al., 2005; Zolfaghari et al., 2009).

4) **Fast:** the administration of PSs and laser illumination are completed within hours, much faster than the action of antibiotics.

5) **Lack of selection of photo-resistant microbial cells** (Jori et al., 2006): it is generally believed that microbial cells are hard to develop resistance to ROS. In a test using Zn(II) phthalocyanine to photosensitize *S. aureus, Pseudomonas aeruginosa (P. aeruginosa)* and *Candida albicans (C. albicans)*, both antibiotic susceptible and resistant strains, it was demonstrated that 20 consecutive APDT treatments did not result in any APDT-resistant mutants (Giuliani et al., 2010).

6) **Double selectivity:** both the PSs can be targeted to the microbes and the light can be targeted to the infected sites.

1.2.3 Application of APDT

Because of the above mentioned advantages, APDT has a wide range of applications to treatment of different microbial infections. The so far reported candidate infectious diseases for ADT are summarized in Fig. 1-6 (Dai et al., 2009).
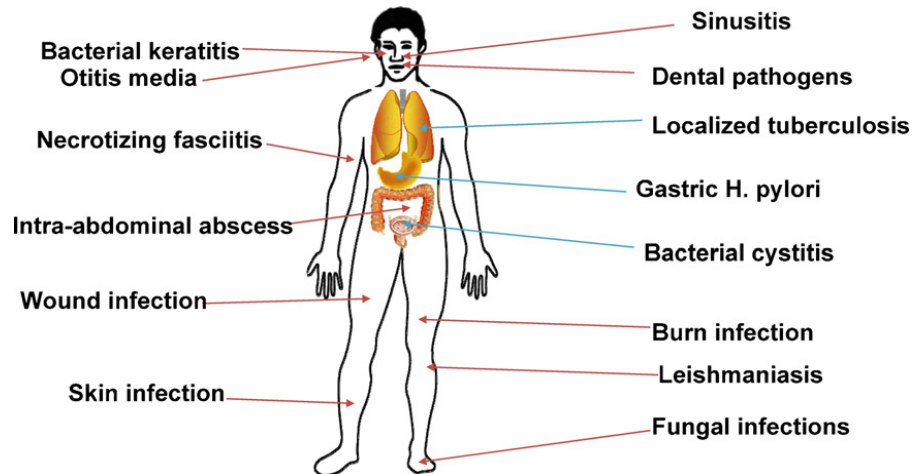
Figure 1-6 Candidate infectious diseases for APDT. A wide variety of localized infections could be clinically treated by antimicrobial PDT. Cited from (Dai et al., 2009).

1.2.3.1 **Treatment of skin associated bacterial infections**

Indications for APDT are first of all the treatment of local and superficial skin infections, such as wound infection, burn infection, soft tissue infection, and acne vulgaris, especially the nosocomial infections caused by multi-resistant bacteria, because of the easy accessibility of light source.

For instance, burn wounds are often associated with infections caused by *S. aureus*, *P. aeruginosa* and *C. albicans*. The antimicrobial PDI of multi-resistant *P. aeruginosa* in burn wounds was studied in third-degree burned mice, indicating that the PS, hypocrellin B, was effective to inactivate *P. aeruginosa* by 2 $\log_{10}$, and subsequently delayed and diminished bloodstream invasion (Hashimoto et al., 2010; Hashimoto et

15

al., 2009). Lambrechts *et al.* used meso-mono-phenyl-tri(N-methyl-4-pyridyl)-porphyrin to treat the third degree burn wounds infected with *S. aureus* in mice, and achieved a fast reduction of more than 98% of the bacteria (Lambrechts et al., 2005b).

The first Phase II study for a topical APDT of infected wound was carried out by a UK company, Photopharmica, which has reported promising proof-of-concept data with its lead candidate PPA 904 for the treatment of microbial disease in wounds. The compound was well tolerated, and no treatment-related adverse events were reported. Now this company is organizing its Phase II b trial for chronic leg ulcer (Photopharmica, 2007).

APDT has shown obvious efficacy in the treatment of acne vulgaris, which is often associated with infection caused by *Propionibacterium acnes* (Kim and Armstrong, 2011). The company, Photocure ASA, is developing a methylaminolevulinate-loaded cream, Visonac™, for the APDT of acne vulgaris. The cream is applied to the acne area, which is subsequently illuminated with red light after a short incubation time. In the completed proof-of-concept study, Visonac™ significantly reduced the number of inflammatory acne lesions than placebo PDT measured 10 weeks after treatment. Now Visonac™ is in the Phase II clinical trial (Photocure, 2011).

1.2.3.2 Treatment of dental infections

Until now the most successful commercial application of APDT is the treatment of dental infections. As shown in Table 1-1, Methylene blue and Toluidine blue are being clinically used as an adjuvant treatment of chronic periodontitis, endodontics, peri-implant disease, gingivitis and caries. After application of a PS, light is delivered into the target area precisely using a fiber optic cable, as shown in Fig.1-7, thus avoiding the disturbances of the microflora at other sites and the adjacent host tissues.

In this treatment, there is no need to anaesthetize the area and inactivation of bacteria is achieved within short span of time, thus beneficial to both operator and the patient (Raghavendra et al., 2009). The additional application of APDT resulted in the reduction in the numbers of bacteria in the periodontal pockets or in the root canal system (Ng et al., 2011; Pinheiro et al., 2010), and a significantly higher reduction of bleeding scores than using scaling and root planning alone (Chondros et al., 2009).

Figure 1-7 Activation of the PSs in the mesiobuccal pocket of tooth 16 (Stephan, 2011).

1.2.3.3 Antifungal therapy

APDT is also effective in the treatment of fungal infections. A variety of fungal species have already been proved to be susceptible to APDT (Donnelly et al., 2008; Lambrechts et al., 2005a; Smijs and Pavel, 2011). Lambrechts *et al.* used a cationic porphyrin to successfully inactivate *Candida albicans*, whose cytoplasmic membrane was found to be the target organelle of APDT (Lambrechts et al., 2005a). Smijs's group found a cationic porphyrin "Sylsens B" effective towards *Trichophyton rubrum*, creating the possibility of efficiently treating nail infections and remaining spores in hair follicle; this group also showed potential usefulness of APDT in treatment of clinical dermatophytoses, *e.g.* 5-aminolevulinic acid (ALA) combined with red light was shown to be efficacious after repeated sessions in the *in vivo* treatment of onychomycosis, namely, fungal nail infection caused by various dermatophytes (Smijs

and Pavel, 2011). Carmen *et al.* treated the patient diagnosed with onychomycosis using methyl-aminolevulinate, and achieved mycological and clinical cure without reoccurrence after 12 months (Carmen et al., 2011). Now it is more and more accepted that PDT has a good prospect to become a worthy alternative to established antifungal drugs for the treatment of superficial fungal infections.

1.2.3.4 Other infections

APDT has also been proved to be effective against other infections, including viral infections (Chen et al., 2011b; Rossi et al., 2009), leishmaniasis (Akilov et al., 2009), gastric *Helicobacter pylori* infection (Lembo et al., 2009; Leszczynska et al., 2009), mycobacterial infection (Shih and Huang, 2011), demonstrating again that APDT has a broad spectrum of applications and is prospective to become a worthy alternative to established antimicrobial drugs.

In summary, APDT is an attractive treatment of various microbial infections. However, this therapy is still in its developing period, and has a long way to go before wide application in practice. On one side, new PSs are being synthesized and tested; on the other side, suitable PSs delivery systems may further improve the APDT. In spite of the vast number of studies published in the field of APDT, a rational approach to formulation design has not taken place. This may be because this filed is dominated by clinicians and basic scientists, rather than those involved in pharmaceutical formulation development (Cassidy et al., 2009).

1.3. Liposomes for delivery of Photosensitizers

1.3.1 Liposomes

Liposomes are spherical vesicles composed of one or more concentric lipid bilayers surrounding an aqueous phase. Since the discovery by Bangham (Bangham and Horne, 1964), liposomes have been extensively investigated and have emerged as excellent drug carriers due to their powerful solubilizing capacity of varieties of compounds and many superior characteristics.

The application of liposomes as drug carriers is illustrated in Fig. 1-8: the hydrophobic drugs can be incorporated into the lipid bilayers, whilst the hydrophilic drugs can be encapsulated into the aqueous phase; stealth liposomes may be obtained by stubbing PEG on the surface; cell-targeting liposomes may be prepared by coupling targeting ligands to the surface of liposomes. Therefore, liposomes have a broad range of applications in the pharmaceutical industries, as summarized in Table 1-2.
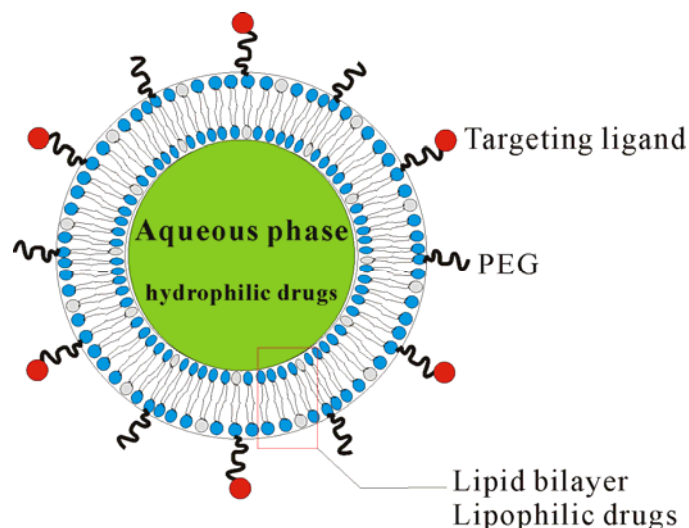
Figure 1-8 Structure of a unilamellar liposome and its application for drug delivery.

Table 1-2. Liposomes in the pharmaceutical industry. Modified from (Lasic, 1995).

Liposome Utility	Current Applications	Disease States Treated
Solubilization	Amphotericin B, minoxidil, benzoporphyrin	Fungal infections, age-related macular degeneration
Site-Avoidance	Amphotericin B – reduced nephrotoxicity, doxorubicin – decreased cardiotoxicity	Fungal infections, cancer
Sustained-Release	Systemic antineoplastic drugs, hormones, corticosteroids, drug depot in the lungs	Cancer, biotherapeutics
Drug protection	Cytosine arabinoside, interleukins	Cancer, etc.
RES Targeting	Immunomodulators, vaccines, antimalarials, macrophage-located diseases	Cancer, MAI, tropical parasites
Specific Targeting	Cells bearing specific antigens	Wide therapeutic applicability
Extravasation	Leaky vasculature of tumours, inflammations, infections	Cancer, bacterial infections
Accumulation	Prostaglandins	Cardiovascular diseases
Enhanced Penetration	Topical vehicles	Dermatology
Drug Depot	Lungs, sub-cutaneous, intra-muscular, ocular	Wide therapeutic applicability

1.3.2 Liposomes for the treatment of microbial infections

One important application of liposomes lies in the treatment of microbial infections, *i.e.* entrap antibiotics to enhance their antimicrobial activity and pharmacokinetic properties (Drulis-Kawa and Dorotkiewicz-Jach, 2010). A variety of antibiotics were successfully encapsulated into liposomes, endowing them specific characteristics. One such successful example is Ambisome® (amphotericin B incorporated in Liposomes for fungal infections), which has already been approved by FDA in 1997. The advantages of liposomes for antibiotics delivery were well discussed in the literature (Bakker-Woudenberg et al., 2005; Drulis-Kawa and Dorotkiewicz-Jach, 2010; Salem et al., 2005), such as:

- improving pharmacokinetics and biodistribution;

- decreasing toxicity of the drugs;

- enhancing activity against intracellular pathogens;

- enhancing activity against extracellular pathogens, in particular, to overcome bacterial drug resistance;

- target selectivity.

Considering the advantages of liposomes in the treatment of microbial infections, it is believed that liposomes will also be a promising formulation for APDT, especially in the treatment of local infections.

1.3.3   Liposomes for APDT

Compared with the intensive study of liposomes for antibiotics delivery, the study of using liposomes to deliver PSs for APDT is still in its infancy, as only a few studies have been published. Nevertheless, the so far published work still shed light on the application of liposomes in this field.

1.3.3.1 Enhancement of the APDT efficiency

Liposomes can significantly enhance the APDT efficiency of PSs, both towards gram-positive and gram-negative bacteria. Nisnevitch *et al*. enclosed methylene B and neutral red NR in liposomes. These liposomes exerted a stronger antimicrobial effect than free PSs for the tested bacteria, including both gram-positive and gram-negative bacteria (Nisnevitch et al., 2010). The enhancement of antimicrobial effect towards gram-negative bacteria was attributed to a fusion mechanism of liposomes with bacteria, thus delivering drugs into bacteria in a concentrated form and increasing the cytotoxicity. This mechanism is in accordance with the fusion of antibiotic containing liposomes with gram-negative bacteria, which was directly observed by scanning electron microscopy or flow cytometry (Mugabe et al., 2006; Sachetelli et al., 2000). In the case of gram-positive bacteria, it was considered that liposomes could release their content nearby cell surface after the interaction with the external peptidoglycan

barrier.

Ferro *et al.* incorporated porphyrin PSs into liposomes composed of pure cationic lipid, DOTAP. They found that the cationic liposomes promoted the tighter binding of liposomes with MRSA, then the cationic lipid disturbed the cell wall, enhanced its permeability to the PSs, leading to effective photoinactivation of MRSA (Ferro et al., 2006; Ferro et al., 2007).

1.3.3.2 Reduction of the PSs dosage

Since the antimicrobial effect can be enhanced by liposomes, the dosage of PSs may be reduced, so as to reduce the side effects to host tissues. For example, liposome-encapsulated 5-aminolevulinic acid (ALA) was recently studied for PACT of acne vulgaris. The concentration of liposome-encapsulated ALA was reduced significantly by a factor of 40 compared to its cream formulation and still induced the same skin fluorescence (Christiansen et al., 2007). Further clinical studies proved that the 0.5% Liposome-encapsulated ALA improved inflammatory acne with minimal side effects in Asians, and therefore was superior to 20% ALA cream in the treatment of acne vulgaris (An et al., 2011; de Leeuw et al., 2010). This is because liposomes could help delivery certain drugs to the sebaceous glands, *e.g.* antiandrogen in liposomes was mainly localized in sebaceous glands, while alcoholic solution favored the localization of the drug into the stratum corneum (Bernard et al., 1997).

1.3.3.3 Solubilization of hydrophobic PSs

A portion of the PSs are hydrophobic and cannot be directly administrated to infection sites. In this case, liposomes serve as a good carrier to solubilize these hydrophobic PSs. For example, temoporfin is a potent generation II photosensitizer,

but its high lipophilicity limits its application. Fortunately, temoporfin is able to be incorporated into liposomes well. It was reported that temoporfin-loaded liposomes (Fospeg®) caused a 4-5 $\log_{10}$ reduction of *S. aureus* (Engelhardt et al., 2010). Bombelli *et al.* used cationic surfactants to prepare new cationic liposomes as vehicles of temoporfin for APDT and achieved sufficient APDT effect (Bombelli et al., 2008).

1.4 Aim of the study

Summarizing the introduction above, the situation of microbial infections as well as antibiotic-resistance is deteriorating, APDT is a promising modality to treat microbial infections, and liposomes are an attractive drug delivery system in the treatment of infections. However, liposomes are still seldom explored for APDT, and the limited study mainly focused on the passive delivery of PSs. Thus we wonder if the APDT could be further improved by using bacteria-targeting liposomes. During the search for suitable liposomal formulations for APDT, a lot of liposomal formulations need to be screened, while the conventional preparation method is slow, limiting the development process of liposomal formulations for APDT. So could we develop a fast high throughput method to screen the liposomal formulations quickly? These questions lead to the aims of our study:

1) **To develop bacteria-targeting liposomes** by coupling different ligands to the surface of liposomes, aiming to increase the delivery of PSs to bacteria and consequently to improve the APDT efficiency. This work is summarized in publication 1 and 2.

2) **To develop a high-throughput method for screening a large number of PS-loaded liposomal formulations** using ethanol injection method and the automatic devices. This work is summarized in Publication 3.

2 Publication overview

2.1 Research Paper:

Antimicrobial peptide modified liposomes for bacteria targeted delivery of temoporfin in photodynamic antimicrobial chemotherapy

Kewei Yang, Burkhard Gitter, Ronny Rüger, Gerhard D. Wieland, Ming Chen, Xiangli Liu, Volker Albrecht, Alfred Fahr

Abstract:

A generation II PS, temoporfin, was incorporated into liposomes, followed by conjugation with a novel antimicrobial peptide (WLBU2) on the liposomal surface for bacteria targeted delivery of temoporfin in photodynamic antimicrobial chemotherapy (PACT). The delivery of temoporfin to MRSA and *P. aeruginosa* was confirmed by fluorescence microscopy and flow cytometry, thus demonstrating that more temoporfin was delivered to bacteria by WLBU2 modified liposomes than by unmodified liposomes. Consequently, the WLBU2 modified liposomes eradicated all MRSA and induced a 3.3 $\log_{10}$ reduction of *P. aeruginosa* in the *in vitro* photodynamic inactivation test. These findings demonstrate that antimicrobial peptide modified liposomes are promising for bacteria targeted delivery of PSs and for improving the PACT efficiency against both gram-positive and gram-negative bacteria in the local infections.

Own contribution to the manuscript:

1) Preparation and characterization of bacteria-targeting liposomes;

2) Culture of bacteria; *in vitro* study of the delivery of temoporfin to bacteria;

3) Data evaluation, interpretation and presentation of the results.

4) Writing of the first version of the manuscript

2.2 Research Paper:

Wheat germ agglutinin modified liposomes for the photodynamic inactivation of bacteria

Kewei Yang, Burkhard Gitter, Ronny Rüger, Volker Albrecht, Gerhard D. Wieland, Alfred Fahr

Abstract:

In this study, a specific lectin, wheat germ agglutinin (WGA), was coupled to the surface of temoporfin-loaded liposomes. MRSA and *P. aeruginosa* were selected to evaluate the WGA modified liposomes in terms of bacteria targeted delivery and *in vitro* photodynamic inactivation test. Fluorescence microscopy revealed that temoporfin was delivered to both kinds of bacteria, while flow cytometry demonstrated that WGA modified liposomes delivered more temoporfin to bacteria compared to non-modified liposomes. Consequently, the WGA modified liposomes eradicated all MRSA and significantly enhanced the PDI of *P. aeruginosa*, suggesting that the WGA modified liposomes are a promising formulation for bacteria targeted delivery of temoporfin and for improving the PDI of both gram-positive and gram-negative bacterial cells.

Own contribution to the manuscript:

1) Preparation and characterization of bacteria-targeting liposomes;

2) Culture of bacteria; *in vitro* study of the delivery of temoporfin to bacteria;

3) Data evaluation, interpretation and presentation of the results.

4) Writing of the first version of the manuscript

2.3 Research Paper:

Fast high-throughput screening of temoporfin-loaded liposomal formulations prepared by ethanol injection method

Kewei Yang, Joseph T. Delaney, Ulrich S. Schubert, Alfred Fahr

Abstract:

A new strategy for the fast and convenient high-throughput screening of liposomal formulations was developed, utilizing the automation of the ethanol injection method. Numerous temoporfin-loaded liposomal formulations were efficiently prepared using a pipetting robot, followed by automated size characterization using a dynamic light scattering plate reader. Step-by-step small liposomes were prepared with high incorporation efficiency, and an optimized formulation was obtained for each lipid, which were unilamellar spheres with a diameter of about 50 nm and were very stable for over 20 weeks. The results illustrate this approach to be promising for the fast high-throughput screening of liposomal formulations.

Own contribution to the manuscript:

1) Experiment design;

2) Performance of all the experiments except Cryo-TEM;

3) Data evaluation, interpretation and presentation of the results.

4) Writing of the first version of the manuscript

3 Publications

3.1 Antimicrobial peptide modified liposomes for bacteria targeted delivery of temoporfin in photodynamic antimicrobial chemotherapy

Kewei Yang, Burkhard Gitter, Ronny Rüger, Gerhard D. Wieland, Ming Chen, Xiangli Liu, Volker Albrecht, Alfred Fahr

Pages in the dissertation: 30~38 (9 pages)

Photochemical & Photobiological Sciences

PAPER

Antimicrobial peptide-modified liposomes for bacteria targeted delivery of temoporfin in photodynamic antimicrobial chemotherapy

Kewei Yang,[a] Burkhard Gitter,[b] Ronny Rüger,[a] Gerhard D. Wieland,[b] Ming Chen,[a] Xiangli Liu,[a] Volker Albrecht[b] and Alfred Fahr*[a]

Photodynamic antimicrobial chemotherapy (PACT) and antimicrobial peptides (AMPs) are two promising strategies to combat the increasing prevalence of antibiotic-resistant bacteria. To take advantage of these two strategies, we integrated a novel antimicrobial peptide (WLBU2) and a potent generation II photosensitizer (temoporfin) into liposomes by preparing WLBU2-modified liposomes, aiming at bacteria targeted delivery of temoporfin for PACT. WLBU2 was successfully coupled to temoporfin-loaded liposomes using a functional phospholipid. The delivery of temoporfin to bacteria was confirmed by fluorescence microscopy and flow cytometry, thus demonstrating that more temoporfin was delivered to bacteria by WLBU2-modified liposomes than by unmodified liposomes. Consequently, the WLBU2-modified liposomes eradicated all methicillin-resistant *Staphylococcus aureus* (MRSA) and induced a 3.3 $\log_{10}$ reduction of *Pseudomonas aeruginosa* in the *in vitro* photodynamic inactivation test. These findings demonstrate that the use of AMP-modified liposomes is promising for bacteria-targeted delivery of photosensitizers and for improving the PACT efficiency against both gram-positive and gram-negative bacteria in the local infections.

Introduction

A major challenge of combating infectious diseases is the increasing emergence of antibiotic resistance amongst pathogenic bacteria despite the continuous development of antibiotics. For instance, the methicillin-resistant,[1] mupirocin-resistant[2] or vancomycin-resistant[3] strains of bacteria are quite hard to kill, attracting much attention nowadays. Particularly, the recently isolated *Escherichia coli* and *Klebsiella pneumoniae* carrying New Delhi metallo-beta-lactamases (NDM-1) are highly resistant to all antibiotics except tigecycline and colistin.[4] Therefore, it is emergent to look for alternative antimicrobial strategies. To date, photodynamic therapy (PDT) is emerging as one of the most promising strategies.[5,6]

PDT involves the use of a photosensitizer (PS), oxygen and light, mostly delivered by laser. The PS is triggered by light from its ground energy level singlet state to an activated state, followed by transferring energy to the surrounding oxygen, leading to the generation of reactive oxygen species (ROS), *e.g.* singlet oxygen.[5] These ROSs are highly reactive, so that they can oxidize varieties of biological molecules, *e.g.* proteins, nucleic acids and lipids, resulting in cytotoxicity.[7] PDT is mainly used in the treatment of tumors in clinics, but is also used in the treatment of other diseases, *e.g.* age-related macular degeneration.[8] In addition, PDT has attracted significant attention in the last decades as a potential strategy to treat microbial infections, especially those caused by antibiotic-resistant species. The antimicrobial application of PDT is often termed as **p**hotodynamic **a**ntimicrobial **c**hemo**t**herapy (PACT)[6,9–11] or **p**hoto**d**ynamic **i**nactivation (PDI).[12] Compared to traditional antibiotics therapy, PACT has the following advantages. Firstly, PACT possesses a broad spectrum of action, and many antibiotic-resistant strains have been reported to be efficiently inactivated, because ROSs are toxic to almost all bacteria.[12–15] Secondly, it is believed that bacteria will not easily develop resistance against ROSs, so PACT is of low mutagenic potential.[5,16] Thirdly, PACT is more phototoxic to bacteria than to mammalian cells. It was observed that human cells (keratinocytes and fibroblasts) could survive PACT in certain conditions that were lethal to microorganisms, so that the bacteria could be selectively removed.[9,17–19] Because of these advantages, PACT has been employed to combat a number of bacteria, mostly during the local microbial infections, such as skin-associated bacteria,[19–21] bacteria of periodontal pockets[16] and the oral cavity.[22] Several products were already developed based on PACT, *e.g.* for the treatment of acne vulgaris and infected leg ulcers.[23,24] The available results confirm that PACT is a very promising approach to combat bacterial infections, especially the antibiotic-resistant species.

Currently we are studying temoporfin as the model of PSs for PACT. Temoporfin is one of the most potent generation II PSs, which is activated at 652 nm wavelength with a depth of light

[a]Department of Pharmaceutical Technology, Friedrich-Schiller-University Jena, Lessingstrasse 8, D-07743, Jena, Germany. E-mail: alfred.fahr@uni-jena.de; Fax: +49-3641-949902; Tel: +49-3641-949901
[b]biolitec AG, Jena, Germany

penetration in skin of about 1 cm,[25] and thereby is suitable for the treatment of local infections. It was found that temoporfin could photodynamically inactivate *S. aureus* effectively, and might be a promising candidate for PACT of staphylococcal infections in wounds.[26–28] However, temoporfin cannot be administrated alone, since it is highly hydrophobic with a log *P* of 9.24,[29] thus a suitable delivery system is essential for the administration of temoporfin. Among the different drug delivery systems, liposomes are an attractive choice and suitable for the incorporation of highly hydrophobic PSs.[12–14,26,30,31] For example, biolitec AG developed a liposomal formulation of temoporfin, Fospeg®, which was proved to be effective in the PACT against *Staphylococcus aureus* (*S. aureus*).[28] Bombelli *et al.* developed another kind of novel temoporfin-loaded cationic liposomes, which featured the same bactericidal activity as free temoporfin, and hence, as the authors claimed, enlarged the prospective of exploitation of temoporfin in PACT through the development of target specificity in these formulations.[26] When these liposomes are applied to the local infection site, temoporfin is delivered not only to bacteria, but also to the cells nearby, causing certain side effects after laser illumination. Therefore, it is desirable to develop bacteria-targeting liposomes which bind specifically to bacteria, consequently increasing the chance to deliver temoporfin directly to bacteria while reducing the nonspecific delivery to other cells, and finally leading to improved PACT efficiency.

A promising source of bacteria-targeting ligands may come from antimicrobial peptides (AMPs), a kind of cationic amphipathic peptides (CAPs), which are found ubiquitously in most classes of life forms, where they function as major effectors of the innate immune system.[32] The cationic nature of AMPs enables them to interact with the negatively charged lipids in bacterial membranes, such as teichoic acids in gram-positive bacteria and lipopolysaccharides (LPS) in gram-negative bacteria, while their amphipathic nature enables their penetration into bacterial membranes and the formation of membrane pores, causing damage to bacteria.[33] This mode of action promises both low susceptibility to antibiotics resistance and a broad spectrum of activities against a vast variety of microorganisms. Besides naturally occurring AMPs, a lot of synthetic AMPs were obtained based on the systematic variation of natural AMPs, aiming to improve antibacterial activity and reduce cytotoxicity. For instance, Deslouches *et al.* synthesized different multimers of a 12-residue lytic base unit (LBU) peptide composed only of arginine and valine residues and investigated the relationship between their length/tryptophan substitution and antimicrobial activity.[34] A 24-residues peptide named WLBU2 showed not only high antimicrobial activity towards *Pseudomonas aeruginosa* (*P. aeruginosa*) and *S. aureus*, but also high antimicrobial selectivity in the co-culture model of *P. aeruginosa* and primary human skin fibroblasts. Further studies confirmed that WLBU2 was able to kill *P. aeruginosa* in human serum and whole blood.[35] WLBU2 was also proved to be active *in vitro* against *Chlamydia trachomatis* and would be an active ingredient for a topical antimicrobial formulation targeting *Chlamydia trachomatis*.[36] These results suggest that WLBU2 has a specific and effective binding to various species of microbes, and therefore may be a potential bacteria-targeting ligand for bacteria-targeting drug delivery systems, *e.g.* liposomes.

To combat the increasing emergence of antibiotic resistance, we intended to develop a novel bacteria-targeting liposomal formula-

tion for improvement of PACT, taking use of the AMPs' bacteria-targeting ability. This strategy was demonstrated by conjugating WLBU2 to the surface of temoporfin-loaded liposomes and by studying their PACT effect on both gram-positive and gram-negative bacteria.

Experimental

Materials

1,2-Dipalmitoyl-*sn-glycero*-3-phosphocholin (DPPC) and 1,2-distearoyl-*sn-glycero*-3-phosphoethanolamine-N-[methoxy(polyethylene glycol)-2000] (mPEG$_{2000}$-DSPE, ammonium salt) were obtained from Genzyme Pharmaceuticals (Cambridge, MA, USA). 1,2-Distearoyl-*sn-glycero*-3-phosphoethanolamine-N-[3-(*N* - succinimidyloxyglutaryl) aminopropyl (polyethyleneglycol) - 2000-carbamyl] (NHS-PEG$_{2000}$-DSPE) was purchased from NOF Cooperation (Tokyo, Japan). N-[1-(2,3-Dioleoyloxy)propyl]-N,N,N-trimethylammonium methylsulfate (DOTAP, methyl sulfate salt) was purchased from Boehringer Ingelheim GmbH (Ingelheim, Germany). Temoporfin, *i.e.* 3,3′,3″,3‴-(7,8-dihydroporphyrin-5,10,15,20-tetrayl)tetraphenol (mTHPC) and its liposomal formulation, Foslip®, were gifts from biolitec AG (Jena, Germany). WLBU2 was custom-made by Centic Biotec (Weimar, Germany). All other chemicals were of analytical grade.

Bacteria

The microbial strains were supplied by the German Collection of Microorganisms and Cell Cultures (DSMZ, Braunschweig, Germany). *S. aureus* DSM11729 is the methicillin-resistant species (MRSA) and is gram-positive. *P. aeruginosa* DSM1117 is a gram-negative species.

Preparation of liposomes and modification with WLBU2

Liposomes consisting of 30 mM phospholipids and 1.5 mg ml^{-1} temoporfin were prepared using the Film-Hydration-Extrusion technique.[30] Briefly, DPPC, DOTAP, NHS-PEG$_{2000}$-DSPE and mPEG$_{2000}$-DSPE were dissolved in chloroform with a molar ratio of 80:15:2:3, containing 2 mol% NHS-PEG$_{2000}$-DSPE. Temoporfin dissolved in methanol was mixed with the phospholipid solution. The organic solvent was removed using a rotary evaporator (BÜCHI Vacobox B-177, BÜCHI, Switzerland) at 55 °C. The obtained lipid/drug film was hydrated using borate buffer (pH 8.0) followed by 21 times extrusion through a 100 nm polycarbonate membrane within 20 min, using a LiposoFast® mini-extruder (Avestin, Ottawa, Canada). The conjugation of WLBU2 with liposomes is illustrated in Fig. 1. The WLBU2 was incubated with liposomes at a 1:5 molar ratio of WLBU2 to NHS-PEG$_{2000}$-DSPE. After 2 h incubation at room temperature (RT), the modified liposomes were separated from the free WLBU2 using a Sepharose Cl-4B column, eluted by phosphate buffered saline (PBS) buffer. The liposomes before and after incubation with WLBU2 are named NHS-liposomes and WLBU2-liposomes, respectively. The unmodified liposomes, consisting of DPPC, DOTAP and mPEG$_{2000}$-DSPE at the molar ratio of 80:15:5, were prepared in the same way and used as control (PEG-liposomes). The registered liposomal formulation, Foslip®, was utilized for
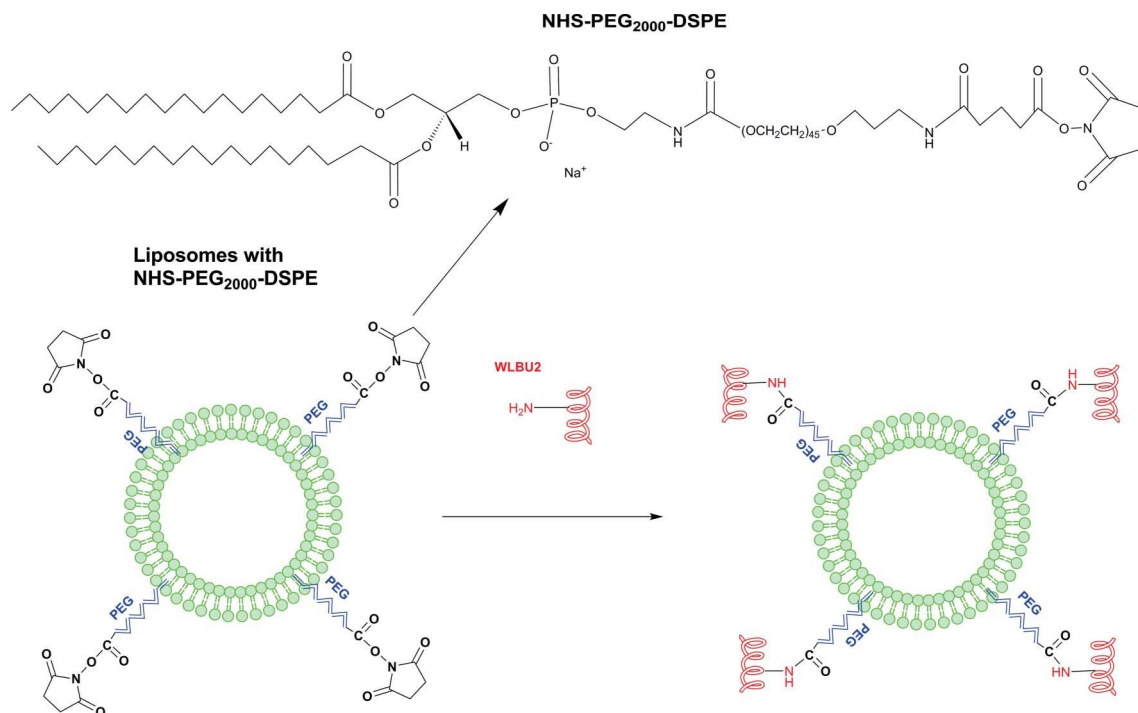
NHS-PEG₂₀₀₀-DSPE

Fig. 1 Scheme of the conjugation of WLBU2 with liposomes incorporating NHS-PEG$_{2000}$-DSPE, including the structure of NHS-PEG$_{2000}$-DSPE.

comparison. This formulation was developed by biolitec AG and was composed of DPPC, 1,2-dipalmitoyl-*sn-glycero*-3-[phospho-*rac*-(1-glycerol)] (DPPG) and Temoporfin (1.5 mg ml⁻¹).

Characterization of liposomes

The conjugation of WLBU2 with the NHS-PEG$_{2000}$-DSPE in the liposomes was confirmed using sodium dodecyl sulfate polyacrylamide gel electrophoresis (SDS-PAGE). Briefly, an aliquot of 10 µL purified WLBU2-liposomes was mixed with equal amount of reducing sample buffer, and applied to a 10–20% precast polyacrylamide gel (Bio-Rad, California, USA). The gel bands were stained by Coomassie blue.

The mean vesicle diameter, polydispersity index and zeta potential of liposomes were measured using photon correlation spectroscopy (PCS) on a Zetasizer Nano ZS (Malvern, Herrenberg, Germany). The liposomes were diluted to a proper concentration using PBS, and the analysis was performed at an angle of 173° and a temperature of 25 °C. Each sample was measured in triplicate.

Bacteria culture

The bacterial cells were grown aerobically overnight at 37 °C in Tryptic Soy Broth (Merck KGaA, Darmstadt, Germany). Cells were harvested by centrifugation and suspended in sterile PBS. The final OD$_{600}$ (optical density at 600 nm, 1 cm) of the bacterial suspensions was adjusted to 0.45 or 0.15, respectively.

Study of the delivery of temoporfin using fluorescence microscope and flow cytometry

Temoporfin-loaded liposomes were incubated with *S. aureus* DSM11729 or *P. aeruginosa* DSM1117 (OD$_{600}$ = 0.45) at 0 °C

for 1h. The ratio of phospholipids to bacteria was based on the *in vitro* PACT test. After 1 h incubation, the bacteria were washed in triplicate with PBS and finally suspended in PBS. For fluorescence microscopy, the bacteria were transferred into 2.5% glutaraldehyde (in 0.17 mM Tris buffer, pH = 7.4). After 1 h fixation, the suspension was spread on a glass slide and observed using a Leica DM-RXP fluorescence microscope (Leica, Wetzlar, Germany). For flow cytometry, the bacteria suspension in PBS was diluted to a proper concentration and submitted to an Epics XL.MCL flow cytometry (Beckman Coulter Inc., Miami, FL, USA). The fluorescence of temoporfin on bacteria was detected using filter 4 (detected range of wavelengths: 660–700 nm).

In vitro experiments on PACT

Both *S. aureus* DSM11729 and *P. aeruginosa* DSM1117 were studied in the *in vitro* PDI test. Briefly, 10 µL temoporfin-loaded liposomes (250 µM or 25 µM temoporfin in liposomes) was incubated with 190 µL bacteria suspension (OD$_{600}$ = 0.15) in sterile black well plates with clear bottoms (Costar 3603, Corning Inc., USA) at RT in the dark. 1 µL free temoporfin in ethanol was mixed with bacteria in the same condition for comparison. After 90 min or 180 min incubation, the bacteria suspension was illuminated using a 652 nm laser (1 W cm⁻², 100 s, 100 J cm⁻²). After this procedure, the bacteria suspension was inoculated on an agar plate using a jet spiral plater (Eddy Jet, IUL Instruments GmbH, Königswinter, Germany). After overnight culture the colonies on the plate were counted using an automatic colony counter (Countermat Flash, IUL Instruments GmbH, Königswinter, Germany). Both the incubation with bacteria and the counting of bacteria on each plate were repeated in triplicate. The bacteria without laser illumination were also counted to examine the dark

Table 1 The diameter, polydispersity index and zeta potential of liposomes ($n = 3$)

Liposomes	Diameter (nm)	Polydispersity index	Zeta potential (mV)
NHS-liposomes[a]	102.7 ± 1.5	0.128 ± 0.037	1.44 ± 0.45
WLBU2-liposomes	136.6 ± 1.6	0.213 ± 0.024	-1.71 ± 1.67
PEG-liposomes	114.6 ± 0.6	0.147 ± 0.004	7.69 ± 0.95
Foslip®	117.5 ± 1.2	0.105 ± 0.010	-48.2 ± 9.00

[a] Liposomes containing NHS-PEG$_{2000}$-DSPE before conjugation with WLBU2.

toxicity of free temoporfin and temoporfin-loaded liposomes, defined as the intrinsic toxicity of the compounds in the absence of light.

Results

Characterization of liposomes

Table 1 lists the diameter and polydispersity index of the liposomes. After extrusion through the polycarbonate membrane (pore size 100 nm), the average diameter of NHS-liposomes was well controlled around 100 nm with a narrow distribution, being comparable with the size of Foslip®. After conjugation with WLBU2, the average diameter of liposomes increased to 136.6 nm with a higher polydispersity index. Meanwhile, the zeta potential changed from almost neutral before conjugation to a little negative afterwards, while Foslip® was very negatively charged.

Previous experiments demonstrated that the phospholipids could not be detected on this SDS-PAGE gel, but WLBU2 could be detected quite well. As shown in Fig. 2, the pure WLBU2 was detected at around 14 kDa, which is four fold the molecular weight of a single WLBU2 (Molecular weight: 3.5 kDa), implying that the detected WLBU2 is a tetramer. In the WLBU2-liposomes a band above the pure WLBU2 band was detected, which was identified to be the WLBU2 conjugate with NHS-PEG$_{2000}$-DSPE, i.e. WLBU2-PEG$_{2000}$-DSPE. The molecular weight difference of about 3~6 kDa between these two bands indicates that one or two NHS-PEG$_{2000}$-DSPE (molecular weight: 3.0 kDa) were conjugated with a tetramer of WLBU2.

Fig. 2 Detection of the conjugation of WLBU2 with NHS-PEG$_{2000}$-DSPE in WLBU2-liposomes using SDS-PAGE.

Fluorescence microscopy

The bacteria and bacteria aggregates could be observed easily using the fluorescence microscope (Fig. 3). When the bacteria were illuminated by green light, red fluorescence of temoporfin was observed around the bacteria, implying that temoporfin was
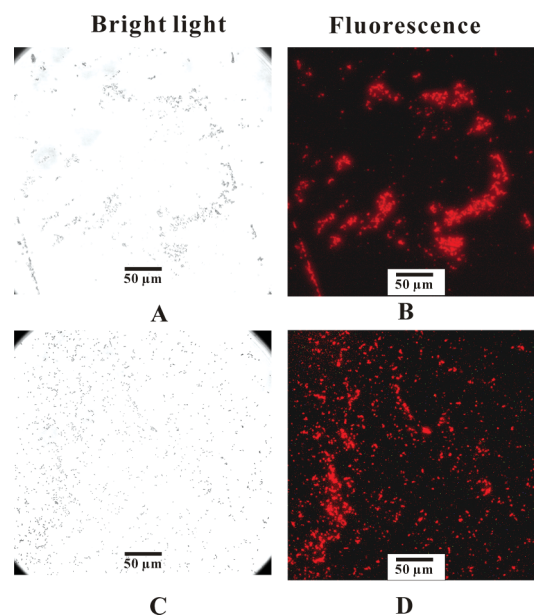
Fig. 3 Fluorescence microscopic pictures of *S. aureus* DSM11729 (A and B) and *P. aeruginosa* DSM1117 (C and D) after incubation with WLBU2-liposomes.

successfully delivered to both kinds of bacteria *via* the modified liposomes.

Flow cytometry

Flow cytometry was used to compare the delivery efficiency of temoporfin from different liposomes to bacteria and the results were shown in Fig. 4 and Fig. 5. The x-axis indicates fluorescence intensity of the bacteria and the number besides each peak is the mean fluorescence intensity (MFI). The higher the MFI, the more temoporfin was delivered to bacteria. The delivery of temoporfin to bacteria includes two aspects: part of temoporfin was released from liposomes and transferred into bacteria, while part of temoporfin was still contained in liposomes being bound to bacteria. Both populations of temoporfin could be detected when the bacteria were injected into flow cytometry. As control, temoporfin-loaded liposomes alone were submitted to flow cytometry. These liposomes could not be detected in the used configuration of the device, in accordance with the literature stating that liposomes smaller than 200 nm cannot be detected by this device.[37]

The MFI of *S. aureus* incubated with WLBU2-liposomes was about two times larger than that of *S. aureus* incubated with Foslip® (Fig. 4), indicating that WLBU2-liposomes delivered twice more temoporfin to *S. aureus* than Foslip®. Similarly,
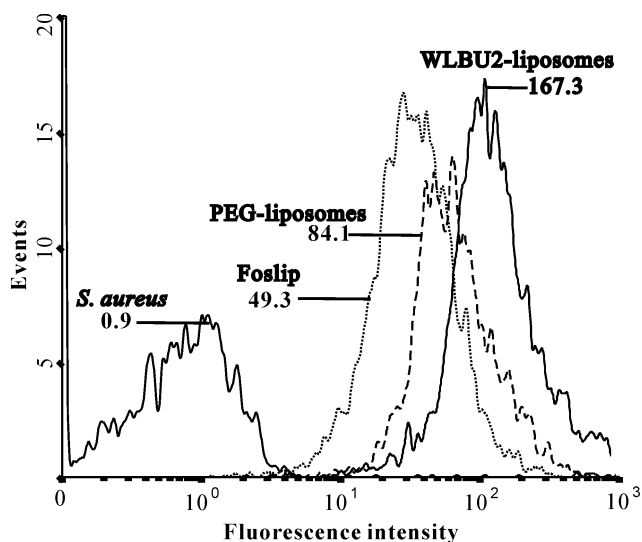
Fig. 4 Temoporfin-loaded liposomes were incubated with *S. aureus* DSM11729 and then the fluorescence caused by the temoporfin delivered to bacteria was analyzed using flow cytometry. The value of each peak represents mean fluorescence intensity.
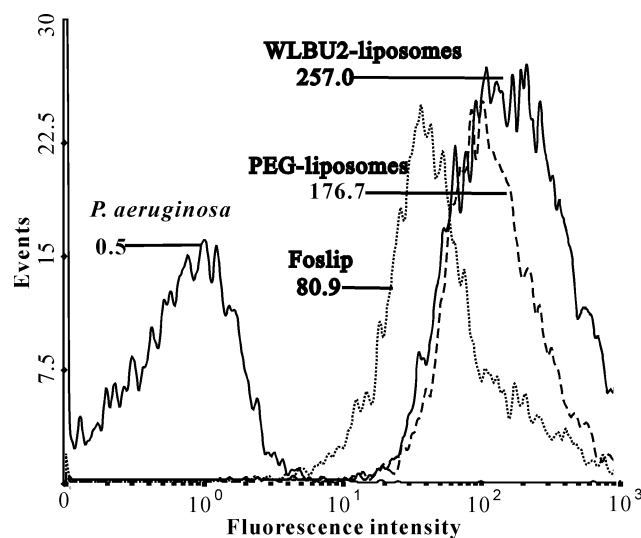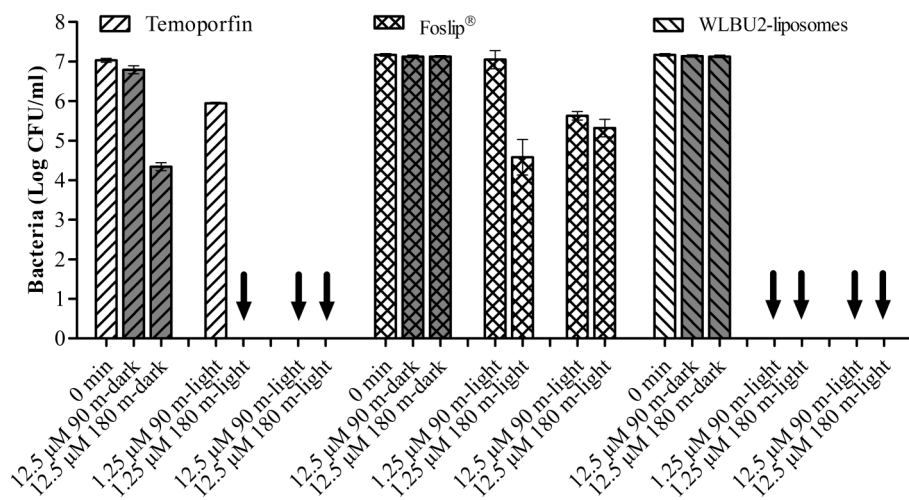
Fig. 5 Temoporfin-loaded liposomes were incubated with *P. aeruginosa* DSM1117 and then the fluorescence caused by the temoporfin delivered to bacteria was analyzed using flow cytometry. The value of each peak represents mean fluorescence intensity.

WLBU2-liposomes delivered approximately the double amount of temoporfin than PEG-liposomes did. Although the MFI of *S. aureus* incubated with Foslip® was smaller than for the other two liposomal formulations, it was still higher than for the untreated bacteria, implying that Foslip® could also deliver some temoporfin to bacteria.

Fig. 5 shows the MFIs of *P. aeruginosa* incubated with all three kinds of liposomes. The order of temoporfin delivery efficiency among these three formulations was the same as the order for *S. aureus*, *i.e.* the WLBU2-liposomes delivered more temoporfin than the unmodified liposomes. Additionally, for each kind of liposomes, the MFIs of *P. aeruginosa* after incubation were higher than those of *S. aureus*, suggesting that the amount of temoporfin delivered to each *P. aeruginosa was more* than to each *S. aureus*.

In vitro experiments on PACT

Fig. 6 shows the $\log_{10}$ unit reduction in the viable count of *S. aureus* when incubated with different temoporfin formulations. Without exposure to light, free temoporfin (dissolved in ethanol) induced a $2.69 \log_{10}$ reduction of bacteria after 180 min incubation, while both Foslip® and WLBU2-liposomes showed no dark toxicity against *S. aureus* (gray bars in Fig. 6), suggesting that the dark toxicity of temoporfin was reduced after incorporation into liposomes, in line with the dark toxicity test on cells where incorporation into liposomes reduced the dark toxicity of temoporfin significantly compared to free temoporfin in solution.[38,39] After laser illumination, free temoporfin was very phototoxic, eradicating all *S. aureus* at 1.25 μM (180 min) and at 12.5 μM (90 and 180 min); Foslip® killed *S. aureus* the least efficiently, achieving its maximal reduction of $2.6 \log_{10}$ at 1.25 μM (180 min);

Fig. 6 Dark toxicity and PACT efficiency of free temoporfin or temoporfin-loaded liposomes on *S. aureus* DSM11729 after incubation at RT for 90 min or 180 min, respectively. The arrows indicate that the bacteria were completely eradicated, and the bars representing dark toxicity results are shaded gray ($n \geq 3$).
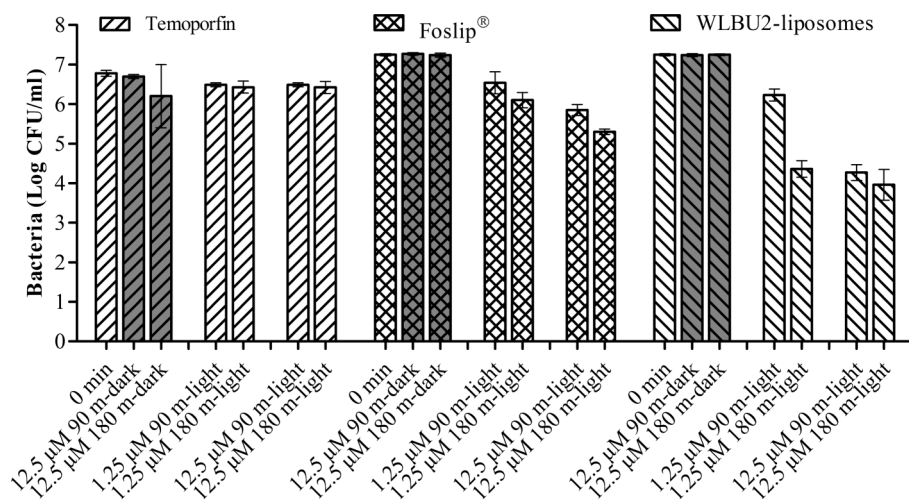
Fig. 7 Dark toxicity and PACT efficiency of free temoporfin or temoporfin-loaded liposomes on *P. aeruginosa* DSM1117 after incubation at RT for 90 min or 180 min, respectively. The bars representing dark toxicity results are shaded gray ($n \geq 3$).

Temoporfin in the WLBU2-liposomes were most efficiently in killing *S. aureus*, removing all *S. aureus* at both concentrations and both time points.

In the tests with *P. aeruginosa* (Fig. 7), neither free temoporfin nor liposomal formulations showed any obvious toxicity after either 90 min or 180 min incubation without laser illumination, implying the temoporfin alone and liposomes constitutes did not cause any bacterial toxicity to *P. aeruginosa*. After exposure to light, free temoporfin only induced maximal 0.36 $\log_{10}$ reduction of *P. aeruginosa*, much less effective than liposomal formulations. WLBU2-liposomes were most effective in killing *P. aeruginosa*, achieving a 3 $\log_{10}$ reduction after 90 min incubation (12.5 µM) and reaching the maximal killing of 3.3 $\log_{10}$ after 180 min incubation, *i.e.* 99.95% of *P. aeruginosa* were killed. However, *P. aeruginosa* seemed to be more resistant to phototoxicity of liposomes than *S. aureus*, as no eradication was obtained. Amongst these three formulations, only WLUB2-liposomes showed the sufficient photoinactivation efficiency which can be considered "antimicrobial", because the use of the term "antimicrobial" requires a minimal 3 $\log_{10}$ reduction of bacteria,[40] which was achieved by the WLBU2-modified liposomes.

Discussion

Liposomes have been studied for drug delivery extensively in the last decades, and targeted delivery with liposomes has been proved to be efficient for various kinds of cells, *e.g.* antibody-modified or lectin-modified liposomes for bacteria-targeting.[41,42] However, little research was done in the preparation of bacteria-targeting liposomes by conjugating AMPs on the surface of liposomes. On the other hand, although numerous PSs and PS conjugates,[11,15,21] as well as many formulations of PSs were studied for the aim of PACT,[12–14,24,26] the targeted delivery of PSs to bacteria *via* bacteria-targeting nanoparticles has been reported rarely.[43] Therefore, we were interested in combing these two strategies, *i.e.* bacteria-targeting delivery of PSs *via* AMP-modified liposomes, aiming to develop a novel strategy to improve the efficiency of PACT.

WLBU2 is a *de novo* engineered antimicrobial peptide, composed predominantly of arginine (13 residues) and valine (8 residues), with 3 tryptophane residues in the hydrophobic face.[34] The amino groups in the 13 arginine residues can react with a novel functional phospholipid (NHS-PEG$_{2000}$-DSPE, Fig. 1) yielding WLBU2-modified liposomes. NHS-PEG$_{2000}$-DSPE is an activated phospholipid, whose succinimidyl residue can easily be replaced by the active amine groups of proteins and peptides. The conjugation *via* NHS-PEG$_{2000}$-DSPE takes place fast and effectively, and the operation is convenient without additional steps to activate neither the phospholipid nor the ligand. Therefore, NHS-PEG$_{2000}$-DSPE was employed to conjugate WLBU2 on the surface of liposomes. Attention must be paid as this NHS group hydrolyzes fast with a hydrolysis half-life of about 20 min (according to the product manual), so the hydration of lipid film and extrusion should be completed as fast as possible.

To prevent the loss of the activity of peptides after conjugation, it is important that the peptides were not over-reacted, *i.e.* to avoid conjugation with too many NHS-PEG$_{2000}$-DSPE per peptide. The SDS-PAGE result in Fig. 2 suggested that one or two NHS-PEG$_{2000}$-DSPE were linked with one WLBU2 tetramer *via* reaction with WLBU22s amino groups. The number is relatively low compared to the 13 arginine residues per peptide, so the antimicrobial activity of WLBU2 was supposed to remain, as proved in the following experiments.

It is notable that the zeta-potential of DOTAP containing liposomes in Table 1 was almost zero, while the similar formulation without mPEG$_{2000}$-DSPE possessed the zeta potential of +30.4 mV (data not shown here). On one side, the NHS-PEG$_{2000}$-DSPE is a negatively charged phospholipid due to DSPE segment, which reduces the zeta potential of liposomes. On the other side, the PEG segment of NHS-PEG$_{2000}$-DSPE forms a hydrated coronal around the phospholipid bilayer, and hence shields the positive charge of the bilayer containing DOTAP. As a result, the zeta potential of the whole liposome was reduced in our measurements from +30.4 mV to almost zero but the bilayer is still positively charged. This specific imparity of charge is essential for preparing WLBU2-modified liposomes. The positively charged bilayer prevents the bilayer from damage by WLBU2 through electrostatic repulsion.

This journal is © The Royal Society of Chemistry and Owner Societies 2011

By contrast, the neutral or negative liposomal bilayer is similar to cell membrane and thus is vulnerable to the membrane penetrating AMP. Moreover, the neutrally charged liposomes are supposed to display little binding to the negatively charged components and surfaces in the physiological environment, which is a big problem for most of cationic formulations when applied *in vivo*. Therefore, our WLBU2-liposomes are ideal for WLBU2 modification and *in vivo* application.

After preparation of WLBU2-liposomes, it was important to check if the delivery of temoporfin to bacteria was increased by WLBU2-liposomes. Theoretically, liposomal temoporfin could be delivered to bacteria *via* three ways. The first pathway is characterized through the binding of liposomes to bacteria, followed by transferring temoporfin from the lipid bilayer into the bacterial cell wall. The second pathway implies fusion of liposomes with the bacterial cell wall, which was confirmed using TEM in the literature.[44,45] The lipid bilayer will fuse with the cell wall and temoporfin is subsequently released *via* lipophilic membraneous pathways directly into bacteria. The third pathway can be described by diffusion *via* water when liposomes are not directly bound to the surface of bacteria. This scenario would imply that temoporfin is released from liposomes into water, followed by diffusion into the cell wall. Since the solubility of temoporfin in water is extremely low, the third pathway can be ignored for short time periods,[46] while the first two pathways are more probable, either alone or in combination.

The fluorescence microscopy using temoporfin as the fluorescence molecule clearly demonstrated that temoporfin was indeed delivered to bacteria, (Fig. 3), while the flow cytometry measurements (Fig. 4 and Fig. 5) reflected how much temoporfin was detected in or around bacteria, and was used to compare the delivery efficiency of temoporfin. In both used bacterial species, the order of delivery efficiency was WLBU2-liposomes > PEG-liposomes > Foslip®. This order supports two hypotheses: the neutral liposomes delivered temoporfin to bacteria more efficiently than negatively charged liposomes, and the surface modification with WLBU2 further increased the delivery efficiency compared to the unmodified liposomes.

Firstly, some liposomal formulations have been reported to be able to fuse with bacteria,[44,45,47] and Fig. 4 and Fig. 5 also showed that Foslip® and PEG-liposomes delivered temoporfin to *S. aureus* and *P. aeruginosa*, which was most likely due to fusion of liposomes with cell walls. Considering that most bacteria have a negatively charged cell wall,[48] the negatively charged Foslip® did not fuse as easily with bacteria as neutral PEG-liposomes and WLBU2-liposomes did, due to the electrostatic repulsion between Foslip® and bacteria. Particularly, the lipid bilayers of PEG-liposomes and WLBU2-liposomes were positively charged in spite of the neutral charge of the whole liposomes. Therefore, the lipid bilayers of these two formulations were more likely to fuse with bacteria through electrostatic interaction, resulting in higher delivery efficiency of temoporfin to bacteria.

Secondly, WLBU2 was reported to be the most bactericidal AMP in the series of LBU and WLBU derivatives, because the residues of WLBU2 were arranged to form an idealized alpha-helical and amphipathic structure, with optimal charge and hydrophobic densities.[34,35] The highly amphipathic and alpha-helical WLBU2 favors strong initial interactions between

the peptide and the highly electronegative components of cell walls, *e.g.* LPS in *P. aeruginosa*. Therefore, the WLBU2 units which were coupled to the surface of liposomes facilitated the binding of liposomes with *S. aureus* and *P. aeruginosa*, and hence enhanced the delivery of temoporfin. In light of these advantages we concluded that WLBU2-liposomes were efficient in temoporfin delivery due to its enhanced binding and fusion potential with bacteria.

In line with the enhanced temoporfin delivery by WLBU2-liposomes, the *in vitro* PACT test proved that WLBU2-liposomes increased the phototoxicity towards both MRSA and *P. aeruginosa*, demonstrated by the eradication of MRSA and the effective PACT against *P. aeruginosa* (Fig. 6 and Fig. 7). In the case of MRSA, WLBU2-liposomes significantly killed more bacteria than the other two formulations at 1.25 μM after 90 min incubation ($p < 0.05$). Although free temoporfin in ethanol also induced a 7 $\log_{10}$ reduction at the higher concentration, considering that temoporfin in ethanol exhibited a 3 $\log_{10}$ dark toxicity to MRSA, the PACT efficiency of WLBU2-liposomes was still higher than free temoporfin. The high PACT efficiency of WLBU2-liposomes could be attributed to the enhanced delivery of temoporfin discussed in the last two paragraphs, as well as the enhanced penetration of temoporfin into cell walls due to the synergistic effect of WLBU2 and DOTAP. Both WLBU2 and DOTAP have the function to disturb the bacterial cell wall and increase its porosity, increasing the penetration of PSs through the cell wall.[13,14] Subsequently, more temoporfin was delivered to the inner cytoplasmic membrane, leading to increased antibacterial phototoxicity.

Recently, Vince *et al.* conjugated a MRSA-specific peptide to a porphyrin PS which induced a 66% reduction in MRSA growth.[11] Bourre *et al.* used an porphyrin conjugate with cell-penetrating peptides to achieve a 6.6 $\log_{10}$ reduction of normal *S. aureus*.[15] Compared to those peptide-PS conjugates, the WLBU2-modified liposomes were more efficient at utilizing peptides for the delivery of PSs to bacteria, as a few peptides on the surface of liposomes could direct all the PSs in the liposomes to bacteria, while liposomes also enhanced the delivery of PSs to bacteria by fusion, resulting in effective reduction of bacteria, *i.e.* 7 $\log_{10}$ reduction of MRSA.

Compared to *S. aureus*, *P. aeruginosa* is obviously more resistant to PACT. Only WLBU2-liposomes achieved the aim of PACT, *i.e.* killing more than 3 $\log_{10}$ bacteria, while the other two formulations could not achieve sufficient antimicrobial effect (less than 3 $\log_{10}$ reduction). This difference of susceptibility between gram-positive and gram-negative bacteria was already extensively discussed in the literature.[5,6,15,43] The major reason is the complicated structure of the gram-negative bacterial cell wall, *i.e.* the outer membrane composed of LPSs, which forms a physical and functional barrier between the cell and its environment. The free temoporfin induced little PACT effect, because it is difficult for free temoporfin to diffuse through the dense outer membrane. Foslip® killed more *P. aeruginosa* than free temoporfin, as it was reported that liposomes composed of DPPC and DMPG (dimyristoylphosphatidylglycerol) appeared to be effective in disrupting the bacteria membrane, resulting in accumulation of the active substance in the inner membrane.[44] The Foslip® is composed of DPPC and DPPG, and could have the similar effect. WLBU2-liposomes were most efficacious, since both WLBU2 and DOTAP could disturb

the bacteria membrane and hence facilitated the penetration of temoporfin into bacteria, producing a higher reduction of bacteria.

Although WLBU2-modified liposomes were proved to be effective in the improvement of the PACT efficiency of temoporfin against *P. aeruginosa*, no complete eradication was obtained. To kill gram-negative bacteria more efficiently, cationic PSs, instead of the neutral temoporfin, may be incorporated into the WLBU2-modified liposomes, as most of the effective PACT against gram-negative bacteria were achieved by cationic PSs, *e.g.* the cationic *meso*-substituted porphyrins,[49] the chlorin(e6) conjugated with poly-L-lysine,[50] methylene blue and toluidine blue.[51] It is generally accepted that cationic PSs are more effective than neutral or anionic PSs, since cationic PSs bind strongly to the negatively charged cell wall and thereby increase the local concentration of the PSs in the bacteria.[5] According to our results, the WLBU2-modified liposome can also be a potential carrier for increasing the PACT efficiency of these cationic PSs and reducing their cytotoxicity for skin cells, such as the highly positively charged and phototoxic *meso*-substituted porphyrins.[49] In addition, a stepwise approach was proposed to overcome this resistance of gram-negative bacteria to PACT.[5] After a short time incubation with PSs, PSs bind to the outer wall. When the bacteria are illuminated, the outer membrane is damaged, leading to increased permeability of the outer membrane. After a second incubation, more PSs will be transferred into the inner membrane or even into the core of bacteria, thereby causing stronger damage to bacteria after the second illumination.

Last but not least, the possible damage of WLBU2-liposomes to host tissues should be taken into account for the potential clinical application. Firstly, the used concentration of temoporfin and the incubation time are two important parameters for controlling the side effects. For *S. aureus*, eradication was achieved at 1.25 μM temoporfin after 90 min incubation (Fig. 6), so both of the two parameters can be further decreased; as to *P. aeruginosa*, there was no significant difference ($p > 0.05$) among the last three columns for WLBU2-liposomes in Fig. 7, *i.e.* 1.25 μM/180 min, 12.5 μM/90 min and 12.5 μM/180 min, implying that the protocol might be optimized by varying the temoporfin concentration and reducing the incubation time, so as to reduce the possible damage to host tissue while remaining sufficient antimicrobial effect. Secondly, the light dosimetry should be designed properly, *e.g.* by adjusting the fluence and illumination time,[24,28] in order to achieve maximal antimicrobial effect while decreasing the damage to deep tissues.

Conclusion

In this study, we have combined the advantages of PACT, AMPs and bacteria-targeting liposomes by virtue of WLBU2-modified liposomes. These results demonstrate that WLBU2-modified liposomes are a promising formulation for bacteria targeted delivery of temoporfin and for improving the PACT efficiency on both gram-positive and gram-negative bacteria. In future, the WLBU2-modified liposomes may also be used to incorporate other kinds of potent PSs, to improve their PACT efficiency. Using PSs incorporated into WLBU2-modified liposomes will be an attractive perspective for the PACT in localized microbial infections, especially for combating antibiotic-resistant bacteria.

Notes and references

1 B. A. Cunha, *Drugs Today*, 1998, **34**, 691–698.
2 B. D. Cookson, *J. Antimicrob. Chemother.*, 1998, **41**, 11–18.
3 D. M. Sievert, J. T. Rudrik, J. B. Patel, L. C. McDonald, M. J. Wilkins and J. C. Hageman, *Clin. Infect. Dis.*, 2008, **46**, 668–674.
4 K. K. Kumarasamy, M. A. Toleman, T. R. Walsh, J. Bagaria, F. Butt, R. Balakrishnan, U. Chaudhary, M. Doumith, C. G. Giske, S. Irfan, P. Krishnan, A. V. Kumar, S. Maharjan, S. Mushtaq, T. Noorie, D. L. Paterson, A. Pearson, C. Perry, R. Pike, B. Rao, U. Ray, J. B. Sarma, M. Sharma, E. Sheridan, M. A. Thirunarayan, J. Turton, S. Upadhyay, M. Warner, W. Welfare, D. M. Livermore and N. Woodford, *Lancet Infect. Dis.*, 2010, **10**, 597–602.
5 G. Jori, C. Fabris, M. Soncin, S. Ferro, O. Coppellotti, D. Dei, L. Fantetti, G. Chiti and G. Roncucci, *Lasers Surg. Med.*, 2006, **38**, 468–481.
6 G. Jori, *J. Environ. Pathol. Toxicol. Oncol.*, 2006, **25**, 505–519.
7 R. W. Redmond and J. N. Gamlin, *Photochem. Photobiol.*, 1999, **70**, 391–475.
8 J. G. Christie and U. B. Kompella, *Drug Discovery Today*, 2008, **13**, 124–134.
9 M. R. Hamblin and T. Hasan, *Photochem. Photobiol. Sci.*, 2004, **3**, 436–450.
10 M. Wainwright, *J. Antimicrob. Chemother.*, 1998, **42**, 13–28.
11 R. V. Vince, L. A. Madden, C. M. Alonso, H. Savoie, R. W. Boyle, M. Todman, T. Paget and J. Greenman, *Photochem. Photobiol. Sci.*, 2011, **10**, 515–522.
12 T. Tsai, Y. T. Yang, T. H. Wang, H. F. Chien and C. T. Chen, *Lasers Surg. Med.*, 2009, **41**, 316–322.
13 S. Ferro, F. Ricchelli, G. Mancini, G. Tognon and G. Jori, *J. Photochem. Photobiol., B*, 2006, **83**, 98–104.
14 S. Ferro, F. Ricchelli, D. Monti, G. Mancini and G. Jori, *Int. J. Biochem. Cell Biol.*, 2007, **39**, 1026–1034.
15 L. Bourre, F. Giuntini, I. M. Eggleston, C. A. Mosse, A. J. Macrobert and M. Wilson, *Photochem. Photobiol. Sci.*, 2010, **9**, 1613–1620.
16 F. M. Lauro, P. Pretto, L. Covolo, G. Jori and G. Bertoloni, *Photochem. Photobiol. Sci.*, 2002, **1**, 468–470.
17 B. Zeina, J. Greenman, D. Corry and W. M. Purcell, *Br. J. Dermatol.*, 2003, **148**, 229–232.
18 C. M. Cassidy, M. M. Tunney, P. A. McCarron and R. F. Donnelly, *J. Photochem. Photobiol., B*, 2009, **95**, 71–80.
19 P. S. Zolfaghari, S. Packer, M. Singer, S. P. Nair, J. Bennett, C. Street and M. Wilson, *BMC Microbiol.*, 2009, **9**, 27.
20 G. Omar, M. Wilson and S. Nair, *BMC Microbiol.*, 2008, **8**, 111.
21 F. Gad, T. Zahra, K. P. Francis, T. Hasan and M. R. Hamblin, *Photochem. Photobiol. Sci.*, 2004, **3**, 451–458.
22 S. L. Pinheiro, J. M. Donega, L. M. Seabra, M. D. Adabo, T. Lopes, T. H. do Carmo, M. C. Ribeiro and P. F. Bertolini, *Lasers Med. Sci.*, 2009, **25**, 87–91.
23 Photopharmica, Photopharmica targets infected wounds with its photodynamic therapy, http://www.photopharmica.com/news/01_07_07b.htm, accessed on July 2007.
24 C. Horfelt, B. Stenquist, O. Larko, J. Faergemann and A. M. Wennberg, *Acta Derm.-Venereol.*, 2007, **87**, 325–329.
25 H. B. Ris, H. J. Altermatt, R. Inderbitzi, R. Hess, B. Nachbur, J. C. Stewart, Q. Wang, C. K. Lim, R. Bonnett, M. C. Berenbaum and *et al.*, *Br. J. Cancer*, 1991, **64**, 1116–1120.
26 C. Bombelli, F. Bordi, S. Ferro, L. Giansanti, G. Jori, G. Mancini, C. Mazzuca, D. Monti, F. Ricchelli, S. Sennato and M. Venanzi, *Mol. Pharmaceutics*, 2008, **5**, 672–679.
27 A. Kubin, F. Wierrani, R. H. Jindra, H. G. Loew, W. Grunberger, R. Ebermann and G. Alth, *Drugs Exp. Clin. Res.*, 1999, **25**, 13–21.
28 V. Engelhardt, B. Krammer and K. Plaetzer, *Photochem. Photobiol. Sci.*, 2010, **9**, 365–369.
29 M. Chen, X. Liu and A. Fahr, *Int. J. Pharm.*, 2011, **408**, 223–234.
30 J. Kuntsche, I. Freisleben, F. Steiniger and A. Fahr, *Eur. J. Pharm. Sci.*, 2010, **40**, 305–315.

This journal is © The Royal Society of Chemistry and Owner Societies 2011

31 A. M. Garcia, E. Alarcon, M. Munoz, J. C. Scaiano, A. M. Edwards and E. Lissi, *Photochem. Photobiol. Sci.*, 2011, **10**, 507–514.

32 O. E. Sorensen, N. Borregaard and A. M. Cole, *Contrib. Microbiol.*, 2008, **15**, 61–77.

33 S. Rotem and A. Mor, *Biochim. Biophys. Acta, Biomembr.*, 2009, **1788**, 1582–1592.

34 B. Deslouches, S. M. Phadke, V. Lazarevic, M. Cascio, K. Islam, R. C. Montelaro and T. A. Mietzner, *Antimicrob. Agents Chemother.*, 2004, **49**, 316–322.

35 B. Deslouches, K. Islam, J. K. Craigo, S. M. Paranjape, R. C. Montelaro and T. A. Mietzner, *Antimicrob. Agents Chemother.*, 2005, **49**, 3208–3216.

36 M. C. Skinner, A. O. Kiselev, C. E. Isaacs, T. A. Mietzner, R. C. Montelaro and M. F. Lampe, *Antimicrob. Agents Chemother.*, 2009, **54**, 627–636.

37 S. Petersen, A. Fahr and H. Bunjes, *Mol. Pharmaceutics*, 2010, **7**, 350–363.

38 T. Kiesslich, J. Berlanda, K. Plaetzer, B. Krammer and F. Berr, *Photochem. Photobiol. Sci.*, 2007, **6**, 619–627.

39 J. Berlanda, T. Kiesslich, V. Engelhardt, B. Krammer and K. Plaetzer, *J. Photochem. Photobiol., B*, 2010, **100**, 173–180.

40 NCCLS, National Committee for Clinical Laboratory Standards, Villanova, Pennsylvania: NCCLS, 1992.

41 M. Kaszuba, I. G. Lyle and M. N. Jones, *Colloids Surf., B*, 1995, **4**, 151–158.

42 A. M. Robinson, J. E. Creeth and M. N. Jones, *Biochim. Biophys. Acta, Biomembr.*, 1998, **1369**, 278–286.

43 S. Perni, P. Prokopovich, J. Pratten, I. P. Parkin and M. Wilson, *Photochem. Photobiol. Sci.*, 2011, **10**, 712–720.

44 Y. Jia, H. Joly and A. Omri, *J. Liposome Res.*, 2010, **20**, 134–146.

45 B. Pudziuvyte, E. Bakiene, R. Bonnett, P. A. Shatunov, M. Magaraggia and G. Jori, *Photochem. Photobiol. Sci.*, 2011, **10**, 1046–1055.

46 H. Hefesha, S. Loew, X. Liu, S. May and A. Fahr, *J. Control. Release*, 2010, **150**, 279–286.

47 C. Mugabe, M. Halwani, A. O. Azghani, R. M. Lafrenie and A. Omri, *Antimicrob. Agents Chemother.*, 2006, **50**, 2016–2022.

48 N. M. Sanderson, B. Guo, A. E. Jacob, P. S. Handley, J. G. Cunniffe and M. N. Jones, *Biochim. Biophys. Acta, Biomembr.*, 1996, **1283**, 207–214.

49 E. Alves, L. Costa, C. M. Carvalho, J. P. Tome, M. A. Faustino, M. G. Neves, A. C. Tome, J. A. Cavaleiro, A. Cunha and A. Almeida, *BMC Microbiol.*, 2009, **9**, 70.

50 M. R. Hamblin, D. A. O'Donnell, N. Murthy, K. Rajagopalan, N. Michaud, M. E. Sherwood and T. Hasan, *J. Antimicrob. Chemother.*, 2002, **49**, 941–951.

51 M. N. Usacheva, M. C. Teichert and M. A. Biel, *Lasers Surg. Med.*, 2001, **29**, 165–173.

3.2 Wheat germ agglutinin modified liposomes for the photodynamic inactivation of bacteria

Kewei Yang, Burkhard Gitter, Ronny Rüger, Volker Albrecht, Gerhard D. Wieland, Alfred Fahr

The built PDF after submission was shown in the dissertation: 40~76 (37 pages)

Photochemistry and Photobiology
The official journal of the American Society of Photobiology

Wheat germ agglutinin modified liposomes for the photodynamic inactivation of bacteria

SCHOLARONE™
Manuscripts

1   **Wheat germ agglutinin modified liposomes for the**
2   **photodynamic inactivation of bacteria**

3   Kewei Yang[1], Burkhard Gitter[2], Ronny Rüger[1], Volker Albrecht[2], Gerhard D.

4   Wieland[2], Alfred Fahr[*1]

5

6

7   [1]Department of Pharmaceutical Technology, Friedrich-Schiller-University Jena, Jena,

8   Germany

9   [2] biolitec AG, Jena, Germany

10   *Corresponding author e-mail: Alfred.fahr@uni-jena.de (Alfred Fahr)

11

12 **ABSTRACT**

13 Photodynamic inactivation (PDI) of bacteria is a promising approach for combating the

14 increasing emergence of antibiotic resistance in pathogenic bacteria. To further improve

15 the PDI efficiency on bacteria, a bacteria-targeting liposomal formulation was

16 investigated. A generation II photosensitizer (temoporfin) was incorporated into

17 liposomes, followed by conjugation with a specific lectin (wheat germ agglutinin, WGA)

18 on the   liposomal surface. WGA was successfully coupled to temoporfin-loaded

19 liposomes using an activated phospholipid containing N-hydroxylsuccinimide residue.

20 Methicillin-resistant *Staphylococcus aureus* (MRSA) and *Pseudomonas aeruginosa*

21 strains were selected to evaluate the WGA modified liposomes in terms of bacteria

22 targeted delivery and *in vitro* PDI test. Fluorescence microscopy revealed that temoporfin

23 was delivered to both kinds of bacteria, while flow cytometry demonstrated that WGA

24 modified liposomes delivered more temoporfin to bacteria compared to non-modified

25 liposomes. Consequently, the WGA modified liposomes eradicated all MRSA and

26 significantly enhanced the PDI of *Pseudomonas aeruginosa*. In conclusion, the WGA

27 modified liposomes are a promising formulation for bacteria targeted delivery of

28 temoporfin and for improving the PDI efficiency of temoporfin on both gram-positive

29 and gram-negative bacterial cells.

30

31

32   **INTRODUCTION**

33   The increasing emergence of antibiotic resistance in pathogenic bacteria poses a major

34   challenge to healthcare. For example, methicillin-resistant *Staphylococcus aureus*

35   (MRSA), which has developed resistance to beta-lactam antibiotics, has spread

36   throughout the world, causing many untreatable hospital-acquired infections (1).

37   Especially, the recently isolated *Escherichia coli* and *Klebsiella pneumoniae* carrying

38   New Delhi metallo-beta-lactamases (NDM-1), showed high resistance to the powerful

39   "last line antibiotics" used for the most resistant strains (2). Therefore, there is an urgent

40   necessity to find alternative antimicrobial therapies. One of the most promising strategies

41   is photodynamic therapy (PDT).

42   PDT involves the use of a photosensitizer (PS), oxygen and light, mostly delivered by

43   lasers. The PSs are triggered by light from the singlet state in ground energy level to an

44   activated state, which transfers energy to the surrounding oxygen, resulting in reactive

45   oxygen species (ROS), *e.g.* the singlet oxygen. Those ROSs are highly reactive and can

46   oxidize proteins, nucleic acids and lipids, leading to cytotoxicity (3). PDT has been

47   approved for the treatment of certain kinds of tumors and age-related macular

48   degeneration (4-6). In addition, PDT has attracted a lot of attention in the last decades as

49   a promising modality to treat microbial infections, particularly those caused by antibiotic-

50   resistant species, since PDT is found to be effective in the **p**hoto**d**ynamic **i**nactivation

51   (PDI) of bacteria and fungi (7-10). This antimicrobial PDI is endowed with several

52   advantages over the traditional antibiotics therapy. Firstly, the antimicrobial PDI

53   possesses a broad spectrum of actions, and varieties of antibiotic-resistant strains have

54   been reported to be efficiently inactivated (7, 11, 12), because ROSs are toxic to almost

55 all bacteria. Secondly, it is hypothesized that bacteria will not easily develop resistance

56 against ROSs and thereby PSs are lack of selection of photo-resistant microbial cells (13).

57 Thirdly, the antimicrobial PDI is more phototoxic to bacteria than to mammalian cells. It

58 has been shown that human cells (keratinocytes and fibroblasts) could survive the

59 antimicrobial PDI in certain conditions which were lethal to microorganisms, thus the

60 bacteria were selectively removed (14, 12, 15, 16). Based on these advantages, the

61 antimicrobial PDI was already utilized to combat many kinds of bacteria, mostly during

62 local microbial infections, such as skin-associated bacteria (16-18) and bacteria of

63 periodontal pockets (19). Some products were already developed based on this method

64 for the treatment of acne vulgaris (20) and infected leg ulcers (21). The available results

65 imply that the antimicrobial PDI is a very potential treatment method to combat bacterial

66 infections, in particular, the antibiotic-resistant species (11, 22).

67   By now, many of the PSs being studied for PDI of bacteria are based on the

68 tetrapyrrole nucleus, such as porphyrins, chlorins, and phthalocyanines, which are

69 lipophilic and easy to form aggregates in aqueous solution, resulting in the loss of

70 photosensitivity (12, 15, 23, 7, 24). To overcome this problem, suitable PS carriers were

71 designed to deliver PSs, *e.g.* liposomes (23, 25, 26, 11, 27), micelles (7), and

72 nanoparticles (28). Amongst these systems, liposomes are most commonly employed to

73 incorporate lipophilic PSs, and have been proved to enhance the antimicrobial PDI of

74 various PSs, not only because liposomes increase the solubility and stability of PSs, but

75 also because they can facilitate the penetration of PSs into bacteria by means of fusion

76 processes or disturbing the cell walls (29, 11, 30, 26). However, these reported liposomal

77 formulations mainly aimed to deliver PSs passively, while little research was done to

78   apply bacteria-targeting liposomes for PDI of bacteria.

79   We hypothesized that the bacteria-targeting liposomes would be a promising strategy

80   to further improve the PDI of bacteria, since liposomes have been reported to be able to

81   targetedly bind to bacteria after conjugation with certain ligands. For instance, lectin

82   modified liposomes could effectively target to candidal bio-film *in vitro* (31), or skin-

83   associated bacteria, such as *Staphylococcus epidermidis* (32); antibody modified

84   liposomes could target to *Staphylococcus oralis* bio-film (33). Therefore, we were

85   interested in combining these two strategies, *i.e.* PDI of bacteria and bacteria-targeting

86   liposomes, and intended to develop a bacteria-targeting liposomal formulation, which can

87   increase the delivery of PSs to bacteria and consequently improve the PDI efficiency on

88   bacteria. To achieve this aim, a natural lectin, wheat germ agglutinin (WGA), was

89   selected as the bacteria-targeting ligand, while a generation II PS, temoporfin, was used

90   as a model of PSs. Temoporfin was incorporated into liposomes followed by conjugation

91   of WGA at the liposomal surface. The bacteria targeted delivery of liposomal temoporfin

92   was studied using MRSA and *Pseudomonas aeruginosa* (*P. aeruginosa*) as model

93   organisms of gram-positive and gram-negative bacteria, respectively. Finally, the

94   liposomes were tested in terms of their *in vitro* PDI of both bacterial strains.

95   **MATERIALS AND METHODS**

96   **Materials**: 1,2-distearoyl-*sn*-glycero-3-phosphoethanolamine-*N*-[methoxy(polyethylene

97   glycol)-2000] (mPEG$_{2000}$-DSPE, ammonium salt) and 1,2-Dipalmitoyl-*sn*-glycero-3-

98   phosphocholin (DPPC) were purchased from Genzyme Pharmaceuticals (Cambridge,

99   MA,   USA).   1,2-Distearoyl-*sn*-glycero-3-phosphoethanolamine-*N*-[3-(*N*-

100   succinimidyloxyglutaryl)aminopropyl(polyethyleneglycol)-2000-carbamyl]   (NHS-

101   PEG$_{2000}$-DSPE) was obtained from NOF Corporation (Tokyo, Japan). *N*-[1-(2,3-

102   dioleoyloxy)propyl]-*N,N,N*-trimethylammonium methylsulfate (DOTAP, methyl sulfate

103   salt) was supplied by Boehringer Ingelheim GmbH (Ingelheim, Germany). Wheat germ

104   agglutinin was purchased from Sigma-Aldrich (Steinheim, Germany). Temoporfin, *i.e.*

105   3,3',3'',3'''-(7,8-dihydroporphyrin-5,10,15,20-tetrayl)tetraphenol   (mTHPC)   and   its

106   liposomal formulation, Foslip®, were kindly gifted by biolitec AG (Jena, Germany). The

107   pure ethanol ($\geq$ 99.9%) was purchased from Merk KGaA (Darmstadt, Germany). All

108   other chemicals were of analytical grade.

109   **Bacteria**: The microbial strains were purchased from the German Collection of

110   Microorganisms and Cell Cultures (DSMZ, Braunschweig, Germany). *Staphylococcus*

111   *aureus* DSM11729 is gram-positive and is a strain of MRSA. *Pseudomonas aeruginosa*

112   DSM1117 (*P. aeruginosa*) is a gram-negative species.

113   **Preparation of liposomes and modification with WGA**: Liposome dispersions

114   consisting of 30 mM phospholipids and containing 1.5 mg/ml temoporfin were produced

115   using the Film-Hydration-Extrusion technique (34). Briefly, DPPC, DOTAP, NHS-

116   PEG$_{2000}$-DSPE and mPEG$_{2000}$-DSPE were dissolved in chloroform with a molar ratio of

117   80:15:2:3. Temoporfin was dissolved in methanol and then mixed with the phospholipid

118   solution. The organic solvent was removed using a rotary evaporator (BÜCHI Vacobox

119   B-177, BÜCHI, Switzerland) at 55 °C. The obtained lipid/drug film was hydrated using

120   borate buffer (pH 8.0) followed by 21 times extrusion through a 100 nm polycarbonate

121   membrane within 20 min, using a LiposoFast® mini-extruder (Avestin, Ottawa, Canada).

122   The conjugation of WGA with liposomes is illustrated in Fig. 1. The liposomes were

123 incubated with WGA at a 20:1 molar ratio of NHS-PEG$_{2000}$-DSPE to WGA. After 2 h

124 incubation at room temperature (RT), the modified liposomes were separated from the

125 free WGA using a Sepharose Cl-4B column, eluted by phosphate buffered saline (PBS)

126 solution. The liposomes before and after incubation with WGA are termed as NHS-

127 liposomes and WGA-liposomes, respectively. The registered liposomal temoporfin

128 formulation, Foslip$^{®}$, was used for comparison. This formulation is composed of DPPC,

129 1,2-Dipalmitoyl-*sn*-glycero-3-[phospho-*rac*-(1-glycerol)] (DPPG) and temoporfin (1.5

130 mg/ml).

131 **Characterization of liposomes**: Sodium dodecyl sulfate polyacrylamide gel

132 electrophoresis (SDS-PAGE according to Laemmli) was employed to detect the

133 conjugation of WGA with the NHS-PEG$_{2000}$-DSPE in the liposomes (35). Briefly, 20 µL

134 purified WGA-liposomes were mixed with equal amount of non-reducing sample buffer,

135 and applied to a 8% discontinuous polyacrylamide gel. The gel bands were stained by

136 SYPRO$^{®}$ Ruby Protein Stains (Bio-Rad, California, USA) and visualized using an UV

137 Transilluminator (Intas, Göttingen, Germany). Before photographing of the gel, the

138 displayed color on screen was inverted to get a white background.

139 Mean vesicle size and zeta potential of liposomes were measured using Photon

140 correlation spectroscopy (PCS) and Laser Doppler Velocimetry, respectively, on a

141 Zetasizer Nano ZS (Malvern, Herrenberg, Germany). The liposomes were diluted to a

142 proper concentration using PBS, and the measurement was performed at an angle of 173

143 ° and a temperature of 25°C. Each sample was measured three times.

144 **Bacteria culture:** *S. aureus* DSM11729 and *P. aeruginosa* DSM1117 were cultivated

145 aerobically overnight at 37°C in Tryptic Soy Broth (Merck KGaA, Darmstadt, Germany).

146 Bacteria were harvested by centrifugation and suspended in sterile PBS. The final OD_{600}

147 (optical density at 600nm, 1cm) of the bacterial suspensions was adjusted to 0.45 or 0.15,

148 respectively.

149 **Study of the delivery of temoporfin**: *S. aureus* DSM11729 or *P. aeruginosa*

150 DSM1117 (OD_{600}=0.45) were incubated with temoporfin-loaded liposomes at 0 °C for

151 1h. The ratio of phospholipids to bacteria was based on the PDI test. After 1 h incubation,

152 the bacteria were washed three times and finally suspended in PBS. For fluorescence

153 microscopy, the bacteria were transferred into 2.5% glutaraldehyde (in 0.169 mM Tris

154 buffer, pH=7.4). After 1 h fixation, the suspension was spread on a glass slide and

155 observed using a Leica DM-RXP fluorescence microscope (Leica, Wetzlar, Germany).

156 For flow cytometry, the bacteria suspension was diluted to a proper concentration and

157 submitted to an Epics XL.MCL flow cytometer (Beckman Coulter Inc., Miami, FL,

158 USA). The fluorescence of temoporfin on bacteria was detected using filter 4 (Detected

159 range of wavelengths: 660~700 nm).

160 *In vitro* **PDI of bacteria:** Both *S. aureus* DSM11729 and *P. aeruginosa* DSM1117

161 were studied in the *in vitro* PDI tests. In brief, 190 µL bacteria suspension (OD_{600}=0.15)

162 were incubated with 10 µL temoporfin-loaded liposomes (250 µM or 25 µM temoporfin

163 in liposomes) in sterile black well plates with clear bottoms (Costar 3603, Corning Inc.,

164 USA) at RT in the dark. As control, 1 µl ethanolic temoporfin solution (2.5 mM or 250

165 µM) was added to bacteria to obtain a final temoporfin concentration of 12.5 µM or 1.25

166 µM. After 90 or 180 min incubation, the bacteria suspension was illuminated using a 652

167 nm laser (1 W/cm^2, 100s, 100 J/cm^2). Then the bacteria suspension was inoculated on an

168 agar plate using a jet spiral plater (Eddy Jet, IUL Instruments GmbH, Königswinter,

169 Germany). After overnight culture in an incubator at 37 °C, the colonies on the plate were

170 counted using an automatic colony counter (Countermat Flash, IUL Instruments GmbH,

171 Königswinter, Germany). Both the incubation with bacteria and the counting of bacteria

172 on each plate were repeated three times. The bacteria without laser illumination were also

173 counted to evaluate the dark toxicity of free temoporfin and temoporfin-loaded

174 liposomes, defined as the intrinsic toxicity of the compounds in the absence of light.

175 **RESULTS**

176 **Characterization of liposomes**

177 The diameter and polydispersity index of the liposomes are listed in Table 1. The mean

178 diameter of NHS-liposomes was well controlled around 100 nm with a narrow size

179 distribution after extrusion through the polycarbonate membrane (pore size 100 nm),

180 being comparable with liposomes in the Foslip® formulation. After conjugation with

181 WGA, the size of liposomes increased slightly to 103.8 nm, while the size distribution

182 was still narrow. The zeta potential changed from almost neutral before conjugation to

183 slightly negative value after conjugation, while Foslip® was quite negatively charged due

184 to the negatively charged phospholipid-DPPG.

185 <Table 1>

186 According to previous experiments, the phospholipids could not be detected on this

187 SDS-PAGE gel (data not shown here), but WGA could be detected quite well. Fig. 2

188 shows that the pure WGA could be detected at around 29 kDa, representing dimeric

189 WGA (36). In the WGA-liposomes a band above the pure WGA's band was detected,

190   which was identified to be the WGA conjugate with NHS-PEG$_{2000}$-DSPE. The molecular

191   weight difference of about 3~6 kDa between these two bands implied that one or two

192   NHS-PEG$_{2000}$-DSPE molecules (Molecular weight: 3.0 kDa) were conjugated with one

193   dimeric WGA. Based on the calculation of the band intensity using ImageJ (developed by

194   National Institutes of Health), the conjugation efficiency of WGA with liposomes was

195   about 50%.

196   <Figure 2>

197   **Fluorescence microscopy**

198   Under illumination by green light, obvious red fluorescence emitted by temoporfin was

199   observed around the bacteria which were incubated with NHS-liposomes and WGA-

200   liposomes. The red fluorescence of bacteria incubated with Foslip$^{®}$ was relatively weak,

201   so that no obvious red fluorescence was shown in pictures S1 and P1. For both species of

202   bacteria, the bacteria incubated with WGA-liposomes exhibited the highest fluorescence,

203   demonstrating that WGA-liposomes delivered temoporfin to bacteria most efficiently

204   among the three formulations. The fluorescence in P2 seems to be no less than that in P3.

205   Therefore, the quantitative comparison was further performed using flow cytometry.

206   <Figure 3>

207   **Flow cytometry**

208   The delivery efficiency of temoporfin from different liposomes to bacteria was compared

209   using flow cytometry, as shown in Fig. 4 and Fig. 5. The x-axis means fluorescence

210   intensity of the bacteria and the number besides each peak is the mean fluorescence

211   intensity (MFI) of the bacteria. The more temoporfin was delivered to bacteria, the higher

212   was the MFI. The delivery of temoporfin to bacteria comprises two aspects: part of

213   temoporfin was released from liposomes and transferred into bacteria, while part of

214   temoporfin remained in the liposomes being bound to bacteria. Both fractions of

215   temoporfin could be detected when the bacteria were analyzed by flow cytometry. As

216   control, temoporfin-loaded liposomes alone were submitted to flow cytometry. These

217   liposomes could not be detected in the used configuration of this device, in line with the

218   literature data (37).

219   <Figure 4>

220   <Figure 5>

221   In Fig. 4, *S. aureus* incubated with WGA-liposomes showed the strongest fluorescence

222   , meaning that WGA-liposomes delivered 4.5 fold more temoporfin to the bacteria than

223   NHS-liposomes and 25.4 fold more temoporfin than Foslip® did. Although the MFI of *S.*

224   *aureus* incubated with Foslip® was smaller than those for the other two liposomal

225   formulations, it was still higher than the MFI of untreated bacteria, implying that Foslip®

226   could also deliver some temoporfin to bacteria.

227   Figure 5 shows the MFIs of *P. aeruginosa* incubated with all three kinds of liposomes.

228   The order of temoporfin delivery efficiency among them is the same as the order for *S.*

229   *aureus*, *i.e.* the WGA-liposomes delivered more temoporfin than the unmodified

230   liposomes. Here, the WGA-liposomes delivered 1.4 fold more temoporfin to the bacteria

231   than NHS-liposomes and 11.2 fold more temoporfin than Foslip® did.

232   **Dark Toxicity Test**

233   The survival of bacteria without laser illumination after incubation with liposomes (dark

234   toxicity) was tested for temoporfin alone and liposomal temoporfin. In Fig. 6, all

235   liposomal formulations showed no dark toxicity against *S. aureus*, while free temoporfin

236   (dissolved in ethanol) induced a 0.24 and 2.69 $\log_{10}$ reduction of bacteria after 90 min

237   and 180 min incubation, respectively. In experiments with *P. aeruginosa* (Fig.7), neither

238   free temoporfin nor Foslip[®] showed any obvious toxicity. By contrast, NHS-liposomes

239   and WGA-liposomes induced a 0.45 and 0.37 $\log_{10}$ reduction, respectively, after 180 min

240   incubation.

241   <Figure 6>

242   <Figure 7>

243   *In vitro* **PDI of bacteria**

244   For *in vitro* PDI test, bacteria were incubated with temoporfin at two concentrations: 1.25

245   μM and 12.5 μM. Fig.6 and Fig.7 show the survival bacteria numbers after PDI. As to *S.*

246   *aureus* (Fig.6), free temoporfin was very bactericidal, eradicating all *S. aureus* at 12.5 μM

247   (90 and 180 min) and at 1.25 μM (180 min); Foslip[®] killed *S. aureus* the least efficiently,

248   achieving its maximal reduction of 2.6 $\log_{10}$; NHS-liposomes caused only an incremental

249   phototoxicity compared to Foslip[®]; the WGA modified liposomes, WGA-liposomes, were

250   the most effective liposomal formulation, achieving antimicrobial effect in all cases, *i.e.*

251   > 3 $\log_{10}$ reduction (38), and eradicated even all *S. aureus* at higher concentration.

252   In the tests with *P. aeruginosa* (Fig. 7), free temoporfin and NHS-liposomes showed a

253   slight phototoxicity, achieving maximal 0.3 and 0.6 $\log_{10}$ reduction, respectively. In

254   comparison, Foslip[®] and WGA-liposomes induced a significant reduction of *P.*

255   *aeruginosa*. Particularly, WGA-liposomes were more phototoxic than Foslip[®] in certain

256   circumstances, *i.e.* 12.5 μM/90 min and 1.25 μM/180 min , resulting in maximal 2 $\log_{10}$

257   reduction at 12.5 μM (90 min incubation). However, *P. aeruginosa* seemed to be more

258   resistant to PDI than *S. aureus*, as no eradication was obtained.

DISCUSSION

259

260   In this study, we combined the advantages of antimicrobial PDI and targeted drug

261   delivery systems, and focused on the targeted delivery of the PS (temoporfin) to bacteria

262   using WGA modified liposomes, aiming to develop a new method to improve the PDI of

263   bacteria.

264   To prepare WGA modified liposomes, a functional phospholipid, NHS-PEG$_{2000}$-DSPE

265   (Fig.1), was utilized. NHS-PEG$_{2000}$-DSPE is an activated phospholipid, whose *N*-

266   hydroxysuccinimidyl (NHS) residue can easily be replaced by active amine groups of

267   proteins. Attention should be paid as this NHS residue hydrolyzes fast with a hydrolysis

268   half-life of about 20 min (according to the product manual), so the hydration of lipid film

269   and extrusion should be finished as soon as possible. After 2 h incubation of the prepared

270   liposomes with WGA, the NHS-PEG$_{2000}$-DSPE was either conjugated with WGA or

271   hydrolyzed into carboxyl acid, so the conjugation process was terminated automatically.

272   This conjugation technique was fast, effective and convenient without additional steps to

273   activate neither the phospholipid nor the ligand. Therefore, NHS-PEG$_{2000}$-DSPE was

274   used for the surface modification of liposomes in our experiment. The result from SDS-

275   PAGE (Fig. 2) suggested that one or two NHS-PEG$_{2000}$-DSPE were linked with one

276   WGA dimer via reaction with WGA's amino groups, so the targeting ability of WGA to

277   bacteria was supposed to remain, as previous study proved that the WGA still bound

278   efficiently to bacteria after its amino groups were thiolated and connected with

279   phospholipids (32).

280   It is noteworthy that the zeta-potential of NHS-liposomes and WGA-liposomes were

281   near zero (Table 1), while the similar formulation without PEG segment exhibited a zeta

282   potential of +30.4 mV (data not shown here). One reason is that the NHS-PEG$_{2000}$-DSPE

283   is negatively charged as shown in Fig. 1, which reduces the zeta potential of liposomes

284   by charge compensation. In addition, the PEGylated phospholipids (NHS-PEG$_{2000}$-DSPE)

285   form a hydrated layer surrounding the phospholipid bilayer, and hence shield the positive

286   charge of the bilayer containing DOTAP (39). As a result, the zeta potential of the whole

287   liposome was reduced in our measurements from +30.4 mV to almost zero, but the

288   bilayer was hypothesized to be still positively charged, because there were more cationic

289   DOTAP than NHS-PEG$_{2000}$-DSPE in the bilayer. Compared to cationic liposomes, these

290   liposomes are supposed to display less binding to the negatively charged components and

291   surfaces in the physiological environment, which is a big problem for most of cationic

292   formulations in the *in vivo* application.

293   With temoporfin as fluorescent molecule, the fluorescence microscopy revealed that

294   temoporfin was indeed delivered to bacteria by WGA-liposomes (Fig.3), while the flow

295   cytometry measurements reflected how much temoporfin was detected in or around

296   bacteria, and was used to compare the delivery efficiency of temoporfin (Fig. 4 and Fig.

297   5). For both employed bacterial strains *(S. aureus and P. aeruginosa)*, the order of

298   delivery efficiency was WGA-liposomes > NHS-liposomes > Foslip[®], demonstrating that

299   our special neutral liposomal formulations delivered temoporfin to bacteria more

300   efficiently than the negatively charged formulation, and the surface modification with

301   WGA further increased the delivery efficiency compared to the non-modified liposomes.

14

302   WGA-liposomes and NHS-liposomes, despite displaying a neutral zeta potential

303   consists of a positively charged lipid bilayer, which exhibits a less favorable packing

304   environment for temoporfin as negatively charged bilayer will do, and therefore, a higher

305   rate of transferring temoporfin to other membranes was observed (40). In addition,

306   Reshetov *et al.* showed that part of temoporfin was localized in the PEG shell of

307   PEGylated liposomes and was released faster than from Foslip[®] (41).

308   Besides the conventional transfer, the binding or adsorption of liposomes to bacteria

309   played an important role concerning drug delivery to bacteria, since the intimacy between

310   liposomes and bacteria resulted in fast temoporfin transfer from the lipid bilayer into the

311   bacterial cell wall. Considering that most bacteria have a net negative charge on the cell

312   surface (42), the negatively charged Foslip[®] will not bind as easy with bacteria as the

313   NHS-liposomes and WGA-liposomes displaying a neglectable zeta potential did, due to

314   the electrostatic repulsion between bacteria and Foslip[®]. Therefore, both WGA-liposomes

315   and NHS-liposomes delivered more temoporfin to bacteria than Foslip[®] did.

316   Furthermore, WGA has a high specificity for *N*-acetylglucosamine and *N*-

317   acetylneuraminic acid and binds to oligosaccharides which contain those two residues

318   (36). As peptidoglycans in bacterial cell walls are rich in *N*-acetylglucosamine residues,

319   and some lipopolysaccharides also contain the residues, WGA may be attracted to

320   bacteria (43). It was alrready reported that WGA bearing liposomes targeted effectively to

321   bio-film of a skin associated strain: *Staphylococcus epidermis* (32), and WGA bound to *P.*

322   *aeruginosa* (44). Our results showed that WGA-liposomes delivered more temoporfin

323   than NHS-liposomes, indicating that the conjugated WGA on the surface of liposomes

324   also facilitated the binding of liposomes with *S. aureus* and *P. aeruginosa,* and thus

325   enhanced the delivery of temoporfin.

326   Based on the above discussions we concluded that WGA-liposomes were efficient in

327   temoporfin delivery due to its fast release of temoporfin and enhanced binding potential

328   with bacteria. We also noticed that WGA modification increased the delivery efficiency

329   for *S. aureus* more intensively than for *P. aeruginosa* by comparing the difference

330   between WGA-liposomes and NHS-liposomes in both fluorescence micrographs and

331   flow cytometry measurements, suggesting that WGA binds to *P. aeruginosa* less

332   efficiently than to *S. aureus*. This difference is related to the different concentration of *N*-

333   acetylglucosamine on the bacterial surface. Gram positive bacteria's peptidoglycan-

334   containing cell walls are exposed directly to the external medium and therefore the *N*-

335   acetylglucosamine in peptidoglycan is easily accessible for WGA binding. By contrast, *P.*

336   *aeruginosa*'s peptidoglycan is shielded by the outer membrane, only a small part of

337   peptidoglycans may be released to the surface. Additionally, a small amount of

338   lipopolysaccharides on the surface of *P. aeruginosa* also contain *N*-acetylglucosamine.

339   However, the total amount of *N*-acetylglucosamine on the surface of *P. aeruginosa* is still

340   lower than that of *S. aureus* (44). That is why WGA-liposomes bind to *S. aureus* more

341   efficiently than to *P. aeruginosa*.

342   The increased delivery of temoporfin to bacteria by WGA-liposomes was supposed to

343   result in enhanced killing efficiency against bacteria, which was confirmed in the *in vitro*

344   test on the PDI of MRSA (Fig. 6). The order of PDI efficiency against MRSA among the

345   three liposomal formulations was in agreement with the order of delivery efficiency.

346   WGA-liposomes presented obvious improvement of antimicrobial PDI compared to

347   NHS-liposomes and Foslip®. Although this improvement could be explained by the

348   superior delivery of temoporfin from WGA-liposomes, we need to point out that the

349   cationic lipid in the liposomes, *i.e.* DOTAP, was believed to contribute to this

350   improvement, too. This hypothesis was supported by the reports that DOTAP containing

351   liposomes facilitated the uptake of PSs into MRSA, and thus enhanced the antibacterial

352   phototoxicity of PSs, most likely because DOTAP binds to the negatively charged cell

353   wall, may disturb it and increase its porosity, resulting in enhanced penetration of PSs

354   into cytoplasmic membrane (26, 11). Although in Fig. 6 the bactericidal efficiency of free

355   temoporfin dissolved in ethanol was comparable with that of WGA-liposomes, the

356   intrinsic PDI efficiency of free temoporfin is probably smaller than WGA-liposomes,

357   considering that temoporfin in ethanol exhibited a 2.7 $\log_{10}$ dark toxicity. From a

358   pharmaceutical point of view, the liposomal formulation is more suitable than the ethanol

359   solution for a potential topical application, and is potential to reduce possible side effects

360   on the surrounding mammalian cells, as the liposomal temoporfin was less toxic to

361   mammalian cells than free temoporfin without light activation (45). Therefore, the WGA-

362   liposomes are promising for antimicrobial PDI of MRSA.

363   Compared to MRSA, *P. aeruginosa* was less susceptible to temoporfin in the PDI test

364   (Fig. 7). In contrast with the porous cell wall of gram-positive bacteria, the outer

365   boundary of gram-negative bacteria consists of an inner cytoplasmic membrane and an

366   outer membrane which are separated by the peptidoglycan-containing periplasm (12).

367   The outer membrane has a very heterogeneous composition, *e.g.* proteins with porin

368   function, lipopolysaccharides and lipoproteins, giving the outer surface a quasi-

369   continuum of densely packed negative charges (13, 46). This highly organized system

370   forms a physical and functional barrier between the cell and its environment, and hence

371   limits the permeation of PSs into cells. Consequently, neutral or anionic PSs generally

372   only bind efficiently to and photodynamically inactive gram-positive bacteria, but not

373   in the case of gram-negative bacteria (8, 46). Different approaches have been devised to

374   overcome this barrier. One strategy is to use cationic PSs, *e.g.* the cationic *meso-*

375   substituted porphyrins (47), the chlorin(e6) conjugated with poly-L-lysine (48),

376   methylene blue and toluidine blue (49). These cationic PSs gain access across the outer

377   membrane via the self-promoted uptake pathway, *i.e.* cationic PSs bind to the negatively

378   charged bacteria, cause alterations in the outer membrane permeability, and thereby

379   render hydrophobic PSs deep penetration inside bacterial cells, where the generated

380   ROSs execute fatal damage (50). Alternatively, the dense outer membrane may be

381   disturbed by the additives, *e.g.* EDTA and polycationic peptide polymyxin B nonapeptide,

382   which both increase the permeability of the outer membrane and allow PSs to penetrate to

383   an inner location (8, 46). In addition, liposomes also have the function to disturb the outer

384   membrane, since some liposomal formulations were able to fuse with bacteria effectively

385   and disturb their cell walls (29, 30, 11).

386   In line with the above analysis, temoporfin alone induced little reduction of *P.*

387   *aeruginosa*, because it is neutral and could not penetrate through the outer membrane

388   easily. By contrast, amongst the three liposomal formulations, WGA-liposomes achieved

389   the highest PDI efficiency against *P. aeruginosa*. It is already evident that free temoporfin

390   could not photoinactivate *P. aeruginosa* effectively, so the obtained photoinactivation was

391   attributed to other factors, most likely, the disturbance of the outer membrane triggered

392   by liposomes. One big advantage of liposomes for antimicrobial application is their

393   potential to fuse with bacteria, which was already confirmed using TEM, *e.g.* certain

394   DPPC-based liposomal formulations fused with as much as 57.8% of *P. aeruginosa*

395   bacteria (29, 30). WGA-liposomes could intensively associated with bacteria because of

396   WGA's affinity to cell walls, not only resulting in higher delivery efficiency (Fig. 5), but

397   also further increasing the fusing potential of the positively charged liposomal bilayer

398   with the negatively charged cell walls. Subsequently, temoporfin was released via

399   lipophilic membraneous pathway directly into bacteria, together with the cationic lipid,

400   DOTAP. Then the transferred DOTAP disturbs the outer membrane, helping deliver

401   temoporfin to the inner location of the cell wall and photoinactivate *P. aeruginosa*

402   efficiently. Our result proved that the WGA modified liposomes increased the PDI

403   efficiency of temoporfin compared to the unmodified liposomes and free temoporfin,

404   with a maximal 2 $\log_{10}$ killing of *P. aeruginosa*, which was, as far as we know, the first

405   time to be reported in the literature using temoporfin, suggesting that this formulation

406   helped to overcome the outer membrane barrier of *P. aeruginosa*.

407   Besides temoporfin, we hypothesize that this formulation will also be helpful for the

408   improvement of other PSs, *e.g.* the highly cationic and phototoxic meso-substituted

409   porphyrins (47), as well as the other reported liposomal formulations for the PDI of

410   bacteria (23, 25, 11, 26).

411   Last but not least, the PDI protocol needs to be further optimized to reduce the

412   possible damage to the mammalian cells. There was no significant difference ($p > 0.05$)

413   between the last two columns for WGA-liposomes in Fig. 6 (12.5 µM/90min and 12.5

414   µM/180min), neither was there among the last three columns for WGA-liposomes in

415   Fig.7 (1.25 µM/180min, 12.5 µM/90min and 12.5 µM/180min), implying that the similar

416   PDI efficiency could be achieved using less than 12.5 µM temoporfin or shorter

417 incubation period than 90 min. In addition, the PDI of gram-negative bacteria is not

418 satisfying and may be further enhanced using a stepwise approach proposed by Jori *et al.*

419 (13). This approach is based on the idea that the PSs, near to or associated with the outer

420 membrane, will cause photodamage to the outer membrane to some extent after a

421 preliminary illumination, leading to increased permeability of the cell wall. Then the

422 bacteria are further incubated with PSs, and more PSs would be translocated into the

423 inner membrane or even into the core of bacteria, causing stronger PDI of bacteria after

424 the second illumination.

425 **CONCLUSION**

426 In this study, we have combined the advantages of bacteria-targeting liposomes and

427 antimicrobial PDI, *i.e.* prepared WGA modified liposomes for bacteria targeted delivery

428 of temoporfin. The results demonstrate that our WGA modified liposomal formulation is

429 promising for bacteria targeted delivery and for improving the PDI efficiency of

430 temoporfin against both *MRSA* than *P. aeruginosa*, although the effect on *P. aeruginosa* is

431 not superior and needs to be further improved. What's more, this bacteria-targeting

432 strategy can also be applied to other effective PSs as well as their liposomal formulations,

433 with the potential to combat antibiotic-resistant bacteria and reduce their cytotoxicity to

434 skin cells. Antimicrobial PDI using PSs incorporated into bacteria-targeting liposomes

435 will be an attractive approach for the treatment of localized microbial infections.

436

Publication 2
Photochemistry and Photobiology

439   Research (BMBF, project No. 0312028).

440   **REFERENCES**

441   1. Cunha, B. A. (1998) Antibiotic resistance. *Drugs Today (Barc)* **34,** 691-8.

442   2. Kumarasamy, K. K., M. A. Toleman, T. R. Walsh, J. Bagaria, F. Butt, R. Balakrishnan, U.

443   Chaudhary, M. Doumith, C. G. Giske, S. Irfan, P. Krishnan, A. V. Kumar, S. Maharjan, S.

444   Mushtaq, T. Noorie, D. L. Paterson, A. Pearson, C. Perry, R. Pike, B. Rao, U. Ray, J. B.

445   Sarma, M. Sharma, E. Sheridan, M. A. Thirunarayan, J. Turton, S. Upadhyay, M. Warner, W.

446   Welfare, D. M. Livermore and N. Woodford (2010) Emergence of a new antibiotic resistance

447   mechanism in India, Pakistan, and the UK: a molecular, biological, and epidemiological study.

448   *Lancet Infect. Dis.* **10,** 597-602.

449   3. Redmond, R. W. and J. N. Gamlin (1999) A compilation of singlet oxygen yields from

450   biologically relevant molecules. *Photochem. Photobiol.* **70,** 391-475.

451   4. Christie, J. G. and U. B. Kompella (2008) Ophthalmic light sensitive nanocarrier systems.

452   *Drug Discov. Today* **13,** 124-34.

453   5. Wilson, B. C. and M. S. Patterson (2008) The physics, biophysics and technology of

454   photodynamic therapy. *Phys. Med. Biol.* **53,** R61-109.

455   6. Lorenz, K. J. and H. Maier (2008) Squamous cell carcinoma of the head and neck.

456   Photodynamic therapy with Foscan. *HNO* **56,** 402-9.

457   7. Tsai, T., Y. T. Yang, T. H. Wang, H. F. Chien and C. T. Chen (2009) Improved Photodynamic

458   Inactivation of Gram-Positive Bacteria Using Hematoporphyrin Encapsulated in Liposomes

459   and Micelles. *Lasers Surg. Med.* **41,** 316-322.

460   8. Huang, L., T. Dai and M. R. Hamblin (2010) Antimicrobial photodynamic inactivation and

461   photodynamic therapy for infections. *Methods Mol. Biol.* **635,** 155-73.

462 9. Smijs, T. G. and S. Pavel (2011) The susceptibility of dermatophytes to photodynamic

463 treatment with special focus on Trichophyton rubrum. *Photochem. Photobiol.* **87,** 2-13.

464 10. Kishen, A., M. Upadya, G. P. Tegos and M. R. Hamblin (2010) Efflux pump inhibitor

465 potentiates antimicrobial photodynamic inactivation of Enterococcus faecalis biofilm.

466 *Photochem. Photobiol.* **86,** 1343-9.

467 11. Ferro, S., F. Ricchelli, D. Monti, G. Mancini and G. Jori (2007) Efficient photoinactivation of

468 methicillin-resistant Staphylococcus aureus by a novel porphyrin incorporated into a poly-

469 cationic liposome. *INT J BIOCHEM CELL B* **39,** 1026-1034.

470 12. Hamblin, M. R. and T. Hasan (2004) Photodynamic therapy: a new antimicrobial approach to

471 infectious disease? *Photochem. Photobiol. Sci.* **3,** 436-50.

472 13. Jori, G., C. Fabris, M. Soncin, S. Ferro, O. Coppellotti, D. Dei, L. Fantetti, G. Chiti and G.

473 Roncucci (2006) Photodynamic therapy in the treatment of microbial infections: basic

474 principles and perspective applications. *Lasers Surg. Med.* **38,** 468-81.

475 14. Zeina, B., J. Greenman, D. Corry and W. M. Purcell (2003) Antimicrobial photodynamic

476 therapy: assessment of genotoxic effects on keratinocytes in vitro. *Br. J. Dermatol.* **148,** 229-

477 32.

478 15. Cassidy, C. M., M. M. Tunney, P. A. McCarron and R. F. Donnelly (2009) Drug delivery

479 strategies for photodynamic antimicrobial chemotherapy: from benchtop to clinical practice. *J.*

480 *Photochem. Photobiol. B* **95,** 71-80.

481 16. Zolfaghari, P. S., S. Packer, M. Singer, S. P. Nair, J. Bennett, C. Street and M. Wilson (2009)

482 In vivo killing of Staphylococcus aureus using a light-activated antimicrobial agent. *BMC*

483 *Microbiol.* **9,** 27.

484 17. Omar, G., M. Wilson and S. Nair (2008) Lethal photosensitization of wound-associated

485 microbes using indocyanine green and near-infrared light. *BMC Microbiol.* **8,** 111.

486 18. Gad, F., T. Zahra, K. P. Francis, T. Hasan and M. R. Hamblin (2004) Targeted photodynamic

487 therapy of established soft-tissue infections in mice. *Photochem. Photobiol. Sci.* **3,** 451-8.

488   19. Pinheiro, S. L., J. M. Donega, L. M. Seabra, M. D. Adabo, T. Lopes, T. H. do Carmo, M. C.

489   Ribeiro and P. F. Bertolini (2010) Capacity of photodynamic therapy for microbial reduction

490   in periodontal pockets. *Lasers Med. Sci.* **25,** 87-91.

491   20. Horfelt, C., B. Stenquist, O. Larko, J. Faergemann and A. M. Wennberg (2007)

492   Photodynamic therapy for acne vulgaris: a pilot study of the dose-response and mechanism of

493   action. *Acta Derm. Venereol.* **87,** 325-9.

494   21. Photopharmica (2007) Photopharmica targets infected wounds with its photodynamic therapy.

495   Available at: http://www.photopharmica.com/news/01_07_07b.htm. Accessed on July 2007.

496   22. Dai, T., G. P. Tegos, T. Zhiyentayev, E. Mylonakis and M. R. Hamblin (2010) Photodynamic

497   therapy for methicillin-resistant Staphylococcus aureus infection in a mouse skin abrasion

498   model. *Lasers Surg. Med.* **42,** 38-44.

499   23. Engelhardt, V., B. Krammer and K. Plaetzer (2010) Antibacterial photodynamic therapy using

500   water-soluble formulations of hypericin or mTHPC is effective in inactivation of

501   Staphylococcus aureus. *Photochem. Photobiol. Sci.* **9,** 365-9.

502   24. Sibani, S. A., P. A. McCarron, A. D. Woolfson and R. F. Donnelly (2008) Photosensitiser

503   delivery for photodynamic therapy. Part 2: systemic carrier platforms. *Expert Opin. Drug*

504   *Deliv.* **5,** 1241-54.

505   25. Bombelli, C., F. Bordi, S. Ferro, L. Giansanti, G. Jori, G. Mancini, C. Mazzuca, D. Monti, F.

506   Ricchelli, S. Sennato and M. Venanzi (2008) New cationic liposomes as vehicles of m-

507   tetrahydroxyphenylchlorin in photodynamic therapy of infectious diseases. *Mol. Pharm.* **5,**

508   672-9.

509   26. Ferro, S., F. Ricchelli, G. Mancini, G. Tognon and G. Jori (2006) Inactivation of methicillin-

510   resistant Staphylococcus aureus (MRSA) by liposome-delivered photosensitising agents. *J.*

511   *Photochem. Photobiol. B* **83,** 98-104.

512   27. Dragicevic-Curic, N., S. Winter, D. Krajisnik, M. Stupar, J. Milic, S. Graefe and A. Fahr

513   (2010) Stability evaluation of temoporfin-loaded liposomal gels for topical application. *J.*

514   *Liposome Res.* **20,** 38-48.

515   28. Schwiertz, J., A. Wiehe, S. Grafe, B. Gitter and M. Epple (2009) Calcium phosphate

516   nanoparticles as efficient carriers for photodynamic therapy against cells and bacteria.

517   *Biomaterials* **30,** 3324-31.

518   29. Jia, Y., H. Joly and A. Omri (2010) Characterization of the interaction between liposomal

519   formulations and Pseudomonas aeruginosa. *J. Liposome Res.* **20,** 134-46.

520   30. Mugabe, C., M. Halwani, A. O. Azghani, R. M. Lafrenie and A. Omri (2006) Mechanism of

521   Enhanced Activity of Liposome-Entrapped Aminoglycosides against Resistant Strains of

522   Pseudomonas aeruginosa. *Antimicrob. Agents Chemother.* **50,** 2016-2022.

523   31. Sudheesh, M. S., V. Jain, G. Shilakari and D. V. Kohli (2009) Development and

524   characterization of lectin-functionalized vesicular constructs bearing amphotericin B for bio-

525   film targeting. *J. Drug Target.* **17,** 148-58.

526   32. Kaszuba, M., I. G. Lyle and M. N. Jones (1995) The targeting of lectin-bearing liposomes to

527   skin-associated bacteria. *Colloid Surface B* **4,** 151-158.

528   33. Robinson, A. M., J. E. Creeth and M. N. Jones (1998) The specificity and affinity of

529   immunoliposome targeting to oral bacteria. *Biochim. Biophys. Acta* **1369,** 278-86.

530   34. Kuntsche, J., I. Freisleben, F. Steiniger and A. Fahr (2010) Temoporfin-loaded liposomes:

531   physicochemical characterization. *Eur. J. Pharm. Sci.* **40,** 305-15.

532   35. Laemmli, U. K. (1970) Cleavage of structural proteins during the assembly of the head of

533   bacteriophage T4. *Nature* **227,** 680-5.

534   36. Nagata, Y. and M. M. Burger (1974) Wheat germ agglutinin. Molecular characteristics and

535   specificity for sugar binding. *J. Biol. Chem.* **249,** 3116-22.

536   37. Petersen, S., A. Fahr and H. Bunjes (2010) Flow cytometry as a new approach to investigate

537   drug transfer between lipid particles. *Mol. Pharm.* **7,** 350-63.

538   38. NCCLS (1992) Methods for determining bactericidal activity of antimicrobial agents;

539   tentative guidelines M26-T. National Committee for Clinical Laboratory Standards, Villanova,

540   Pennsylvania: NCCLS.

541   39. Dadashzadeh, S., N. Mirahmadi, M. H. Babaei and A. M. Vali (2010) Peritoneal retention of

542   liposomes: Effects of lipid composition, PEG coating and liposome charge. *J. Control.*

543   *Release* **148,** 177-86.

544   40. Hefesha, H., S. Loew, X. Liu, S. May and A. Fahr (2010) Transfer mechanism of temoporfin

545   between liposomal membranes. *J. Control. Release.*

546   41. Reshetov, V., D. Kachatkou, T. Shmigol, V. Zorin, M. A. D'Hallewin, F. Guillemin and L.

547   Bezdetnaya (2011) Redistribution of meta-tetra(hydroxyphenyl)chlorin (m-THPC) from

548   conventional and PEGylated liposomes to biological substrates. *Photochem. Photobiol. Sci.*

549   42. Sanderson, N. M., B. Guo, A. E. Jacob, P. S. Handley, J. G. Cunniffe and M. N. Jones (1996)

550   The interaction of cationic liposomes with the skin-associated bacterium Staphylococcus

551   epidermidis: effects of ionic strength and temperature. *Biochim. Biophys. Acta* **1283,** 207-14.

552   43. Avni, I., R. C. Arffa, J. B. Robin and N. A. Rao (1987) Lectins for the identification of ocular

553   bacterial pathogens. *Metab. Pediatr. Syst. Ophthalmol.* **10,** 45-7.

554   44. Strathmann, M., J. Wingender and H. C. Flemming (2002) Application of fluorescently

555   labelled lectins for the visualization and biochemical characterization of polysaccharides in

556   biofilms of Pseudomonas aeruginosa. *J. Microbiol. Methods* **50,** 237-48.

557   45. Berlanda, J., T. Kiesslich, V. Engelhardt, B. Krammer and K. Plaetzer (2010) Comparative in

558   vitro study on the characteristics of different photosensitizers employed in PDT. *Journal of*

559   *Photochemistry and Photobiology B-Biology* **100,** 173-180.

560   46. Malik, Z., H. Ladan and Y. Nitzan (1992) Photodynamic inactivation of Gram-negative

561   bacteria: problems and possible solutions. *J. Photochem. Photobiol. B* **14,** 262-6.

562   47. Alves, E., L. Costa, C. M. Carvalho, J. P. Tome, M. A. Faustino, M. G. Neves, A. C. Tome, J.

563   A. Cavaleiro, A. Cunha and A. Almeida (2009) Charge effect on the photoinactivation of

564   Gram-negative and Gram-positive bacteria by cationic meso-substituted porphyrins. *BMC*

565   *Microbiol.* **9,** 70.

566   48. Hamblin, M. R., D. A. O'Donnell, N. Murthy, K. Rajagopalan, N. Michaud, M. E. Sherwood

567   and T. Hasan (2002) Polycationic photosensitizer conjugates: effects of chain length and

568   Gram classification on the photodynamic inactivation of bacteria. *J. Antimicrob. Chemother.*

569   **49,** 941-51.

570   49. Usacheva, M. N., M. C. Teichert and M. A. Biel (2001) Comparison of the methylene blue

571   and toluidine blue photobactericidal efficacy against gram-positive and gram-negative

572   microorganisms. *Lasers Surg. Med.* **29,** 165-73.

573   50. Minnock, A., D. I. Vernon, J. Schofield, J. Griffiths, J. H. Parish and S. B. Brown (2000)

574   Mechanism of uptake of a cationic water-soluble pyridinium zinc phthalocyanine across the

575   outer membrane of Escherichia coli. *Antimicrob. Agents Chemother.* **44,** 522-7.

576

577

26

578   Table 1. The diameter, polydispersity index and zeta potential of liposomes as measured

579   by PCS and Laser Doppler Velocimetry. (n=3)

Liposomes	Diameter (nm)	polydispersity index	Zeta potential (mV)
NHS-liposomes	102.7±1.5	0.128±0.037	1.44±0.45
WGA-liposomes	103.8±1.0	0.078±0.001	-8.61±0.45
Foslip®	117.5±1.2	0.105±0.010	-48.2±9.00

580

581   **FIGURE CAPTIONS**

582   **Figure 1.** Scheme of the conjugation of WGA with liposomes composed of DPPC,

583   DOTAP, NHS-PEG$_{2000}$-DSPE and mPEG$_{2000}$-DSPE (molar ratio of 80:15:2:3). The amino

584   group reactive anchor lipid NHS-PEG$_{2000}$-DSPE was used for the conjugation of WGA to

585   the vesicle surface.

586   **Figure 2.** SDS-PAGE of free WGA and liposome-conjugated WGA after coupling to

587   NHS-PEG$_{2000}$-DSPE containing liposomes and purification via Sepharose CL4B column.

588   **Figure 3.** Fluorescence micrographs of *S. aureus* DSM11729 and *P. aeruginosa*

589   DSM1117 after incubation with Foslip®, NHS-liposomes and WGA-liposomes,

590   respectively.

591   **Figure 4.** Flow cytometry analysis of *S. aureus* DSM11729 incubated with temoporfin-

592   loaded liposomes: Foslip®, liposomes before conjugation (NHS-liposomes) and after

593   conjugation with WGA (WGA-liposomes). The value of each peak represents mean

594   fluorescence intensity (MFI).

595   **Figure 5.** Flow cytometry analysis of *P. aeruginosa* DSM1117 incubated with

596   temoporfin-loaded liposomes: Foslip®, liposomes before conjugation (NHS-liposomes)

597   and after conjugation with WGA (WGA-liposomes). The value of each peak represents

598   mean fluorescence intensity (MFI).

599   **Figure 6.** Dark toxicity and PDI efficiency of free temoporfin or temoporfin-loaded

600   liposomes on *S. aureus* DSM11729 after incubation at RT for 90min or 180 min,

601   respectively. The arrows indicate that the bacteria were completely eradicated, and the

602   bars representing dark toxicity results were labeled grayly. (n ≥ 3)

603   **Figure 7.** Dark toxicity and PDI efficiency of free temoporfin or temoporfin-loaded

604   liposomes on *P. aeruginosa* DSM1117 after incubation at RT for 90 min or 180 min,

605   respectively. The bars representing dark toxicity results were labeled grayly. (n ≥ 3)

606

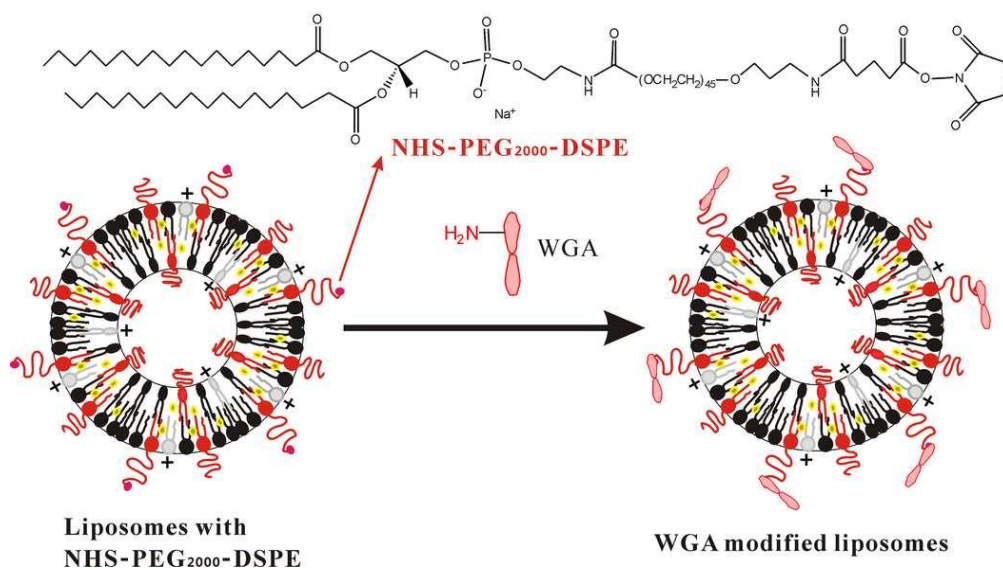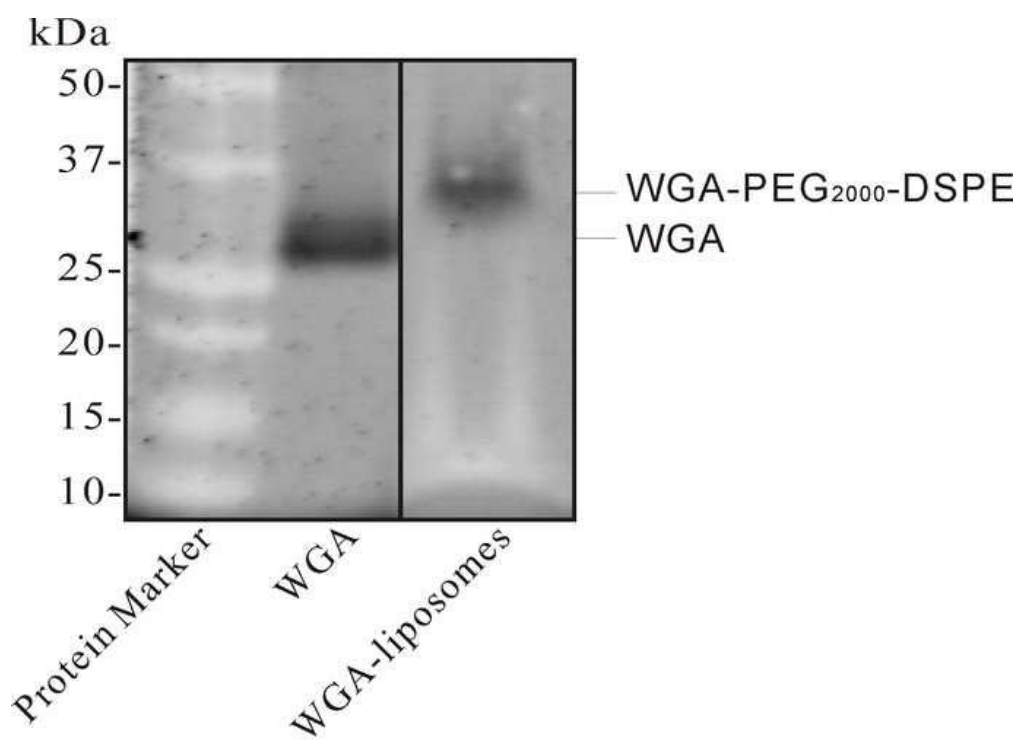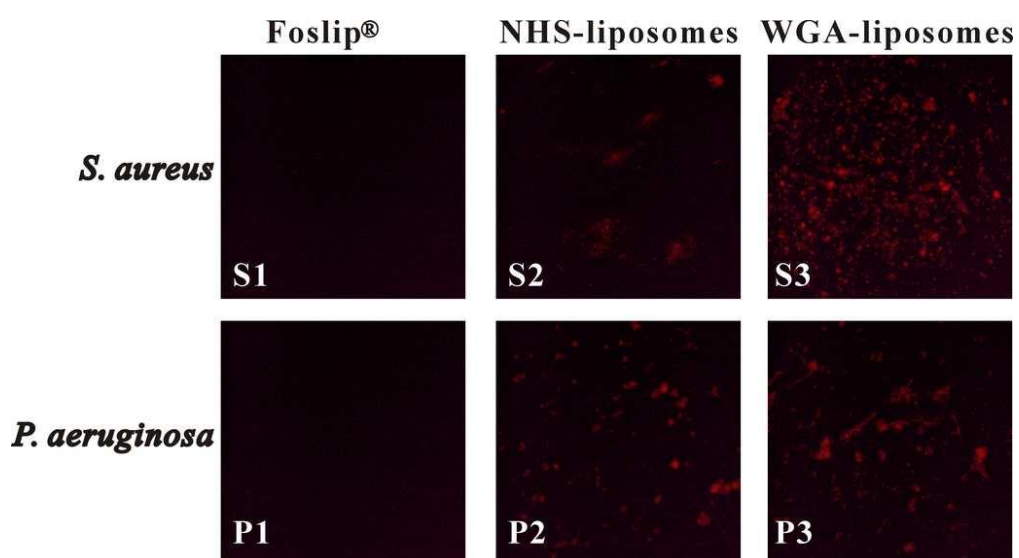Figure 1. Scheme of the conjugation of WGA with liposomes composed of DPPC, DOTAP, NHS-PEG2000-DSPE and mPEG2000-DSPE (molar ratio of 80:15:2:3). The amino group reactive anchor lipid NHS-PEG2000-DSPE was used for the conjugation of WGA to the vesicle surface.
89x49mm (300 x 300 DPI)

Figure 2. SDS-PAGE of free WGA and liposome-conjugated WGA after coupling to NHS-PEG2000-DSPE containing liposomes and purification via Sepharose CL4B column.
58x42mm (300 x 300 DPI)

Figure 3. Fluorescence micrographs of S. aureus DSM11729 and P. aeruginosa DSM1117 after incubation with Foslip®, NHS-liposomes and WGA-liposomes, respectively.
87x47mm (300 x 300 DPI)

Figure 4. Flow cytometry analysis of S. aureus DSM11729 incubated with temoporfin-loaded liposomes: Foslip®, liposomes before conjugation (NHS-liposomes) and after conjugation with WGA (WGA-liposomes). The value of each peak represents mean fluorescence intensity (MFI).
75x71mm (300 x 300 DPI)

Figure 5. Flow cytometry analysis of P. aeruginosa DSM1117 incubated with temoporfin-loaded liposomes: Foslip®, liposomes before conjugation (NHS-liposomes) and after conjugation with WGA (WGA-liposomes). The value of each peak represents mean fluorescence intensity (MFI).
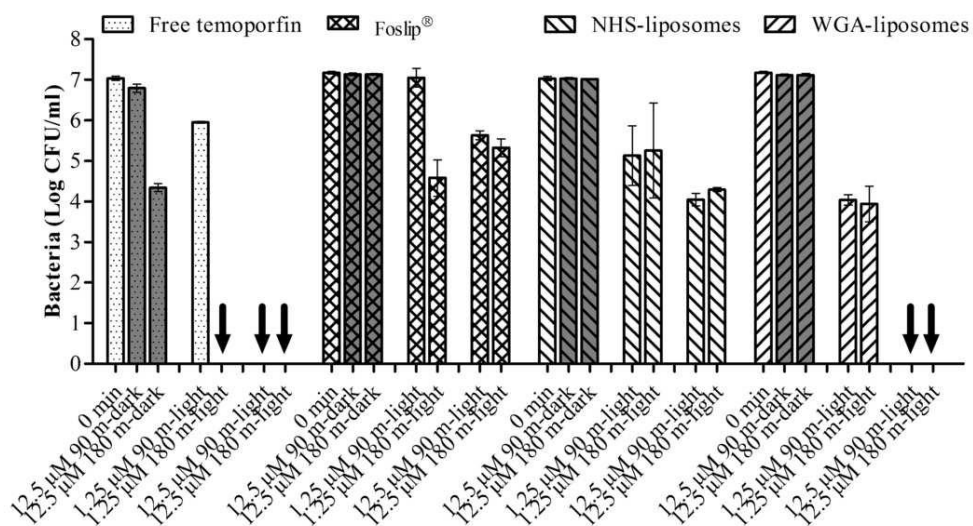81x79mm (300 x 300 DPI)

Fig. 6. Dark toxicity and PDI efficiency of free temoporfin or temoporfin-loaded liposomes on S. aureus DSM11729 after incubation at RT for 90min or 180 min, respectively. The arrows indicate that the bacteria were completely eradicated, and the bars representing dark toxicity results were labeled grayly. (n ≥ 3)
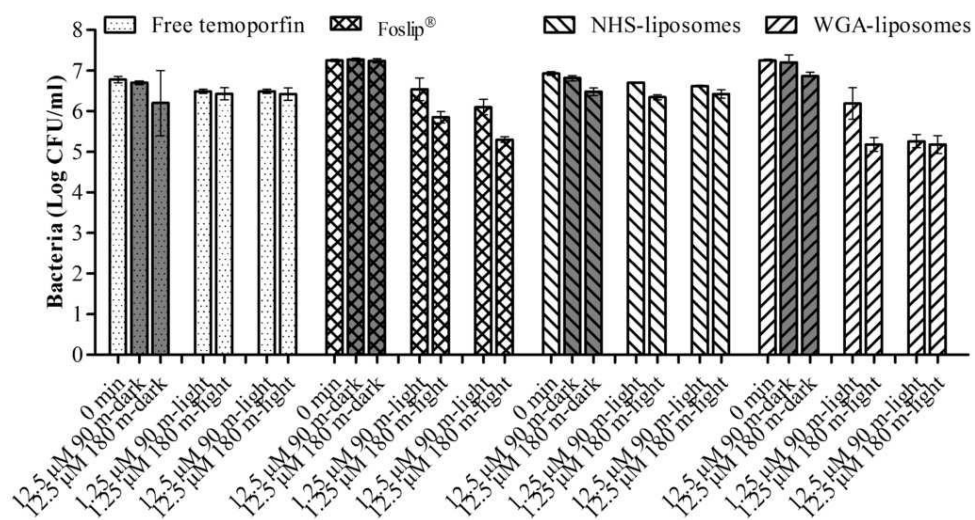91x52mm (300 x 300 DPI)

Fig. 7. Dark toxicity and PDI efficiency of free temoporfin or temoporfin-loaded liposomes on P. aeruginosa DSM1117 after incubation at RT for 90 min or 180 min, respectively. The bars representing dark toxicity results were labeled grayly. (n ≥ 3)
90x50mm (300 x 300 DPI)

3.3 Fast high-throughput screening of temoporfin-loaded liposomal formulations prepared by ethanol injection method

Kewei Yang, Joseph T. Delaney, Ulrich S. Schubert, Alfred Fahr

Pages in the dissertation: 78~88 (11 pages)

informa
healthcare

RESEARCH ARTICLE

Fast high-throughput screening of temoporfin-loaded liposomal formulations prepared by ethanol injection method

Kewei Yang,[1] Joseph T. Delaney,[2,3,4] Ulrich S. Schubert,[2,3,4] and Alfred Fahr[1]

[1]Department of Pharmaceutical Technology, Friedrich Schiller University Jena, Jena, Germany, [2]Laboratory of Organic and Macromolecular Chemistry (IOMC) and Jena Center for Soft Matter (JCSM), Friedrich Schiller University Jena, Jena, Germany, [3]Laboratory of Macromolecular Chemistry and Nanoscience, Eindhoven University of Technology, Eindhoven, The Netherlands, and [4]Dutch Polymer Institute (DPI), Eindhoven, The Netherlands

Abstract
A new strategy for fast, convenient high-throughput screening of liposomal formulations was developed, utilizing the automation of the so-called ethanol-injection method. This strategy was illustrated by the preparation and screening of the liposomal formulation library of a potent second-generation photosensitizer, temoporfin. Numerous liposomal formulations were efficiently prepared using a pipetting robot, followed by automated size characterization, using a dynamic light scattering plate reader. Incorporation efficiency of temoporfin and zeta potential were also detected in selected cases. To optimize the formulation, different parameters were investigated, including lipid types, lipid concentration in injected ethanol, ratio of ethanol to aqueous solution, ratio of drug to lipid, and the addition of functional phospholipid. Step-by-step small liposomes were prepared with high incorporation efficiency. At last, an optimized formulation was obtained for each lipid in the following condition: 36.4 mg·mL^{-1} lipid, 13.1 mg·mL^{-1} mPEG$_{2000}$-DSPE, and 1:4 ethanol:buffer ratio. These liposomes were unilamellar spheres, with a diameter of approximately 50 nm, and were very stable for over 20 weeks. The results illustrate this approach to be promising for fast high-throughput screening of liposomal formulations.

Keywords: Liposome, ethanol injection method, temoporfin, ethosome, pipetting robot

Introduction

Liposomes are nanoscopic vesicles consisting of an aqueous core enclosed in one or more phospholipid bilayers. Over the past few decades, liposomes have been widely studied as the drug delivery system for numerous bioactive compounds. A few techniques have evolved for the preparation of liposomes on a laboratory scale, such as thin-film hydration, sonication, freeze-dried rehydration, reverse-phase evaporation, detergent depletion, high-pressure homogenization, and organic solvent injection (Jesorka and Orwar, 2008; Lasch et al., 2003; Mozafari, 2005). Although a diverse array of preparative techniques have been demonstrated in the scientific literature, the number of these applied commercially is still rather limited because of the consideration of process costs and operation complexity (Justo and Moraes, 2010; Mozafari,

2005). These practical limitations function as bottlenecks to a wider application of liposomes. Therefore, the need exists to develop feasible preparation strategies suitable for both laboratory-scale study in the development of formulations and scalable manufacture.

Among the various techniques, the ethanol-injection method shows the largest potential for scale-up (Justo and Moraes, 2010; Wagner et al., 2002). In 1973, Batzri and Korn introduced the ethanol-injection method by injecting an ethanolic solution of phospholipids into water, resulting in liposomal suspensions containing 2.5–7.5% of ethanol (Batzri and Korn, 1973). Since then, this method was further developed, for example, by reverse injecting water into ethanolic solution and increasing the final concentration of ethanol to as high as 67% (Jaafar-Maalej et al., 2010; Maitani et al., 2007).

1

RIGHTSLINK

By simply injecting an ethanolic lipid solution in water or reversely under proper stirring conditions, a spontaneous liposome formation occurs as soon as the ethanolic solution comes into contact with the aqueous phase, yielding small liposomes with a narrow distribution in a single step, without the need of extrusion or sonication (Batzri and Korn, 1973; Jaafar-Maalej et al., 2010; Stano et al., 2004). Many advantages of the ethanol-injection method have been reported in the literature, including the method's simplicity, low cost, fast implementation, reproducibility, and mild conditions, which do not cause lipid degradation or oxidative alterations (Jaafar-Maalej et al., 2010; Justo and Moraes, 2010). Because of these advantages, the ethanol-injection method has been studied for the delivery of different kinds of drugs, including lipophilic drugs (Cortesi et al., 2010; Jaafar-Maalej et al., 2010; Stano et al., 2004), hydrophilic drugs (Jaafar-Maalej et al., 2010), proteins and genes (Maitani et al., 2007), and is considered to be among the most practical, scalable means of liposome production. In addition, the ethanol-injection method is especially useful for the preparation of ethosomal systems, which are patented liposomal systems containing 20–50 weight% of ethanol and ethosomes, namely, "soft" vesicles formed from phospholipids in the presence of water and ethanol and sometimes glycols (Touitou, 1996, 1998). Ethosomes showed enhanced penetration through the *stratum corneum* (SC) into the deeper layer of the skin (Dragicevic-Curic et al., 2009; Godin and Touitou, 2003; Touitou et al., 2000) resulting from the synergistic penetration-enhancing effect of liposomes and ethanol. Therefore, ethosomes are of great interest for dermal and transdermal drug administration.

Although liposomes can easily be prepared by the ethanol-injection method, there are still many factors that directly affect the formation and final properties of liposomes, such as the lipid concentration in ethanol, the ratio of ethanol to aqueous solution, the choice of lipids, the addition of stabilizers, and the ratio of drug to lipid—to name only a few. A wide variety of lipids are now commercially available, and the selection of lipids is based on numerous practical considerations (e.g., delivery routes, as well as physical-chemical characteristics of utilized drugs). The composition of liposomes is also critical to determine the structure and performance attributes (especially in combination with the drug of interest), and the relationship between these factors and the resulting liposomes is complex and not readily predictable *ab initio*. Consequently, the relationship between the aforementioned factors and the general properties of the liposome system must be studied empirically in detail. With all these considerations in mind, the rigorous development of an optimal formulation is complex and time-consuming. Traditionally, large numbers of samples are prepared and characterized manually and often sequentially. This work is labor intensive, and perhaps most significantly, often exhibits a high degree of sample variability because of human faults. Therefore, a solution was sought out to automate this process, allowing for more controlled, uniform preparation of samples in a systemic, programmable, standardized, and miniaturized format.

In this study, using the ethanol-injection method, temoporfin was selected as the drug incorporated into liposomes. Temoporfin is one of the most potent second-generation photosensitizers (Brown et al., 2004) and is already clinically used as part of the photodynamic therapy (PDT) for treatment of squamous-cell carcinoma of the head and neck (Lorenz and Maier, 2008). When temoporfin is illuminated with an excitation wavelength of 652 nm, it is activated from its ground energy-level singlet state to an activated state, which then transfers energy to the surrounding oxygen, resulting in the generation of reactive oxygen species (ROS), for example, singlet oxygen. These ROS are highly reactive and can oxidize many biological molecules, such as proteins, nucleic acids, and lipids, leading to cytotoxicity (Redmond and Gamlin, 1999). Temoporfin has been shown to be effective in the PDT of early or recurrent oral carcinomas (Biel, 2002), refractory oral carcinomas (Biel, 2002), and primary nonmelanomatous tumors of the skin of the head and neck (Kubler et al., 1999). In addition, PDT has attracted significant attention in the last decade as a promising modality to treat microbial infections, particularly antibiotic-resistant species, and thereby is termed as photodynamic antimicrobial chemotherapy or photodynamic inactivation (Hamblin and Hasan, 2004; Jori, 2006; Wainwright, 1998). It has already been demonstrated that temoporfin killed *Staphylococcus aureus* effectively (Engelhardt et al., 2010).

However, temoporfin is highly hydrophobic and cannot be administrated directly. The commercial intravenous (i.v.) injection formulation, Foscan® (biolitec AG, Jena, Germany), consists of temoporfin dissolved in a mixture of water, ethanol, and propylene glycol. Foscan requires slow injection to avoid drug precipitation at the injection site, nevertheless still with a more than 10% occurrence probability of injection-site pain (biolitec AG, 2008). Further, Foscan showed a highly unusual pharmacokinetic profile, where a minimum concentration in plasma was reached after 45 minutes and a maximum concentration was obtained after approximately 10 hours (Glanzmann et al., 1998). To solve this problem, liposomal formulations were developed to incorporate temoporfin. The first evaluated liposomal formulation, Foslip®, and its pegylated counterpart, Fospeg®, have already been evaluated in some detail, showing high incorporation efficiency (Kuntsche et al., 2010), improvements in pharmacokinetics (Buchholz et al., 2005), and faster accumulation in tumors than Foscan (Lassalle et al., 2009). Hence, the liposomal formulations are ideal for systemic administration. However, Foslip and Fospeg are prepared using a film-hydration method, with size control accomplished by high-pressure extrusion (Kuntsche et al., 2010). Film hydration and extrusion is a

complicated, difficult approach for large-scale manufacture. By contrast, and in light of the previously mentioned technical advantages, the ethanol-injection method seems to be a more attractive prospect for the scale-up of production. Additionally, it has been reported that temoporfin-loaded ethosomes enhance the penetration through SC, compared to Foslip (Dragicevic-Curic et al., 2009). Consequently, the liposomes prepared by ethanol injection are also of great interest for the topical application of temoporfin (e.g., PDT of skin-associated tumors or infections).

The aim of this study was to take advantage of both ethanol injection and automation to develop a fast, convenient method for high-throughput screening of temoporfin-loaded liposomal formulations. To achieve this aim, a large number of liposomal formulations were prepared quickly and systematically using a pipetting robot, followed by a high-throughput characterization of liposomes, to investigate, step-by-step, the interplay between different parameters relating to the optimization of new formulations. Finally, one optimal formulation for each lipid was selected, whose morphology and stability were studied in greater depth.

Methods

Materials

Egg phosphatidylcholine (EPC), Lipoid S75, and Lipoid S100 were supplied by Lipoid GmbH (Ludwigshafen, Germany). Temoporfin (i.e., 3,3′,3″,3‴-(7,8-dihydroporphyrin-5,10,15,20-tetrayl)tetraphenol; mTHPC) was a generous gift supplied from biolitec AG. 1,2-distearoyl-*sn*-glycero-3-phosphoethanolamine-*N*-[methoxy(polyethylene glycol)2000] (mPEG$_{2000}$-DSPE) was purchased from Genzyme Pharmaceuticals (Cambridge, Massachusetts, USA). Phosphate-buffered saline solution (PBS; pH 7.4) was composed of 140 mM of NaCl and 10 mM of Na$_2$HPO$_4$ and KH$_2$PO$_4$, respectively, which were purchased from Sigma-Aldrich (Steinheim, Germany). All other chemicals were of analytical grade and also purchased from Sigma-Aldrich.

Preparation of liposomes using a pipetting robot

The FasTrans® pipetting robot (Analytik Jena AG, Jena, Germany) was equipped with 200-µL tips and was used to prepare liposomes in a 96-well plate by the ethanol-injection method, as shown in Figure 1. To accomplish
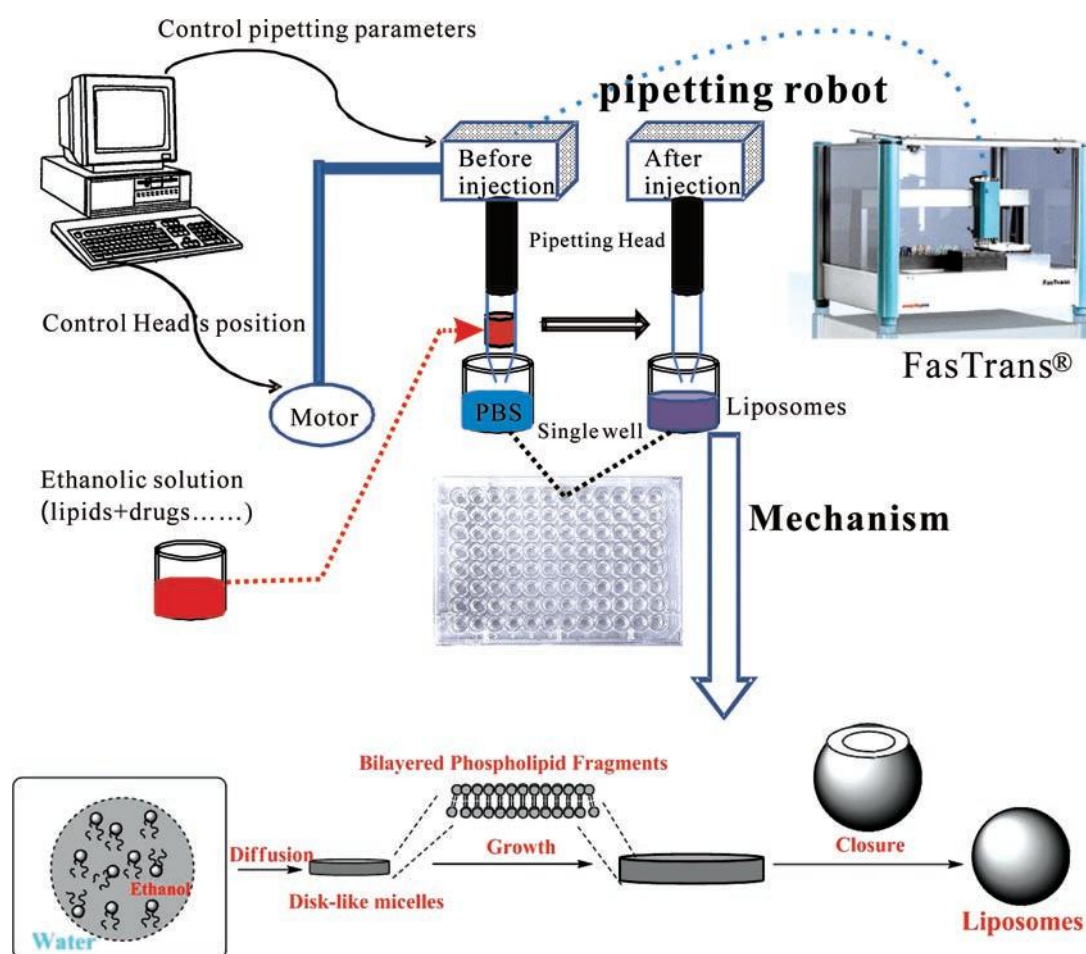

Figure 1. Scheme of the automation of the ethanol injection using a pipetting robot and the underlying mechanism of liposome formation. The position of the pipetting head and the pipetting parameters (e.g., volume and mixing speed) are adjustable by program. After injection of the ethanolic solution into the aqueous phase, ethanol diffuses into water, and liposomes are formed via intermediately formed, disk-like micelles.

this, PBS solution, pure ethanol, and ethanolic lipid stock solutions (both with and without temoporfin) were loaded into reservoirs in the system and dispensed by the pipetting robot as stock solutions. The pipetting steps were set up in the FasTrans process program. Briefly, specific volumes of PBS solution were dispensed into the target wells, and in a separate set of wells, concentrated ethanolic lipid solutions and temoporfin stock solutions were combined and diluted to the desired concentrations in a separate well plate; these diluted ethanolic lipid-drug solutions were then injected into PBS according to the desired volume. To ensure effective mixing of each formulation and to disperse the mixtures effectively, each mixture was purged completely and aspirated three times at a flow rate of 105 µL·s^{-1}. In this study, the lipids chosen included EPC, Lipoid S75, and Lipoid S100, and their liposomal formulations are referred to hereafter as Liposome-EPC, Liposome-S75, and Liposome-S100, respectively. Although ethosomes were obtained in several formulations containing more than 20 weight% of ethanol, they were still discussed in terms of liposomes for consistency of evaluation.

Determination of particle size, size distribution, and zeta potential

Mean particle size and size distribution (i.e., polydispersity index; PDI) were measured using dynamic light scattering (DLS) on a DynaPro™ DLS plate reader (Wyatt Technology Corp., Santa Barbara, California, USA), which was equipped with a 10-mW He-Ne laser (832.5 nm) and operated at an angle of 173 degrees and a temperature of 25°C. Aliquots of the prepared 100 µL liposome suspensions were subsequently transferred into a 96-well quartz plate and measured by the DLS plate reader. Each sample was scanned 10 times, and the acquisition time was fixed at 30 seconds. Mean hydrodynamic diameter of the liposomes was calculated from the intensity of the scattered light using the Dynamics 6.12.0.3 software (Wyatt Technology). Zeta-potential measurements were performed using a Zetasizer Nano ZS (Malvern, Herrenberg, Germany), as reported in the literature (Kuntsche et al., 2010).

Effect of lipid concentration in ethanol on the size of liposomes

The lipid ethanolic stock solution was diluted by ethanol to the concentrations of 5, 10, 20, 30, 40, 50, 60, 70, 80, and 100 mg·mL^{-1}, respectively. Aliquots of 13.5 µL ethanolic lipid solution were pipetted into 180 µL of PBS solution using the pipetting robot. Each formulation was prepared in triplicate. Sizes of liposomes were characterized using the DLS plate reader.

Effect of ethanol:buffer ratios on the size of liposomes

Lipids were dissolved in ethanol at the concentration of 40 mg·mL^{-1}. Different amounts of ethanolic solution were pipetted into the PBS solution using the following ethanol:buffer ratios by volume: 1:30, 1:20, 1:13, 1:9, 1:5, 1:4, 1:3, 1:2, and 1:1. Sizes of liposomes were characterized using the DLS plate reader.

Incorporation of temoporfin into liposomes

Temoporfin and the respective lipids were codissolved in ethanol at different ratios of temoporfin to lipid. The concentration of lipid was fixed at 40 mg·mL^{-1}, whereas concentrations of temoporfin were 0.5, 1, 2, or 3 mg·mL^{-1}, respectively. The ethanolic solution was dispensed into the PBS solution at the volume ratio of 1:4. Sizes of liposomes were characterized using the DLS plate reader.

Incorporation efficiency was measured as follows. Liposomes were first prepared using the pipetting robot. An aliquot of these liposomes were extruded 21 times through a polycarbonate membrane (pore size, 100 nm), using a LiposoFast® miniextruder (Avestin, Ottawa, Ontario, Canada). Next, both the original liposomes and the extruded liposomes were destroyed by the 50-fold dilution of the formulation in methanol, followed by measuring the absorbance of temoporfin at the wavelength of 645 ± 10 nm, using the Fluostar microplate reader (BMG LABTECH GmbH, Offenburg, Germany). The concentration of temoporfin in the extruded liposomes, divided by that in the original liposomes, was used to quantify incorporation efficiency.

Adding functional phospholipid to modify liposome surface

To modify liposome features, mPEG$_{2000}$-DSPE was incorporated into liposomes. The lipids, temoporfin and mPEG$_{2000}$-DSPE, were codissolved in ethanol. The total molar concentration of lipids and mPEG$_{2000}$-DSPE was fixed at the same value as that of 40 mg·mL^{-1} of pure lipid, whereas the molar percentage of mPEG$_{2000}$-DSPE increased gradually (i.e., 1, 3, 5, 7, and 9%, respectively). The concentration of temoporfin was kept constant at 0.5 mg·mL^{-1}. Thereafter, aliquots of 36 µL of the ethanolic solution were injected into 144 µL of PBS solution to prepare liposomes, followed by characterization of size and zeta potential.

Visualization of liposomes by cryogenic transmission electron microscopy

Based on the aforementioned high-throughput screening of the liposomal formulations, one optimal formulation was determined for each lipid and visualized using cryogenic transmission electron microscopy (Cryo-TEM) to study their shape and lamellarity. For each sample, an aliquot of 5 µL of the corresponding liposome dispersion was deposited onto a perforated coated net of copper. Excess was removed from the samples with a sheet of filter paper. Samples were quickly frozen with liquid ethane (–170 to–180°C) in a cryo-box (Carl Zeiss NTS GmbH, Oberkochen, Germany). Excess ethane was removed by blotting samples in the cold, and samples were placed, with the help of a cryo-transfer device (Gatan 626-DH; Gatan, Inc., Pleasanton, California, USA), in a precooled Cryo-TEM (Philips CM 120) operated on 120 kV.

Stability of liposomes

The three optimal formulations for each lipid were prepared in large scale for studying their stability. A large amount of the selected formulations were prepared in one batch and stored at 4 and 23°C (room temperature), respectively. After 1, 2, 3, 4, 10, and 20 weeks, respectively, the sizes of the liposomes were measured.

Statistical analysis

All reported size measurements present mean values ± standard deviation ($n > 12$). Statistical analysis was carried out with the Student's t test, using Microsoft Excel 2007 (Microsoft Corp., Redmond, Washington, USA). A value of $P < 0.05$ was considered statistically significant.

Results and discussion

Effect of lipid concentration in ethanol on size of liposomes

After the injection of the ethanolic solution into the PBS solution, followed by triplicate mixing via purging and aspirating, the mixtures became opalescent, indicating that liposomes were formed. In general, the dispersions became increasingly intensely opalescent as the lipid concentration increased. The measured diameter and respective PDI values of the liposomes are shown in Figure 2. The diameter of liposomes increased gradually as the concentration of lipid in the injected ethanol increased. For each measured lipid concentration value, the Liposome-EPC based formulations exhibited the smallest measured average liposome size among the three kinds of liposomes investigated, with values ranging from 61 to 177 nm. When the lipid concentration was increased to more than 50 mg·mL^{-1}, the PDI began to rise to values higher than 0.1. The size of Liposome-S75 increased from 98 (5 mg·mL^{-1}) to 198 nm (60 mg·mL^{-1}) and finally reached 273 nm (100 mg·mL^{-1}), although during this change, PDI values did not increase considerably until the lipid concentration was above 100 mg·mL^{-1}. The size of Liposome-S100 was comparable with that of Liposome-EPC when the lipid concentration was equal or less than 40 mg·mL^{-1}. However, above 40 mg·mL^{-1}, the size increased more dramatically than in the case of Liposome-EPC. In particular, at concentrations greater than 60 mg·mL^{-1}, the size increased sharply and finally reached 2,157 nm at 100 mg·mL^{-1}. In confluence with this observation, the PDI values of liposomes at higher concentrations of more than 50 mg·mL^{-1} also increased sharply to 0.326, which was the upper measurement limit of the DLS plate reader.

Here, the size of liposomes was measured as the most important index to evaluate the formation of liposomes. To understand the relationship between parameters and size, a well-known nonequilibrium model of vesicle formation was introduced to illustrate the formation of liposomes in the ethanol-injection method (Figure 1) (Antonietti and Förster, 2003; Jahn et al., 2010; Lasic, 1988).

During the diffusion of ethanol into water, lipid molecules initially dissolved in ethanol become exposed to an increasingly polar environment with decreasing capacity for lipid solvation. At a critical polarity, lipid molecules aggregate and form disk-like or oblate micelles as an intermediate structure, which grow through coalescence and/or the integration of solubilized lipid molecules. These disk-like micelles are also called bilayered phospholipid fragments (BPFs) (Lasic, 1988). As the polarity of the surrounding microfluidic environment continues to increase, these BPFs close and form liposomes to eliminate exposure of the lipid hydrocarbon tails (Jahn et al., 2010). Therefore, the size of liposomes is related to microfluidic formation, as well as the growth and closure processes of the intermediate structures, which will be discussed below, respectively.

The lipid concentration in the injected solution plays an important role in the determination of the outcome of particle size (Domazou and Luisi, 2002). As a general rule, the lower the lipid concentration in the injected solution, the smaller the liposomes will be. On the other hand, increased lipid concentration facilitates the loading of drugs in liposomes. As a result of these conflicting phenomena, it is necessary to achieve a balance between liposome size and total drug loading. With this in mind, the lipid concentration in ethanol was studied first to obtain the suitable range of lipid concentrations for the ethanol-injection method. As shown in Figure 2, both size and PDI values increased as the lipid concentration in ethanol increased. The lipid concentration in ethanol affects two aspects of the formulation: the local lipid concentration when the injected ethanol diffused into the buffer and overall lipid concentration when liposomes were finally dispersed in the sample. During the diffusion of injected ethanol in the PBS solution, the high local lipid concentration means a high concentration of BPFs; as a consequence, the short distance between BPFs facilitates their chances for coalescence and increases the possible formation of larger liposomes. Additionally, many liposomes have a tendency toward aggregation during the formation process. The tendency may not be obvious at lower lipid concentrations, but can be strong at higher overall lipid concentrations, leading to greater liposome aggregations. This phenomenon has already been observed in the literature using TEM (Domazou and Luisi, 2002). At higher lipid concentrations (more than 60 mg·mL^{-1}), the size of Liposome-S100 was much bigger than the other two kinds of liposomes and showed the highest PDI values, implying that the aggregation tendency of Liposome-S100 was higher than the others.

Taking into consideration that, for many applications, the size and PDI values of liposomes should generally be as small as possible, while maintaining the overall weight fraction of liposomes as high, the concentration of lipid in the injected ethanol was maintained at 40 mg·mL^{-1} in the following experiments, which was also convenient for the comparison of these three lipids.

6   Kewei Yang et al.

Effect of the ethanol:buffer ratio on size of liposomes

To evaluate the range of ethanol:buffer ratios suitable for the preparation of liposomes, the lipid ethanolic solutions were injected into PBS solution in different ratios by volume, and the particle size was measured (Figure 3). As the ratio of ethanol to PBS solution increased from 1:30 to 1:4, the size of all three kinds of liposomes decreased slightly and reached a minimal value when the ethanol percentage by volume was 20% (ethanol:buffer ratio = 1:4). At percentages greater than 20% ethanol, size increased along with the increase in ethanol percentage. When the ethanol percentage reached 33%, the liposomes were still small, with average diameter values of approximately 200 nm. However, at the highest ethanol percentage of 50%, the size of the liposomes increased to more than 500 nm, in accordance with the observation of aggregations in the 96-well plate. Taken together, liposomes could be readily prepared when the ethanol concentration was in the range of 3.2–33%. For subsequent experiments, the ethanol:buffer ratio of 1:4 was selected, because the measured average liposome size was smallest at this ratio. Nevertheless, the demonstration of the efficacy of higher ethanol concentrations is still of importance for the design of other formulations in the future, as it indicates the accessibility of liposome formulations of high lipid concentrations through this route, which offers the possibility of increasing the loading capacity for drugs. In particular, when the volume ratio of ethanol to buffer is equal to or higher than 1:3, the formulations contain more than 20 weight% of ethanol and, therefore, belong to the ethosome classification, which may lead to enhanced penetration through the SC.

Effect of temoporfin concentration in ethanol on size of liposomes and incorporation efficiency

To check how the incorporation of temoporfin affects size and size distribution of liposomes, different amounts of temoporfin were codissolved into lipid ethanolic solution. The relationship between the concentration of temoporfin and the resulting average diameter of temoporfin-loaded liposomes is shown in Figure 4. Incorporation of temoporfin increased the size of Liposome-EPC gradually (i.e., from 108 to 157 nm) as more and more temoporfin was dissolved in the injected ethanolic solution. In comparison, the size of Liposome-S75 did not change significantly, except that at the
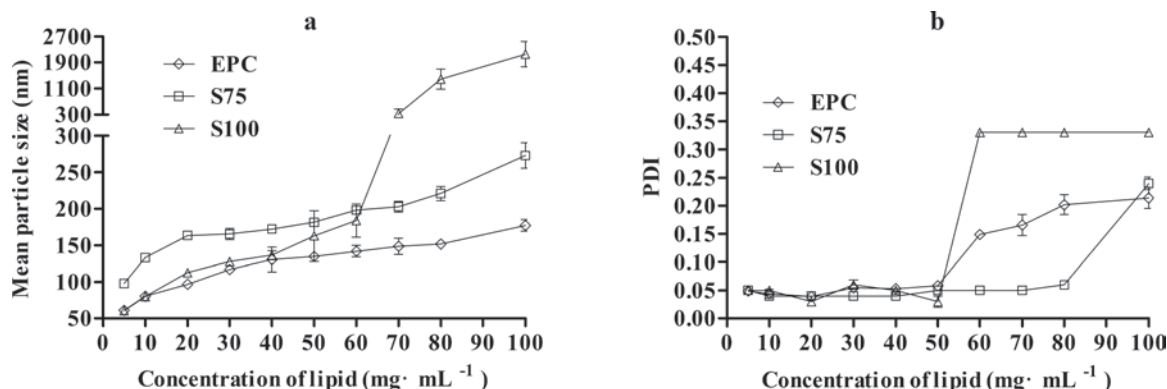

Figure 2. Particle size (**a**) and PDI values (**b**) of liposomes, which were prepared by injection of lipid ethanolic solution at different lipid concentrations, varying from 5 to 100 mg•mL⁻¹ (*n* = 3).
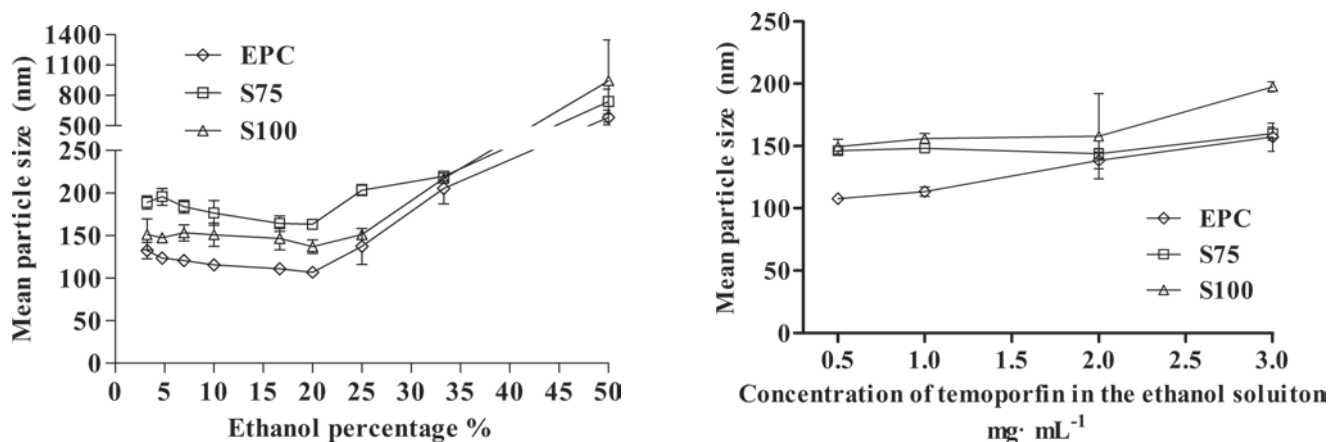

Figure 3. Mean particle size of liposomes, which were prepared in different ethanol:buffer ratios by volume. The resulting ethanol percentage (%) by volume in the final dispersion varied from 3.2 to 50% (*n* = 3).

Figure 4. Mean particle size of liposomes, which were prepared by injecting the ethanolic solution at different temoporfin concentrations. The concentration of lipid in ethanol was 40 mg•mL⁻¹, and the ethanol:buffer ratio was 1:4 (*n* = 3).

highest temoporfin concentration of 3 mg·mL^{-1}, where size increased slightly to 160 nm. The size of Liposome-S100 increased modestly from 150 to 158 nm as the concentration of temoporfin increased from 0.5 to 2 mg·mL^{-1}, then grew up to 198 nm at 3 mg·mL^{-1}. In summary, the increase of size as a function of temoporfin was acceptable in all cases.

In addition to size, incorporation efficiency of drug is also an important factor to be studied for drug-loaded liposomes. Consequently, incorporation efficiency of temoporfin into liposomes was evaluated. As shown in Figure 5, incorporation efficiency of temoporfin in all formulations was consistently above 95% and, in many cases, reached almost 100%. When the concentration of temoporfin in the injected ethanolic solution increased from 0.5 to 3 mg·mL^{-1}, incorporation efficiency did not change significantly, suggesting that this drug is very readily incorporated into liposomes. At least within this concentration range, effectively, all temoporfin was incorporated into liposomes. Especially, when the concentration of temoporfin in ethanolic solution was

3 mg·mL^{-1}, the weight ratio of temoporfin to lipid was 3:40, the same as the ratio used in the well-developed liposomal formulation, Foslip (biolitec AG), containing 1.5 mg·mL^{-1} of temoporfin and 20 mg·mL^{-1} of phospholipids (phosphatidylcholine and phosphatidylglycerol) (Kuntsche et al., 2010). Because temoporfin is a very lipophilic drug with a high logP value of 9.24 (Chen et al., 2011), the high incorporation efficiency of more than 95% confirmed that the ethanol-injection method is promising for incorporation of hydrophobic drugs (Jaafar-Maalej et al., 2010), being a potential alternative to the traditional preparation method.

Based on the results from Figures 4 and 5, temoporfin can be readily incorporated into liposomes by the ethanol-injection method, yielding liposome suspensions with comparable diameters. To save the cost of temoporfin, 0.5 mg·mL^{-1} in the injected ethanolic solution was used in the following experiments.

Modification of liposomes using mPEG$_{2000}$-DSPE

When mPEG$_{2000}$-DSPE was incorporated into liposomes, the size and surface charge of liposomes were supposed to change and, therefore, were measured after adding different amount of mPEG$_{2000}$-DSPE. As shown in Figure 6a, all three kinds of liposomes demonstrated an easily observable decreasing trend in terms of diameter, as the molar percentage of mPEG$_{2000}$-DSPE increased from 0 to 9% (with the exception of the point of Liposome-EPC, containing 1 mol% mPEG$_{2000}$-DSPE). The size of liposomes containing 9 mol% of mPEG$_{2000}$-DSPE decreased significantly, compared to those liposomes without mPEG$_{2000}$-DSPE, and reached a minimal diameter of approximately 50 nm.

In addition to size, stability is another consideration with liposomes. To increase the stability of liposomes, different strategies are utilized, especially using some functional lipids to modify the characteristics of liposomes. For example, cholesterol is used to increase the rigidity of liposomes. Some charged phospholipids are incorporated into liposomes to prepare cationic or anionic liposomes, and thus the liposomes are stabilized via electrostatic repulsion. Polymers containing poly(ethyleneglycol) (PEG) are the most commonly used steric stabilizers for
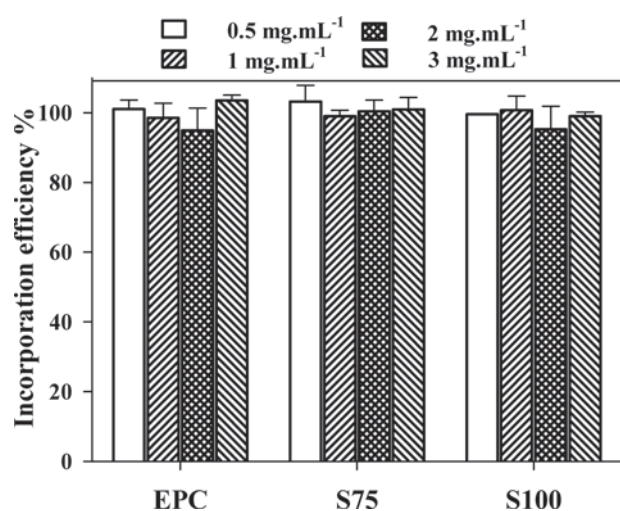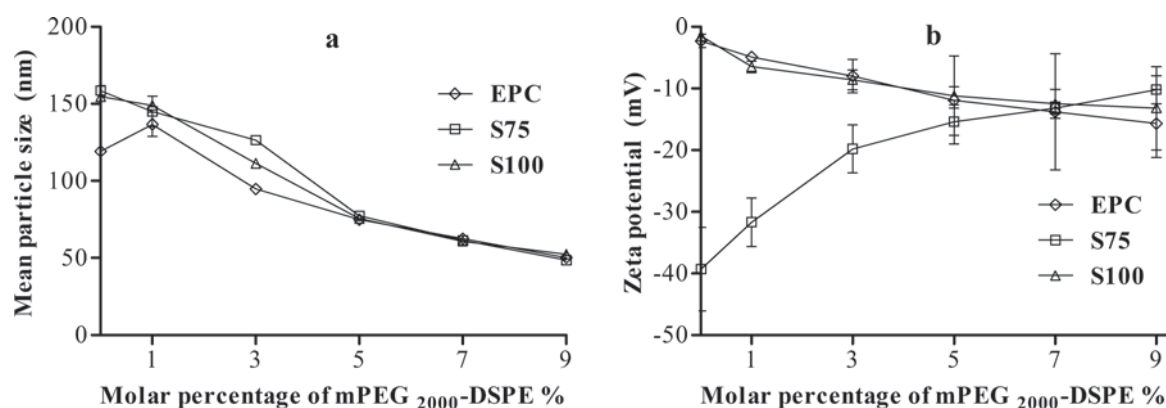

Figure 5. Incorporation efficiency of temoporfin into three types of liposomes, which were prepared by injecting the ethanolic solution at different temoporfin concentrations. The concentration of lipid in ethanol was 40 mg·mL^{-1}, and the ethanol:buffer ratio was 1:4 ($n = 3$).

Figure 6. Particle size (**a**) and zeta potential (**b**) of liposomes containing different amounts of mPEG$_{2000}$-DSPE ($n = 3$).

8   Kewei Yang et al.

liposomes (Knop et al., 2010), as the PEG segments are able to form a hydrated shell around liposomes and thus prevent the aggregation of liposomes.

In this study, $mPEG_{2000}$-DSPE was used to modify liposomes, aiming to increase their stability. As expected, it was found that $mPEG_{2000}$-DSPE helped to decrease the size of liposomes significantly (Figure 6a), which is supposed to make the liposomes more stable. Because of its amphiphilic diblock copolymer nature, $mPEG_{2000}$-DSPE is known to readily form micelles as a result of its extremely low critical micelle concentration of 6.3 μM (Ishida et al., 1999). Johnsson and Edwards reported that the addition of PEG lipid decreased the diameter of discoidal micelles composed of lipid and $mPEG_{2000}$-DSPE or $mPEG_{5000}$-DSPE (Johnsson and Edwards, 2003). Similarly, the addition of $mPEG_{2000}$-DSPE in ethanolic solution reduces the size of intermediate disk-like micelles, consequently yielding smaller liposomes. Additionally, the PEG chains form a hydrophobic coronal on the surface of liposomes, which prevents the aggregation of liposomes and, therefore, reduces the average size of liposomes. It should also be considered that the additional hydrophilic coronal composed of PEG can also increase the size of liposomes, to some extent. This is probably why the diameter of Liposome-EPC, containing 1 mol% of $mPEG_{2000}$-DSPE, was significantly larger than the unmodified liposomes.

In Figure 6b, Liposome-EPC and Liposome-S100 were almost neutrally charged, if no $mPEG_{2000}$-DSPE was present. The higher the percentage of $mPEG_{2000}$-DSPE present, the more negative the Liposome-EPC and Liposome-S100 measurements became. Finally, the zeta potential of liposomes decreased to approximately –15 mV at 9 mol% of $mPEG_{2000}$-DSPE. In contrast, the zeta potential of Liposome-S75 became less negative as more $mPEG_{2000}$-DSPE was incorporated into liposomes, but remained negatively charged with 9 mol% of $mPEG_{2000}$-DSPE.

EPC and S100 are neutral lipids; correspondingly, Liposome-EPC and Liposome-S100 would be liposomes without exhibiting a significant zeta potential. As is known, $mPEG_{2000}$-DSPE is a negatively charged molecule. So, when $mPEG_{2000}$-DSPE was incorporated into the neutral liposomes, the zeta potential of liposomes became negative as the molar percentage of $mPEG_{2000}$-DSPE increased (Figure 6b). In contrast, S75 contained negative components, and thus, Liposome-S75 was negatively charged with a zeta potential of approximately –40 mV.

When a portion of S75 lipids was replaced by $mPEG_{2000}$-DSPE, the charge of the lipid bilayer changed little and remained negative. However, the $mPEG_{2000}$ layer on the surface shields the negative charge of lipids in the bilayer, leading to a reduced negative zeta potential. The more $mPEG_{2000}$-DSPE is contained in liposomes, the stronger is the shielding effect and, consequently, the less negative the liposomes. Therefore, the zeta potential of Liposome-S75 became less negative with increasing percentage of $mPEG_{2000}$-DSPE (Figure 6b). In this situation, $mPEG_{2000}$-DSPE played a multifunctional role, which decreased the zeta potential of neutral liposomes, but increased that of negatively charged liposomes.

Liposomes containing 9 mol% of $mPEG_{2000}$-DSPE displayed the smallest diameter and were still negatively charged. As a result, they were considered to be the most stable of the formulations tested and were thus selected for subsequent stability investigations.

In total, four parameters were investigated step-by-step by preparing and screening 87 formulations in triplicate (i.e., 261 samples) within 1 month, demonstrating that this method is very fast and efficient. As a result, a proper range for each parameter was respectively obtained, providing useful directions for practical formulation development, where the detailed values are determined by the specific requirements (e.g., administration dose and cost considerations). For the study described in this article, the primary aim was the development of the formulation with the smallest size and highest potential for stability; consequently, the following combination was selected: 36.4 mg·mL^{-1} of lipid, 13.1 mg·mL^{-1} of $mPEG_{2000}$-DSPE (9 mol%), and 0.5 mg·mL^{-1} of temoporfin in the ethanolic solution, using a 1:4 ethanol:buffer ratio. The concentration of temoporfin in ethanol used was 0.5 mg·mL^{-1}, but could be increased by up to 3 mg·mL^{-1}. Those liposomes prepared in this condition were selected as the optional formulations for further investigation in the following experiments.

Morphology of the liposomes

Figure 7 shows Cryo-TEM images of the optimal formulations for each lipid. The vesicles were spherical and unilamellar. Most liposomes were smaller than 100 nm in diameter, with an average of approximately 50 nm. The uniformity of Liposomes-S75 was the best, whereas the Liposome-EPC and Liposome-S100 suspensions
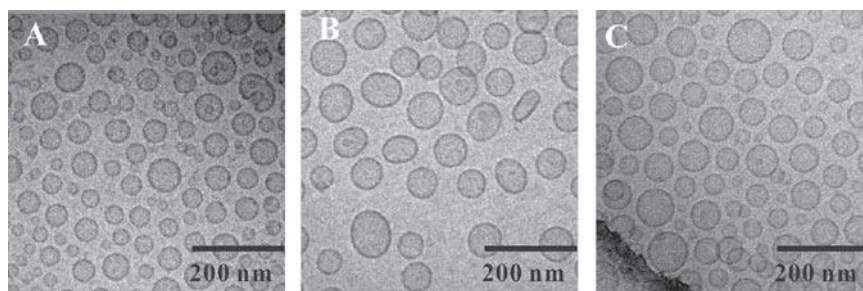

Figure 7. Cryo-TEM images of liposomes. (**A**) Liposome-EPC, (**B**) Liposome-S75, and (**C**) Liposome-S100.

contained some smaller vesicles. The Cryo-TEM images of liposomes in Figure 7 confirmed their small size and narrow size distribution obtained from the DLS plate reader (Figure 6a), suggesting that the high-throughput characterization method using DLS is reliable. The spherical unilamellar morphology, and small size of liposomes, is similar to that of liposomes containing soybean phosphatidylcholine and 20% ethanol, as reported by Dragicevic-Curic et al. (2009), which showed strong penetration enhancement through the skin, so we hypothesize that the three formulations prepared by us are very likely to own the same advantage and are worth performing further investigation in this direction.

Stability of liposomes

The stability of liposomes was examined with respect to mean particle size and PDI values. Figure 8 shows the size and PDI during 20 weeks of storage at 4 or 23°C. When stored at 4°C, the diameter of Liposome-S75 did not change significantly, whereas the diameter of Liposome-EPC and Liposome-S100 increased slightly, by 8 and 12 nm, respectively. In line with the small size increase, the PDI values of Liposome-EPC and Liposome-S100 also increased only slightly, but the PDI values of Liposome-S75 remained constant, confirming that Liposome-S75 was the most stable formulation at 4°C. At 23°C, the size of all three formulations increased slowly during 20 weeks of storage, and the increasing speed of size was bigger than that at 4°C; however, their PDI values did not increase significantly. In addition, the Cryo-TEM showed

that these liposomes were still small unilamellar spheres after 10 weeks of storage (data not shown). Although there was a small increase in size during 20 weeks at 4 or 23°C, these selected formulations could still be considered stable, in view of their diameters being smaller than 100 nm with low PDI values.

The stability study demonstrated that the selected optimal formulations maintained small size and low PDI values within 20 weeks (Figure 8), and the liposomes were more stable at 4 than at 20°C. The aim of adding $mPEG_{2000}$-DSPE to increase liposomal stability was achieved; however, long-term stability still needs to be studied in the future and is already in progress.

Besides the three selected optimal formulations, more liposomal formulations can be prepared for different applications (e.g., the concentration of temoporfin and ethanol may be varied) and many other lipids as well as different drugs can be studied, too. In addition, this method can be further refined. For example, the 96-well plate can be readily replaced by 384- or even 1,536-well plates, to prepare much a smaller amount of liposomes, which is of great use to save drugs and materials—in particular, when the drug supply is scarce or very expensive. Additionally, the use of automated liquid dispensing offers the chance of controlling the flow rate of the injection process, enabling the possibility to study process parameters and their effects on the final performance properties of the formulation. The use of automated pipetting is compatible with liquids with a broad range of viscosities, extending the prospects of solvent/nonsolvent systems
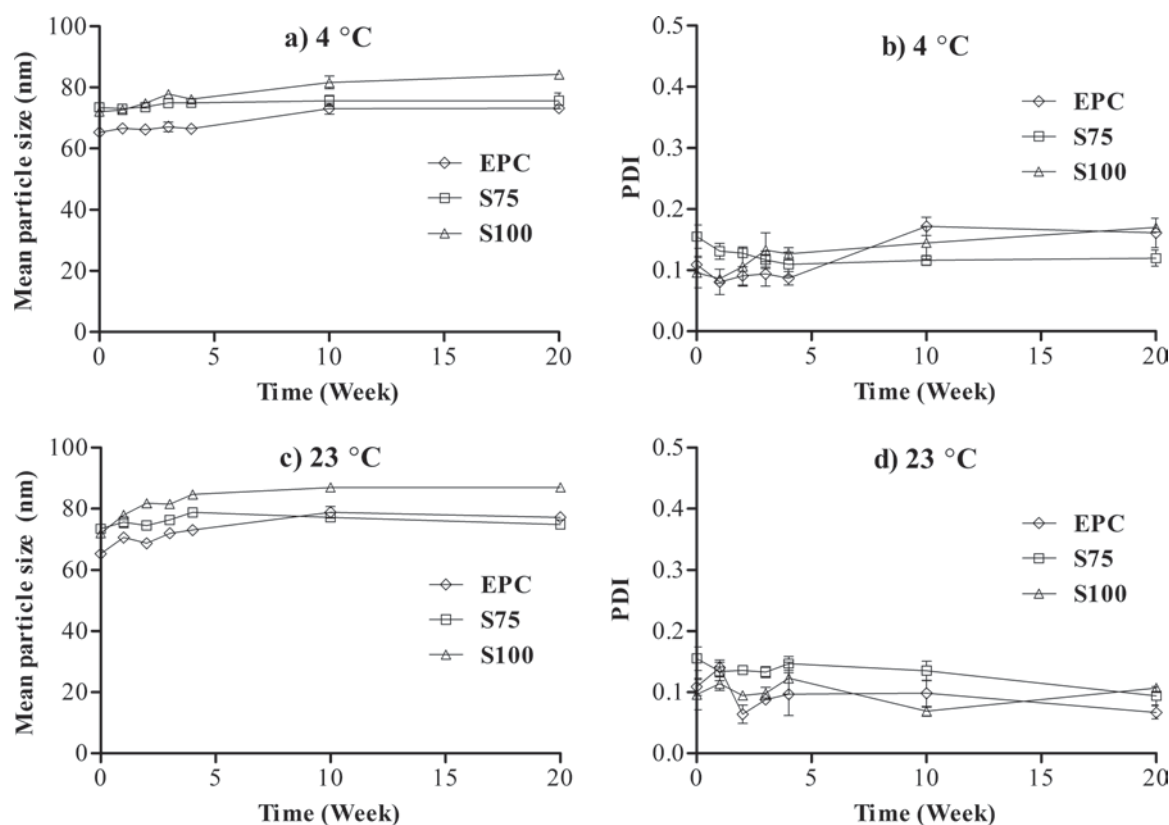

Figure 8. Mean particle size and PDI values of liposomes after storage at 4 or 23°C for 1~20 weeks ($n = 3$).

10   Kewei Yang et al.

beyond ethanol and water. Therefore, the automation of the ethanol-injection method has a broad potential for applications, including both the high-throughput screening of liposomal formulations in the lab and the scale-up of production.

We need to point out that the ethanol in the suspensions needs to be removed for the real production of conventional liposomal formulations where ethanol content should be restricted, whereas removing is unnecessary in the case of ethosomal formulations for topical applications to the skin. Several techniques, such as ultracentrifugation, ultrafiltration, dialysis, rotary evaporation, and gel filtration, were reported to remove ethanol from liposomes easily (Batzri and Korn, 1973; Cortesi et al., 2010; Jaafar-Maalej et al., 2010). Our preliminary experiments confirmed that small liposomes (i.e., 60~~80 nm) could be obtained after the removal of ethanol. In addition, lyophilization, besides cross-flow dialysis, is a more applicable approach for the scale-up of production (Isele et al., 1994; Wagner et al., 2002), which is especially attractive to high-throughput screening of a large number of samples and, therefore, is in the scope of the following study.

Conclusions

This work shows an innovative strategy for the high-throughput screening of liposomal formulations by automation of ethanol injection. Using three kinds of lipids, altogether, 87 different formulations (261 samples) were screened in a high-throughput way. Factors affecting the properties of liposomes were investigated step-by-step, where liposomes were prepared automatically, and, when applicable, were characterized automatically, making it easy and fast to optimize the liposomal formulations of temoporfin. Finally, three optimal liposomes were prepared, which were stable at least for 20 weeks with only a small increase of size. The small liposome diameter of approximately 50 nm enables these formulations to be ideal for i.v. injection, whereas the high content of ethanol makes those liposomes have the potential for dermal and transdermal delivery of temoporfin. The results also lay a good foundation for the development of formulations using other drugs and lipids. In the future, the potential for systematic and topical administration still needs to be investigated. In summary, this high-throughput screening strategy is fast, automated, materially efficient, labor-saving, time-saving, economic, facile, and highly reproducible. This approach is promising for the development of new formulations; because of the nature of the process, the approach is readily amenable to the scale-up of production.

Acknowledgments

Declaration of interest

References

Antonietti, M., Förster, S. (2003). Vesicles and liposomes: a self-assembly principle beyond lipids. Adv Mater 15:1323–1333.

Batzri, S., Korn, E. D. (1973). Single bilayer liposomes prepared without sonication. Biochim Biophys Acta 298:1015–1019.

Biel, M. A. (2002). Photodynamic therapy in head and neck cancer. Curr Oncol Rep 4:87–96.

biolitec AG. (2008). Summary of product characteristics. biolitec AG website. Available at: http://www.biolitecpharma.com/foscan/summary-of-product-characteristics.html. Accessed on August 7, 2008.

Brown, S. B., Brown, E. A., Walker, I. (2004). The present and future role of photodynamic therapy in cancer treatment. Lancet Oncol 5:497–508.

Buchholz, J., Kaser-Hotz, B., Khan, T., Rohrer Bley, C., Melzer, K., Schwendener, R. A., Roos, M., et al. (2005). Optimizing photodynamic therapy: in vivo pharmacokinetics of liposomal meta-(tetrahydroxyphenyl)chlorin in feline squamous cell carcinoma. Clin Cancer Res 11:7538–7544.

Chen, M., Liu, X., Fahr, A. (2011). Skin penetration and deposition of carboxyfluorescein and temoporfin from different lipid vesicular systems: in vitro study with finite and infinite dosage application. Int J Pharm 408:223–234.

Cortesi, R., Romagnoli, R., Drechsler, M., Menegatti, E., Zaid, A. N., Ravani, L., Esposito, E. (2010). Liposomes- and ethosomes-associated distamycins: a comparative study. J Liposome Res 20:277–285.

Domazou, A. S., Luisi, P. L. (2002). Size distribution of spontaneously formed liposomes by the alcohol injection method. J Liposome Res 12:205–220.

Dragicevic-Curic, N., Scheglmann, D., Albrecht, V., Fahr, A. (2009). Development of liposomes containing ethanol for skin delivery of temoporfin: characterization and in vitro penetration studies. Coll Surf B Biointerf 74:114–122.

Engelhardt, V., Krammer, B., Plaetzer, K. (2010). Antibacterial photodynamic therapy using water-soluble formulations of hypericin or mTHPC is effective in inactivation of Staphylococcus aureus. Photochem Photobiol Sci 9:365–369.

Glanzmann, T., Hadjur, C., Zellweger, M., Grosjean, P., Forrer, M., Ballini, J. P., et al. (1998). Pharmacokinetics of tetra(m-hydroxyphenyl) chlorin in human plasma and individualized light dosimetry in photodynamic therapy. Photochem Photobiol 67:596–602.

Godin, B., Touitou, E. (2003). Ethosomes: new prospects in transdermal delivery. Crit Rev Ther Drug Carrier Syst 20:63–102.

Hamblin, M. R., Hasan, T. (2004). Photodynamic therapy: a new antimicrobial approach to infectious disease? Photochem Photobiol Sci 3:436–450.

Isele, U., van Hoogevest, P., Hilfiker, R., Capraro, H. G., Schieweck, K., Leuenberger, H. (1994). Large-scale production of liposomes containing monomeric zinc phthalocyanine by controlled dilution of organic solvents. J Pharm Sci 83:1608–1616.

Ishida, T., Iden, D. L., Allen, T. M. (1999). A combinatorial approach to producing sterically stabilized (Stealth) immunoliposomal drugs. FEBS Lett 460:129–133.

Jaafar-Maalej, C., Diab, R., Andrieu, V., Elaissari, A., Fessi, H. (2010). Ethanol injection method for hydrophilic and lipophilic drug-loaded liposome preparation. J Liposome Res 20:228–243.

Jahn, A., Stavis, S. M., Hong, J. S., Vreeland, W. N., Devoe, D. L., Gaitan, M. (2010). Microfluidic mixing and the formation of nanoscale lipid vesicles. ACS Nano 4:2077–2087.

Jesorka, A., Orwar, O. (2008). Liposomes: technologies and analytical applications. Annu Rev Anal Chem 1:801–832.

Johnsson, M., Edwards, K. (2003). Liposomes, disks, and spherical micelles: aggregate structure in mixtures of gel phase phosphatidylcholines and poly(ethylene glycol)-phospholipids. Biophys J 85:3839–3847.

Jori, G. (2006). Photodynamic therapy of microbial infections: state of the art and perspectives. J Environ Pathol Toxicol Oncol 25:505–519.

Justo, O. R., Moraes, Â. M. (2010). Economical feasibility evaluation of an ethanol injection liposome production plant. Chem Eng Technol 33:15–20.

Knop, K., Hoogenboom, R., Fischer, D., Schubert, U. S. (2010). Poly(ethylene glycol) in drug delivery: pros and cons as well as potential alternatives. Angew Chem Int Ed Engl 49:2–23.

Kubler, A. C., Haase, T., Staff, C., Kahle, B., Rheinwald, M., Muhling, J. (1999). Photodynamic therapy of primary nonmelanomatous skin tumours of the head and neck. Lasers Surg Med 25:60-68.

Kuntsche, J., Freisleben, I., Steiniger, F., Fahr, A. (2010). Temoporfin-loaded liposomes: physicochemical characterization. Eur J Pharm Sci 40:305–315.

Lasch, J., Weissig, V., Brandl, M. (2003). Preparation of liposomes. In: Torchilin, V., Weissig, V. (Eds.), Liposomes: a practical approach, 2nd ed. (pp. 4–16). Oxford, UK: Oxford University Press.

Lasic, D. D. (1988). The mechanism of vesicle formation. Biochem J 256:1–11.

Lassalle, H. P., Dumas, D., Grafe, S., D'Hallewin, M. A., Guillemin, F., Bezdetnaya, L. (2009). Correlation between *in vivo* pharmacokinetics, intratumoral distribution, and photodynamic efficiency of liposomal mTHPC. J Contr Rel 134:118–124.

Lorenz, K. J., Maier, H. (2008). Squamous cell carcinoma of the head and neck. Photodynamic therapy with Foscan. HNO 56:402–409.

Maitani, Y., Igarashi, S., Sato, M., Hattori, Y. (2007). Cationic liposome (DC-Chol/DOPE = 1:2) and a modified ethanol injection method to prepare liposomes, increased gene expression. Int J Pharm 342:33–39.

Mozafari, M. R. (2005). Liposomes: an overview of manufacturing techniques. Cell Mol Biol Lett 10:711–719.

Redmond, R. W., Gamlin, J. N. (1999). A compilation of singlet oxygen yields from biologically relevant molecules. Photochem Photobiol 70:391–475.

Stano, P., Bufali, S., Pisano, C., Bucci, F., Barbarino, M., Santaniello, M., et al. (2004). Novel camptothecin analogue (gimatecan)-containing liposomes prepared by the ethanol injection method. J Liposome Res 14:87–109.

Touitou, E. (1996). Compositions for applying active substances to or through the skin. United States Patent and Trademark Office: (Patent No.) 5540934.

Touitou, E. (1998). Composition for applying active substances to or through the skin. United States Patent and Trademark Office: (Patent No.) 5716638.

Touitou, E., Dayan, N., Bergelson, L., Godin, B., Eliaz, M. (2000). Ethosomes—novel vesicular carriers for enhanced delivery: characterization and skin penetration properties. J Contr Rel 65:403–418.

Wagner, A., Vorauer-Uhl, K., Katinger, H. (2002). Liposomes produced in a pilot scale: production, purification, and efficiency aspects. Eur J Pharm Biopharm 54:213–219.

Wainwright, M. (1998). Photodynamic antimicrobial chemotherapy (PACT). J Antimicrob Chemother 42:13–28.

RIGHTSLINK

4 Discussion

In this dissertation, temoporfin was incorporated into different liposomal formulations for the aim of APDT. To achieve a bacteria-targeting delivery of temoporfin, the surface of liposomes was modified with either an antimicrobial peptide (WLBU2) or a lectin (WGA). Then a high-throughput method based on ethanol injection method was developed to screen other liposomal formulations loading temoporfin. In this section, I will discuss: the improvement of APDT using bacteria-targeting liposomes; how to take use of the high-throughput method to develop more liposomal formulations for APDT; and the potential clinical applications of liposomes for APDT.
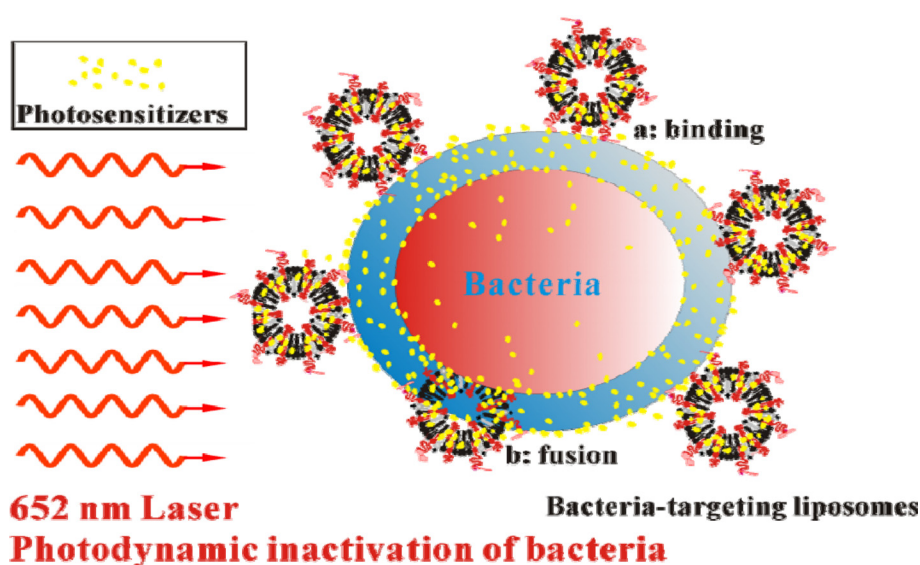
4.1 Improvement of APDT using bacteria-targeting liposomes

In publication 1 and 2, both the WGA-liposomes and the WLBU2-liposomes increased the delivery of temoporfin to *S. aureus* and *P. aeruginosa*. Subsequently, the *in vitro* APDT efficiency was increased, too. These results confirm our previous hypothesis that the bacteria-targeting liposomes do enhance APDT compared to unmodified liposomes.

The delivery of liposomal temoporfin to bacteria is illustrated in Fig. 4-1. Both modified liposomes are able to bind to *S. aureus* and *P. aeruginosa* via their conjugated bacteria-targeting ligands*,* and thus increase the local concentration of temoporfin around bacteria and facilitate the release of temoporfin from liposomes to bacterial cell walls in the vicinity. What is more, the cationic lipid, DOTAP, may gradually translocate in the cell wall because of the electrostatic interaction with the negatively charged cell walls, disturb the cell walls, increase their permeability for temoporfin, and further enhance the translocation of temoporfin into or across the

4 Discussion

cytoplasmic membrane, resulting in effective APDT. In addition, fusion of liposomes with the gram-negative bacterial outer membrane has been extensively studied and proved using different techniques, *e.g.* TEM and flow cytometry (Mugabe et al., 2006; Sachetelli et al., 2000). This fusion phenomenon is a big advantage of liposomes for antibiotics delivery, and may also take place in our experiments, helping overcome the obstacle of the densely packed outer membrane and deliver temoporfin directly into cell walls.

Figure 4-1 The bacteria-targeting liposomes bind to bacteria or even fuse with the bacteria, consequently increase the delivery of temoporfin to bacteria. After light illumination, the photosensitizers (temoporfin) generate reactive oxygen species, *e.g.* $^1O_2$, resulting in photodynamic inactivation of bacteria.

By comparing the results in both publications, it was found that WLBU2-liposomes were obviously more effective than WGA-liposomes with respect to APDT against both species of bacteria: WLBU2-liposomes eradicated MRSA at 1.25 μM after 90 min incubation, while WGA-liposomes eradicated MRSA at 12.5 μM after 90 min incubation; WLBU2-liposomes induced maximal more than 3 $\log_{10}$

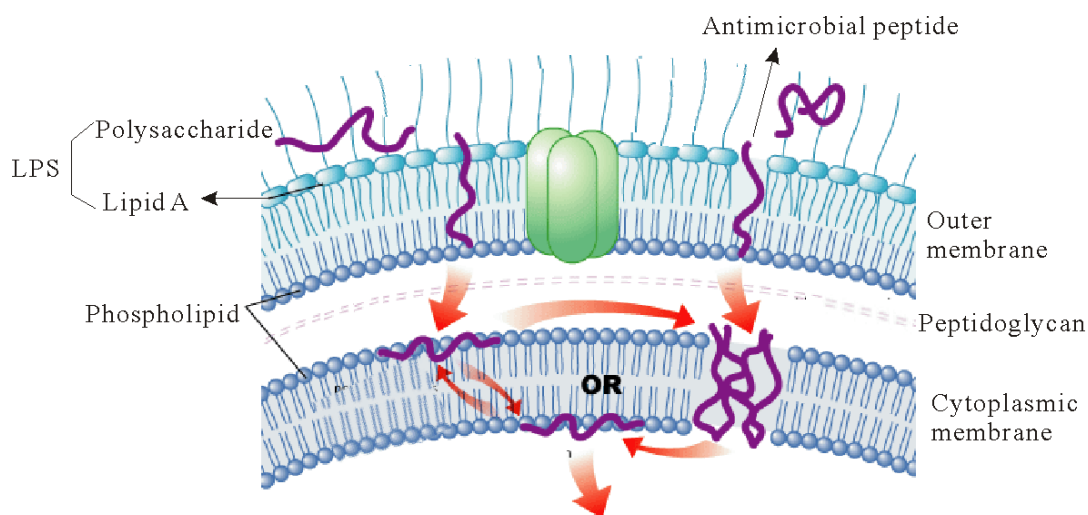reduction of *P. aeruginosa*, whereas WGA-liposomes induced maximal 2 $\log_{10}$ reduction of *P. aeruginosa*. The difference in APDT efficiency suggests that WLBU2 is a better bacteria-targeting ligand than WGA, which is assumed to be caused by the different binding mechanism of the two ligands with bacteria.

WGA recognizes the *N*-acetylglucosamine group, which is prevalent in the peptidoglycan of gram-positive bacterial cell walls (Sizemore et al., 1990) and is also available in the surface of *P. aeruginosa*, although not as much as in *S. aureus* (Avni et al., 1987; Strathmann et al., 2002). Therefore, WGA only helps WGA modified liposomes bind to the surface of bacteria.

The antimicrobial peptide WLBU2 is an amphiphilic cationic peptide, and owns a different bacteria-binding mechanism as compared to WGA. The antimicrobial function of amphiphilic cationic peptides is illustrated by their interaction with gram-negative bacteria in Fig. 4-2. They are proposed to associate with the negatively charged surface of the outer membrane, mainly due to the presence of highly anionic LPS. Then they either neutralize the charge over a patch of outer membrane, creating cracks through which the peptides can cross the outer membrane, or actually bind to the divalent cation binding sites on LPS, and disrupt the densely packed outer membrane. In case of gram-positive bacteria, these peptides may cross the thick porous peptidoglycan layer and approach the cytoplasmic membrane. In both cases, the peptides will further disturb the cytoplasmic membrane as shown in Fig. 4-2 (Hancock, 2001). The peptides' ability to perturb the outer membrane and cytoplasmic membrane will improve the diffusion of temoporfin into the cells, which may explain why the WLBU2 modified liposomes resulted in more effective APDT than the WGA modified liposomes.

Figure 4-2 The interaction of antimicrobial peptide with bacterial outer membrane and cytoplasmic membrane of gram-negative bacteria. Cited from (Wilcox, 2004). LPS: lipopolysaccharide.

4.2 Application of high-throughput screening method to development of liposomal formulations for APDT.

The used liposomes preparation method in Publication 1 and 2 are the traditional film-hydration method, where preparation of one formulation took more than two hours. For preparation of a few samples, this method might be acceptable. But for screening of dozens or hundreds of liposomal formulations, this traditional method is not preferable, because it is both time- and labor-consuming, and the reproducibility is sometimes a problem. To accelerate the development process of liposomal formulations loading temoporfin, we aimed to develop a faster and more convenient preparation method.
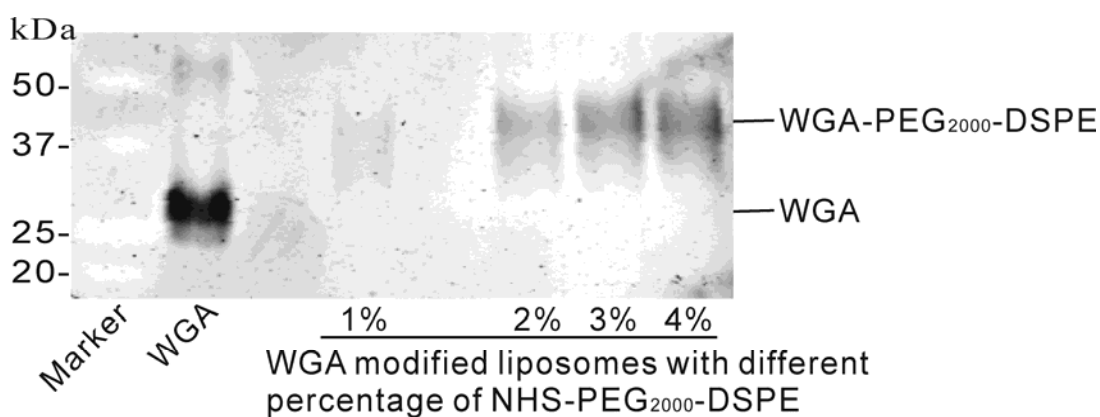
As shown in Publication 3, the high-throughput screening method demonstrates some attractive capabilities, making the fast screening of liposomal formulations possible. This high-throughput strategy is just recently developed, so there remain a lot of opportunities to pioneer new applications, *e.g.* in the field of APDT.

4.2.1 Preparation of bacteria-targeting liposomes

This high-throughput method can be used to prepare a series of bacteria-targeting liposomes quickly within one step. In one experiment, the anchor lipid: DSPE-PEG$_{2000}$-NHS was co-dissolved with temoporfin and EPC in ethanol, while WGA was dissolved in the aqueous phase. The liposomes were prepared in the same way as described in Publication 3. After injection of ethanolic solution, the liposomes were formed and the DSPE-PEG$_{2000}$-NHS was integrated into the lipid bilayer, with some NHS residue on the surface. As soon as the liposomes were formed, the WGA in the aqueous phase started reacting with the anchor lipid. The conjugation of WGA with DSPE-PEG$_{2000}$-NHS was proved using SDS-PAGE (Fig. 4-3). Increasing the concentration of anchor lipid increased the liposome-linked WGA, but did not increase the molecular weight of WGA-PEG$_{2000}$-DSPE conjugates, implying that the average number of anchor lipids linked to one WGA was same in this range of anchor lipid concentration. It will be interesting to test if the increasing conjugated WGA on liposomes will increase the APDT effect.

Figure 4-3 Detection of the conjugation of WGA to liposomes using SDS-PAGE. The liposomes were composed of EPC, DOTAP, mPEG$_{2000}$-DSPE and NHS-PEG$_{2000}$-DSPE. The molar percentage of NHS-PEG$_{2000}$-DSPE varied from 1% to 4%, while the total amount of PEG-lipid was fixed at 9 mol %. The excess WGA and ethanol were removed using ultracentrifuge (150,000g, 1h).

Besides WGA, the other amino-containing ligands may also be linked to liposomes using DSPE-PEG$_{2000}$-NHS, such as peptides and antibodies. This high-throughput method is also suitable for the conjugation reaction using maleimide containing anchor lipids, so as to conjugate thiol group-containing ligands to liposomes.

One advantage of this method is the higher conjugation efficiency compared to that in the film-hydration method (Publication 1 and 2), because the conjugation reaction starts immediately after the contact of DSPE-PEG$_{2000}$-NHS with water, and hence the hydrolysis of NHS residue during film hydration is avoided.

Another special advantage of this method is its economically efficient utilization of the relatively expensive materials, such as the drug and the anchor lipid. In the 96-well plate, the volume of each sample in a single well can be as small as tens of microliters, much smaller than the hundreds of microliters in case of normal film hydration method.

4.2.2 Investigation of liposomal compositions

In publication 1 and 2, only a few liposomal formulations were investigated, but they could probably not be the best formulations for bacteria-targeting delivery of PSs. Therefore, there is still necessity to investigate more liposomal formulations.

Jones *et al* have investigated the interaction between liposomes and bacterial biofilms, and found that the adsorption of liposomes to bacteria was closely related to the bacteria species and liposomal compositions, *e.g.* the molar percentage of the charged phospholipids, the head groups of phospholipids, the charge of liposomes and the concentration of liposomes. There was an optimum adsorption in a certain mol % range of charged phospholipids (Jones et al., 1997; Kaszuba et al., 1997). Higher molar percentage of charged phospholipids would not further increase the adsorption and even decrease the adsorption. Smistad *et al* confirmed this point when studying
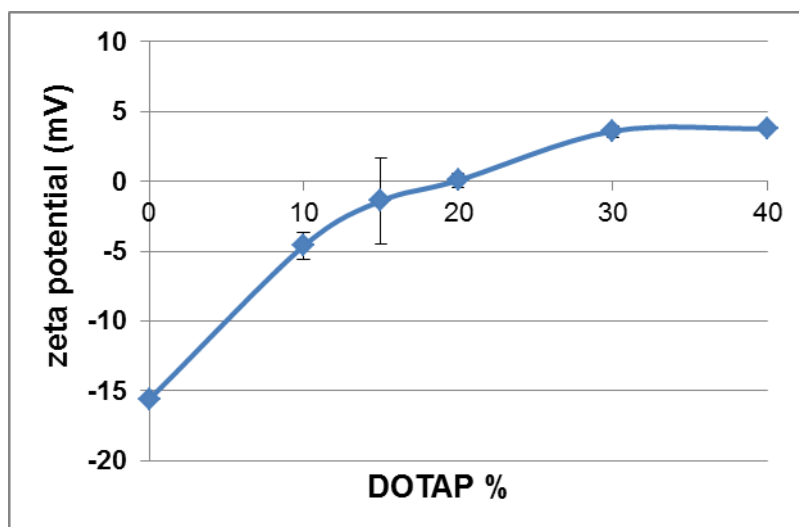
the interaction of various liposomes with *Candida* biofilm, pointing out that high-level amount of cationic lipids would result in less adsorption to *Candida* biofilms. They explained this phenomenon as follows: the adsorption of liposomes with a high level of cationic lipids will be expected to increase the surface potential of cells from negative value to positive value more easily than the liposomes with lower level of positive charge, and in turn prevents further adsorption of positively charged liposomes due to electrostatic repulsion (Smistad et al., 2011). They also showed that a low level of positively charged lipid in the liposomes was less toxic to human buccal cells than liposomes with a high level (Smistad et al., 2007). Therefore, it was suggested that low levels of positive charges would be advantageous.

The above mentioned studies investigated dozens of liposomal formulations with diverse compositions, whose manual preparation took a lot of time and work. In such studies as well as the search for suitable liposomal formulations, our high-throughput method will facilitate the preparation of a big library of diverse liposomes. This application was demonstrated by preparing WGA modified liposomes containing different percentages of DOTAP (0~40%) quickly in one batch, where DOTAP was co-dissolved in the lipid ethanolic solution and injected into PBS buffer. In all cases, WGA was successfully conjugated with liposomes. It is shown in Fig. 4-4 that the zeta potential of liposomes increased from negative to positive, as more DOTAP was incorporated into liposomes. For these formulations, the zeta potential of liposomes with high level of DOTAP (30% and 40%) was only slightly positive because of the shielding effect of PEG layer. The slightly positive charge may be advantageous for binding to bacteria. On the other hand, the high content of DOTAP in the liposomal bilayer may enhance the fusion of liposomes with bacteria and the disturbance to bacterial cell wall. Nevertheless, this experiment is just the first step in such

application. In future, the binding of these liposomes to bacteria and their bacterial toxicity should be investigated in depth, and maybe more formulations will be prepared in one batch.

Figure 4-4 Zeta potential of liposomes with different amount of DOTAP. The liposomes were composed of EPC, DOTAP, mPEG$_{2000}$-DSPE and NHS-PEG$_{2000}$-DSPE. The molar percentage of DOTAP varied from 0% to 40%. The total percentage of PEG-lipids was 9%. (n=3)

Here we stress again that one of the biggest advantages of this method is its potential for fast screening of liposomal formulations. In this experiment, the liposomal formulations with different DOTAP content and the anchor lipid content were prepared in one batch within about 1 hour. By contrast, the preparation of one such formulation using the film-hydration method took more than two hours. So it is clear that the preparation of bacteria-targeting liposomes can be dramatically simplified and accelerated.

4.2.3 Preparation of ethanol-containing liposomes for APDT

This high-throughput method is based on ethanol injection method and is ideal for

the preparation of ethanol-containing liposomes, particularly, ethosomes. Ethosomes were first invented and patented by E. Touitou, and were claimed to be "soft" vesicles formed from phospholipids in the presence of water and high amount of ethanol and sometimes glycols (Touitou, 1996, 1998). The ethosomal formulations refer to the liposomal formulations comprising from 0.5% to 10% phospholipids and from 20% to 50% ethanol.

Ethosomes were shown to be effective for the *in vivo* killing of bacteria and in the treatment of skin infections caused by *S. aureus*, where the rationale behind this work is that ethosomes' permeation enhancing ability facilitates the transport of antimicrobial molecules through the two biological barriers: stratum corneum of the skin and bacterial membrane/cell wall (Godin and Touitou, 2005; Godin et al., 2005). Therefore, we hypothesize that ethosomes are also a promising formulations for delivery of PSs to bacteria, especially the bacteria in skin infections, and will consequently improve APDT.

4.3 Potential clinical application of liposomes in APDT

The work in this dissertation sheds light on the application of liposomes for APDT, and may contribute to the wider application of APDT for the combat with infectious diseases, particularly those caused by multidrug-resistant microbes and unsusceptible to antibiotics.

The most promising application of the developed bacteria-targeting liposomal formulations lies in the field of superficial skin infections, such as skin wound infections, acne vulgaris and skin lesions. Compared to traditional antibiotic therapy, APDT offers a faster and efficacious treatment, normally within a few hours. What's more, using the bacteria-targeting liposomes, APDT can increase the delivery efficiency of PSs to bacteria, facilitate the penetration of PSs into bacteria, and

consequently enhance the antimicrobial therapy. As a result, the administration dose may be decreased, and the side effects will be reduced. Meanwhile, the non-specific delivery of PSs to the host tissues is supposed to be reduced.

The bacteria-targeting liposomes will be of great interest for drug delivery to microbial biofilms. The main problem with biofilms involves the local concentration of bacterial colonies covered by an extracellular matrix of polymeric substances which prevent drug transport to the hidden microbial cells. The advantage of bacteria-targeting liposomes is to target matrix or biofilm bacteria, allowing the drug to be released in the vicinity of the microorganisms and significantly increasing the local drug concentration. This targeted transport was realized using site-specific ligands such as immunoglobulins, oligosaccharides, and proteins (Drulis-Kawa and Dorotkiewicz-Jach, 2010). Jones *et al.* demonstrated that the WGA modified liposomes or antibody modified liposomes could be used for carrying lipophilic bactericides (*e.g.* Triclosan) or hydrophilic antibiotics (*e.g.* vancomycin or benzylpenicillin) and targeted to immobilized bacterial biofilms of oral or skin-associated bacteria (Jones, 2005). The antibiotics in liposomes are more effective than the free antibiotics towards biofilms. So we postulate that our bacteria-targeting liposomes will enhance the delivery of PSs to biofilms, *e.g.* biofilm of MRSA or *P. aeruginosa,* and improve the photodynamic inactivation of bacteria.

The ethanol containing liposomes obtained from the high throughput preparation method may widen the application of APDT to soft tissue infections, which accounts for a fifth of skin infections. Soft tissue infections, *e.g.* furuncles, carbuncles, cystic acne and cellulitis, affect not only the skin surface but also the tissues beneath it. They can affect the dermis and the subcutaneous tissues. The normal antibiotics therapy may take weeks to accumulate sufficient antibiotics in the infected sites and remove

bacteria, while APDT takes effect within a much shorter time (Gad et al., 2004). On the other hand, various studies have proved that the ethanol containing liposomes exhibit strong skin penetration capability, which may help the diffusion of PSs in the infected soft tissues (Chen et al., 2011a; Dragicevic-Curic et al., 2009b; Godin et al., 2005). What's more, the novel synthesized PSs are able to be activated by near infrared (NR) light , which penetrates even deeper in skin than the red light (Schastak et al., 2010). These NR light activated PSs are particularly useful for APDT of soft tissue infections.

The damage to host tissue needs to be taken into account if the liposomal formulations will be applied to local infections *in vivo*. When the liposomal formulations are administrated to the infection site, a portion of temoporfin will also be released to the surrounding cells and probably penetrate into deep tissues. Then the following illumination by laser might cause certain damage to the surrounding cells at the infection site and the deep tissue beneath the infection site. Fortunately, APDT together with liposomes offers many options to minimize the side effects on host tissues:

1) **Administration dose:** it is possible to find a low PS concentration which is safe to human tissues; and liposomes may further decrease the administration dose while remaining the antimicrobial toxicity (An et al., 2011).

2) **Incubation time:** the diffusion of PSs into human cells takes much longer time than that in bacteria, so that efficient APDT may be achieved during a short incubation without harming the host tissues. On the other hand, long incubation time is required for sufficient accumulation of PSs in the infected soft tissues.

3) **Light dosage**: Although deep penetration of light is possible, the light fluence will attenuate exponentially while light penetrates into the tissue, meaning that

most of the energy fluence is absorbed by the upper cells in the light pathway and the damage to the superficial cells is much stronger than the damage to the underlying tissues (Jacques, 2010). For the treatment of superficial infections, low fluence and short wavelength light are advantageous, while for deep skin infections, high fluence and long wavelength light will be required.

4) **Selection of liposomal formulations:** conventional liposomes are suitable for superficial infections, and bacteria-targeting liposomes will increase the ratio of bacteria to human cells in terms of binding with PS-loaded liposomes compared to conventional liposomes; special skin penetrating liposomes are applicable for deep skin infections, *e.g.* ethanol containing liposomes or invasomes (Dragicevic-Curic et al., 2009a).

After all, the photodamage to host tissues will not be a hurdle for PACT since this therapy is well controllable according to the treatment aims.

4.4 Future perspectives

The never-stopping world-wide rise in multi-drug resistance in many classes of pathogenic microbes leads to lessening effectiveness of standard antibiotics, antiviral and anti-parasitic drugs, giving rise to the worrying that the day may come when infections return as the major cause of premature death. In our opinion, APDT is one of the most promising alternative antimicrobial strategies, and liposomes open the possibility to further improve this therapy. However, we are aware that there are still many obstacles to overcome before real clinical applications of the liposomal formulations for APDT. Nonetheless, we are confident that liposomes will play an important role in the development of APDT, and do hope that our study could contribute to this development to some extend and lead to some practical products in future.

5 Summary/Zusammenfassung

As more and more antibiotic-resistant organisms are emerging continuously, the development of new antibiotics falls behind the evolution of antibiotic-resistance. Thus there is an urgent need to search for alternative antibacterial drugs. Nowadays, antimicrobial photodynamic therapy (APDT) has emerged as an efficacious modality to treat various kinds of microbial infections. Meanwhile, liposomes are shown to be an attractive drug delivery system in the treatment of infections and may improve the APDT efficiency. Therefore, the aims of this study are to develop bacteria-targeting liposomes to further improve APDT, and to develop a high-throughput method for screening a large number of PS-loaded liposomal formulations.

In publication 1 and 2, a generation II photosensitizer, temoporfin, was incorporated into liposomes for APDT, afterwards two bacteria-targeting ligands, the antimicrobial peptide WLBU2 and the lectin Wheat Germ Agglutinin (WGA) were successfully coupled to the surface of temoporfin-loaded liposomes, respectively, using an aminogroup-reactive functional lipid: NHS-PEG$_{2000}$-DSPE. The delivery of temoporfin to Methicillin-resistant *Staphylococcus aureus* (MRSA) and *Pseudomonas aeruginosa* (*P. aeruginosa*) was confirmed by fluorescence microscopy and flow cytometry, thus demonstrating that more temoporfin was delivered to bacteria by the modified liposomes than by unmodified liposomes. Consequently, both of the two bacteria-targeting liposomes eradicated all MRSA and enhanced the photodynamic inactivation of *P. aeruginosa* in the *in vitro* photodynamic inactivation test. In particular, WLBU2 seems to be a better bacteria-targeting ligand than WGA. These results demonstrate that the strategy of using bacteria-targeting liposomes is promising for improving the APDT efficiency against both gram-positive and

gram-negative bacteria in the local infections.

To speed up the screening process of liposomal formulations and develop a method suitable for large-scale production of liposomes, a novel strategy for the fast and convenient high-throughput screening of liposomal formulations was developed in Publication 3, utilizing the automation of the ethanol injection method. This strategy was illustrated by the preparation and screening of the liposomal formulation library of temoporfin. To optimize the formulations, different parameters were investigated, including lipid types, lipid concentration, the ratio of ethanol to aqueous solution, the ratio of drug to lipid and the addition of functional phospholipids. Numerous formulations (261 samples) were screened quickly in a high-throughput way. The factors affecting the properties of liposomes were investigated step-by-step, where liposomes were prepared and characterized automatically, making it easy and fast to optimize the liposomal formulations of temoporfin. The obtained optimized liposomes were unilamellar spheres with a diameter of about 50 nm, and were very stable for over 20 weeks. What's more, this high-throughput method is also applicable for preparing bacteria-targeting liposomes of different compositions, showing many advantages over the conventional methods. All the results demonstrate that this high-throughput screening strategy is fast, automated, materially efficient, labor-saving, time-saving, economic, facile, and highly reproducible. This approach is promising for the development of new formulations to enhance APDT; due to the nature of the process, the approach is readily amenable to scale-up of production.

In conclusion, bacteria-targeting liposomes are useful drug delivery system for APDT, and the high-throughput method will facilitate the search for more suitable liposomal formulations. These PS-loaded liposomal formulations have potential clinical applications for the treatment of microbial infections.

Zusammenfassung

Die Anzahl der Antibiotika-resistenten Mikroorganismen steigt stetig und die Entwicklung der Antibiotika-Resistenz schreitet schneller voran, als die Entdeckung neuer wirksamer Antibiotika. Deshalb besteht dringende Notwendigkeit, alternative antibakterielle Medikamente zu entwickeln. Die antimikrobielle photodynamische Therapie (APDT) ist heutzutage eine wirksame Therapie, um verschiedene Arten mikrobieller Infektionen zu behandeln. Inzwischen wurde gezeigt, dass Liposomen ein attraktives Arzneistoffträgersystem in der Behandlung von Infektionen sind und zusätzlich die APDT Effizienz verbessern können.

Die Ziele dieser Arbeit sind:

a) die Entwicklung liposomaler Formu-lierungen zum bakteriellen Targeting für die Verbesserung der APDT und

b) die Entwicklung eines High-Throughput-Verfahrens zum Screening einer Vielzahl von Photosensibilisator (PS) -tragenden   Liposomenformulierungen.

In den Publikationen 1 und 2 wurde ein PS der zweiten Generation (Temoporfin), in Liposomen für die APDT inkorporiert. Anschließend wurden Liganden für das bakterielle Targeting ausgewählt und diese an die Liposomenoberfläche konjugiert. Bei den beiden Liganden handelt es sich um das antimikrobiell-wirksame Peptid WLBU2 und das Lektin Wheat Germ Agglutinin (WGA). Die Kopplung beider Liganden erfolgte mit Hilfe des Aminogruppen-reaktiven Lipids: NHS-PEG$_{2000}$-DSPE. Der Transport des liposomal verpackten Temoporfins zu Methicillin-resistenten *Staphylokokkus aureus* (MRSA) und *Pseudomonas aeruginosa* (*P. Aeruginosa*) wurde mittels Fluoreszenzmikroskopie und Durchfluss-zytometrie bestätigt. Weiterhin wurde durch die Modifikation der Liposomenoberfläche mehr Temoporfin zu den Mikroorganismen transportiert, verglichen mit unmodifizierten Liposomen. Beide

103

ligand-modifizierten-Liposomenspezies konnten in *in vitro* APDT-Untersuchungen alle MRSA töten und die photodynamische Inaktivierung von *P. aeruginosa* verbessern. Insbesondere WLBU2 scheint sich als Ligand für ein liposomales Targeting besser zu eignen als WGA. Die Ergebnisse bestätigen die verbesserte APDT durch die Verwendung von Liposomen, die gegen Bakterien gerichtet sind. Diese Strategie ist ein vielversprechender Ansatz bei der Bekämpfung von lokalen Infektionen ausgelöst durch gram-positive und gram-negative Bakterien.

Zur Beschleunigung des Screening-Prozesses liposomaler Formulierungen und zur Entwicklung geeigneter Verfahren für die Großproduktion von Liposomen wurde eine neue Strategie für das schnelle und bequeme High-Throughput-Screening entwickelt (Publikation 3). Hierbei wurde die Ethanol-Injektion-Methode zur Liposomenerzeugung verwendet und automatisiert. Als Modellarzneistoff diente Temoporfin, welcher in verschiedene liposomale Formulierungen eingebaut wurde. Zur Optimierung der Rezepturen wurden spezielle Parameter untersucht, darunter verschiedene Phospholipid-Kompositionen, Phospholipidkonzentration, das Verhältnis von Ethanol zu wässriger Lösung, das Verhältnis von PS zu Lipid, und der Zusatz von funktionalen Phospholipiden. Zahlreiche liposomale Formulierungen (261 Proben) wurden mit diesem Verfahren generiert und analysiert. Die Faktoren, die die Eigenschaften der Liposomen beeinflussen, wurden nacheinander untersucht. Die Liposomen wurden hergestellt und automatisch charakterisiert, was die Optimierung der liposomalen Formulierungen von Temoporfin einfach und schnell machte. Die erhaltenen optimierten Liposomen waren unilamellare Vesikel mit einem Durchmesser von etwa 50 nm. Diese waren über 20 Wochen lagerstabil. Alle Ergebnisse zeigen, dass diese High-Throughput-Screening-Strategie schnell, automatisiert, effizient, arbeitssparend, zeitsparend, ökonomisch, und hoch

reproduzierbar ist. Dieses Verfahren ist bei der Entwicklung neuer Liposomen-formulierungen zur Verbesserung der APDT vielversprechend und für den Scale-up der Produktion geeignet.

Zusammenfassend sind die Bakterien-Targeting Liposomen ein geeignetes Arzenistoffträgersystem für die APDT. Das High-Throughput-Verfahren wird die Suche nach geeigneten liposomalen Formulierungen erleichtern. Diese PS-haltigen Liposomen haben potenzielle klinische Anwendungen in der Behandlung von mikrobiellen Infektionen.

6 References

Akilov OE, Yousaf W, Lukjan SX, Verma S, Hasan T. (2009). Optimization of Topical Photodynamic Therapy With 3,7-bis(di-n-butylamino)Phenothiazin-5-ium Bromide for Cutaneous Leishmaniasis. *Lasers Surg Med,* 41: 358-65.

Alanis AJ. (2005). Resistance to antibiotics: are we in the post-antibiotic era? *Arch Med Res,* 36: 697-705.

Amalrich XR, 2010. title., Universitat Ramon Llull, Barcelona.

An JS, Kim JE, Lee DH, Kim BY, Cho S, Kwon IH, Choi WW, Kang SM, Won CH, Chang SE, Lee MW, Choi JH, Moon KC. (2011). 0.5% Liposome-encapsulated 5-aminolevulinic acid (ALA) photodynamic therapy for acne treatment. *J Cosmet Laser Ther,* 13: 28-32.

Avni I, Arffa RC, Robin JB, Rao NA. (1987). Lectins for the identification of ocular bacterial pathogens. *Metab Pediatr Syst Ophthalmol,* 10: 45-7.

Baglo Y, Sousa MM, Slupphaug G, Hagen L, Havag S, Helander L, Zub KA, Krokan HE, Gederaas OA. (2011). Photodynamic therapy with hexyl aminolevulinate induces carbonylation, posttranslational modifications and changed expression of proteins in cell survival and cell death pathways. *Photochem Photobiol Sci*.

Dan Bailey, (2011). A Need for New Antibiotics. Available at: http://smellslikescience.com/a-need-for-new-antibiotics/ Accessed on June 2011.

Bakker-Woudenberg IAJM, Schiffelers RM, Storm G, Becker MJ, Guo L, Nejat D. (2005). Long-Circulating Sterically Stabilized Liposomes in the Treatment of Infections, ed. Methods Enzymol. Academic Press, pp. 228-60.

Bangham AD, Horne RW. (1964). Negative Staining of Phospholipids and Their Structural Modification by Surface-Active Agents as Observed in the Electron Microscope. *J Mol Biol,* 8: 660-8.

Bernard E, Dubois JL, Wepierre J. (1997). Importance of sebaceous glands in cutaneous penetration of an antiandrogen: target effect of liposomes. *J Pharm Sci,* 86: 573-8.

Bombelli C, Bordi F, Ferro S, Giansanti L, Jori G, Mancini G, Mazzuca C, Monti D, Ricchelli F, Sennato S, Venanzi M. (2008). New cationic liposomes as vehicles

of m-tetrahydroxyphenylchlorin in photodynamic therapy of infectious diseases. *Mol Pharm,* 5: 672-9.

Capella M, Coelho AM, Menezes S. (1996). Effect of glucose on photodynamic action of methylene blue in Escherichia coli cells. *Photochem Photobiol,* 64: 205-10.

Carmen A, Blanca F, Antonio R, Pablo PS, Fernando L, Josepa G, Yolanda G. (2011). [Photodynamic therapy for onychomycosis. Case report and review of the literature.]. *Rev Iberoam Micol.*

Cassidy CM, Tunney MM, McCarron PA, Donnelly RF. (2009). Drug delivery strategies for photodynamic antimicrobial chemotherapy: from benchtop to clinical practice. *J Photochem Photobiol B,* 95: 71-80.

Chen M, Liu X, Fahr A. (2011a). Skin penetration and deposition of carboxyfluorescein and temoporfin from different lipid vesicular systems: In vitro study with finite and infinite dosage application. *Int J Pharm,* 408: 223-34.

Chen MK, Luo DQ, Zhou H, Huang ZW, Zhang QF, Han JD. (2011b). 5-aminolevulinic Acid-mediated photodynamic therapy on cervical condylomata acuminata. *Photomed Laser Surg,* 29: 339-43.

Chondros P, Nikolidakis D, Christodoulides N, Rossler R, Gutknecht N, Sculean A. (2009). Photodynamic therapy as adjunct to non-surgical periodontal treatment in patients on periodontal maintenance: a randomized controlled clinical trial. *Lasers Med Sci,* 24: 681-8.

Christiansen K, Bjerring P, Troilius A. (2007). 5-ALA for photodynamic photorejuvenation--optimization of treatment regime based on normal-skin fluorescence measurements. *Lasers Surg Med,* 39: 302-10.

Coates AR, Hu Y. (2007). Novel approaches to developing new antibiotics for bacterial infections. *Br J Pharmacol,* 152: 1147-54.

Dai T, Huang YY, Hamblin MR. (2009). Photodynamic therapy for localized infections--state of the art. *Photodiagnosis Photodyn Ther,* 6: 170-88.

de Leeuw J, van der Beek N, Bjerring P, Neumann HA. (2010). Photodynamic therapy of acne vulgaris using 5-aminolevulinic acid 0.5% liposomal spray and intense pulsed light in combination with topical keratolytic agents. *J Eur Acad Dermatol Venereol,* 24: 460-9.

6 References

Donnelly RF, McCarron PA, Tunney MM. (2008). Antifungal photodynamic therapy. *Microbiol Res,* 163: 1-12.

Dragicevic-Curic N, Scheglmann D, Albrecht V, Fahr A. (2009a). Development of different temoporfin-loaded invasomes-novel nanocarriers of temoporfin: characterization, stability and in vitro skin penetration studies. *Colloids Surf B Biointerfaces,* 70: 198-206.

Dragicevic-Curic N, Scheglmann D, Albrecht V, Fahr A. (2009b). Development of liposomes containing ethanol for skin delivery of temoporfin: characterization and in vitro penetration studies. *Colloids Surf. B Biointerfaces,* 74: 114-22.

Drulis-Kawa Z, Dorotkiewicz-Jach A. (2010). Liposomes as delivery systems for antibiotics. *Int J Pharm,* 387: 187-98.

Engelhardt V, Krammer B, Plaetzer K. (2010). Antibacterial photodynamic therapy using water-soluble formulations of hypericin or mTHPC is effective in inactivation of Staphylococcus aureus. *Photochem Photobiol Sci,* 9: 365-9.

Ferro S, Ricchelli F, Mancini G, Tognon G, Jori G. (2006). Inactivation of methicillin-resistant Staphylococcus aureus (MRSA) by liposome-delivered photosensitising agents. *J Photochem Photobiol B,* 83: 98-104.

Ferro S, Ricchelli F, Monti D, Mancini G, Jori G. (2007). Efficient photoinactivation of methicillin-resistant Staphylococcus aureus by a novel porphyrin incorporated into a poly-cationic liposome. *INT J BIOCHEM CELL B,* 39: 1026-34.

Finch R. (2007). Innovation - drugs and diagnostics. *J Antimicrob Chemother,* 60 Suppl 1: i79-82.

Gad F, Zahra T, Francis KP, Hasan T, Hamblin MR. (2004). Targeted photodynamic therapy of established soft-tissue infections in mice. *Photochem Photobiol Sci,* 3: 451-8.

Garcia AM, Alarcon E, Munoz M, Scaiano JC, Edwards AM, Lissi E. (2010). Photophysical behaviour and photodynamic activity of zinc phthalocyanines associated to liposomes. *Photochem Photobiol Sci.*

Giuliani F, Martinelli M, Cocchi A, Arbia D, Fantetti L, Roncucci G. (2010). In vitro resistance selection studies of RLP068/Cl, a new Zn(II) phthalocyanine suitable for antimicrobial photodynamic therapy. *Antimicrob Agents Chemother,* 54: 637-42.

6 References

Godin B, Touitou E. (2005). Erythromycin ethosomal systems: physicochemical characterization and enhanced antibacterial activity. *Curr Drug Deliv,* 2: 269-75.

Godin B, Touitou E, Rubinstein E, Athamna A, Athamna M. (2005). A new approach for treatment of deep skin infections by an ethosomal antibiotic preparation: an in vivo study. *J Antimicrob Chemother,* 55: 989-94.

Hamblin MR, Hasan T. (2004). Photodynamic therapy: a new antimicrobial approach to infectious disease? *Photochem Photobiol Sci,* 3: 436-50.

Hancock RE. (2001). Cationic peptides: effectors in innate immunity and novel antimicrobials. *Lancet Infect Dis,* 1: 156-64.

Hashimoto MCE, Prates RA, Toffoli DJ, Courrol LC, Ribeiro MS, 2010. Prevention of bloodstream infections by photodynamic inactivation of multiresistant Pseudomonas aeruginosa in burn wounds, in: Hamblin, MR, Waynant, RW, Anders, J (Eds.), Proceedings of SPIE p. 75520I.

Hashimoto MCE, Toffoli DJ, Prates RA, Courrol LC, Ribeiro MS, 2009. Photodynamic inactivation of antibiotic resistant strain of Pseudomonas aeruginosa in vivo in: Kessel, DH (Ed.), Proceedings of SPIE p. 73803F.

Huang L, Dai T, Hamblin MR. (2010). Antimicrobial photodynamic inactivation and photodynamic therapy for infections. *Methods Mol Biol,* 635: 155-73.

Jacques SL. (2010). How tissue optics affect dosimetry of photodynamic therapy. *J Biomed Opt,* 15: 051608.

Jia Y, Joly H, Omri A. (2010). Characterization of the interaction between liposomal formulations and Pseudomonas aeruginosa. *J Liposome Res,* 20: 134-46.

Jones MN. (2005). Use of liposomes to deliver bactericides to bacterial biofilms, ed. Liposomes, Pt E. San Diego: Elsevier Academic Press Inc, pp. 211-28.

Jones MN, Song YH, Kaszuba M, Reboiras MD. (1997). The interaction of phospholipid liposomes with bacteria and their use in the delivery of bactericides. *J Drug Targeting,* 5: 25-34.

Jori G. (2006). Photodynamic therapy of microbial infections: state of the art and perspectives. *J Environ Pathol Toxicol Oncol,* 25: 505-19.

Jori G, Fabris C, Soncin M, Ferro S, Coppellotti O, Dei D, Fantetti L, Chiti G, Roncucci G. (2006). Photodynamic therapy in the treatment of microbial infections: basic principles and perspective applications. *Lasers Surg Med,* 38:

6 References

468-81.

Kaszuba M, Robinson AM, Song YH, Creeth JE, Jones MN. (1997). The visualisation of the targeting of phospholipid liposomes to bacteria. *Colloids and Surfaces B-Biointerfaces,* 8: 321-32.

Kim RH, Armstrong AW. (2011). Current state of acne treatment: highlighting lasers, photodynamic therapy, and chemical peels. *Dermatol Online J,* 17: 2.

Kumarasamy KK, Toleman MA, Walsh TR, Bagaria J, Butt F, Balakrishnan R, Chaudhary U, Doumith M, Giske CG, Irfan S, Krishnan P, Kumar AV, Maharjan S, Mushtaq S, Noorie T, Paterson DL, Pearson A, Perry C, Pike R, Rao B, Ray U, Sarma JB, Sharma M, Sheridan E, Thirunarayan MA, Turton J, Upadhyay S, Warner M, Welfare W, Livermore DM, Woodford N. (2010). Emergence of a new antibiotic resistance mechanism in India, Pakistan, and the UK: a molecular, biological, and epidemiological study. *Lancet Infect Dis,* 10: 597-602.

Lambrechts SA, Aalders MC, Van Marle J. (2005a). Mechanistic study of the photodynamic inactivation of Candida albicans by a cationic porphyrin. *Antimicrob Agents Chemother,* 49: 2026-34.

Lambrechts SA, Demidova TN, Aalders MC, Hasan T, Hamblin MR. (2005b). Photodynamic therapy for Staphylococcus aureus infected burn wounds in mice. *Photochem Photobiol Sci,* 4: 503-9.

Lasic DD. (1995). Application of liposomes, in: Sackmann, RLaE, ed. Handbook of Biological Physics. pp. 491-519.

Lembo AJ, Ganz RA, Sheth S, Cave D, Kelly C, Levin P, Kazlas PT, Baldwin PC, 3rd, Lindmark WR, McGrath JR, Hamblin MR. (2009). Treatment of Helicobacter pylori infection with intra-gastric violet light phototherapy: a pilot clinical trial. *Lasers Surg Med,* 41: 337-44.

Leszczynska K, Namiot A, Fein DE, Wen Q, Namiot Z, Savage PB, Diamond S, Janmey PA, Bucki R. (2009). Bactericidal activities of the cationic steroid CSA-13 and the cathelicidin peptide LL-37 against Helicobacter pylori in simulated gastric juice. *BMC Microbiol,* 9: 187.

Livermore DM, Mushtaq S, Warner M, Zhang J, Maharjan S, Doumith M, Woodford N. (2011). Activities of NXL104 combinations with ceftazidime and aztreonam against carbapenemase-Producing Enterobacteriaceae. *Antimicrob*

Agents Chemother, 55: 390-4.

Maisch T. (2009). A new strategy to destroy antibiotic resistant microorganisms: antimicrobial photodynamic treatment. *Mini Rev Med Chem,* 9: 974-83.

Maisch T, Bosl C, Szeimies RM, Lehn N, Abels C. (2005). Photodynamic effects of novel XF porphyrin derivatives on prokaryotic and eukaryotic cells. *Antimicrob Agents Chemother,* 49: 1542-52.

Maisch T, Hackbarth S, Regensburger J, Felgentrager A, Baumler W, Landthaler M, Roder B. (2011). Photodynamic inactivation of multi-resistant bacteria (PIB) - a new approach to treat superficial infections in the 21st century. *J Dtsch Dermatol Ges,* 9: 360-6.

Malik Z, Ladan H, Nitzan Y. (1992). Photodynamic inactivation of Gram-negative bacteria: problems and possible solutions. *J Photochem Photobiol B,* 14: 262-6.

Merchat M, Spikes JD, Bertoloni G, Jori G. (1996). Studies on the mechanism of bacteria photosensitization by meso-substituted cationic porphyrins. *J Photochem Photobiol B,* 35: 149-57.

Minnock A, Vernon DI, Schofield J, Griffiths J, Parish JH, Brown SB. (2000). Mechanism of uptake of a cationic water-soluble pyridinium zinc phthalocyanine across the outer membrane of Escherichia coli. *Antimicrob Agents Chemother,* 44: 522-7.

Moan J, Berg K. (1991). The photodegradation of porphyrins in cells can be used to estimate the lifetime of singlet oxygen. *Photochem Photobiol,* 53: 549-53.

Moan J, Peng Q. (2003). An outline of the hundred-year history of PDT. *Anticancer Res,* 23: 3591-600.

Moran GJ, Krishnadasan A, Gorwitz RJ, Fosheim GE, McDougal LK, Carey RB, Talan DA. (2006). Methicillin-resistant S. aureus infections among patients in the emergency department. *N Engl J Med,* 355: 666-74.

Mugabe C, Halwani M, Azghani AO, Lafrenie RM, Omri A. (2006). Mechanism of Enhanced Activity of Liposome-Entrapped Aminoglycosides against Resistant Strains of Pseudomonas aeruginosa. *Antimicrob Agents Chemother,* 50: 2016-22.

Ng R, Singh F, Papamanou DA, Song X, Patel C, Holewa C, Patel N, Klepac-Ceraj V, Fontana CR, Kent R, Pagonis TC, Stashenko PP, Soukos NS. (2011).

6 References

Endodontic photodynamic therapy ex vivo. *J Endod,* 37: 217-22.

Nisnevitch M, Nakonechny F, Nitzan Y. (2010). Photodynamic antimicrobial chemotherapy by liposome-encapsulated water-soluble photosensitizers. *Bioorg Khim,* 36: 396-402.

Ochsner M. (1997). Photophysical and photobiological processes in the photodynamic therapy of tumours. *J Photochem Photobiol B,* 39: 1-18.

Ohlsen K. (2009). Novel antibiotics for the treatment of Staphylococcus aureus. *Expert Review of Clinical Pharmacology,* 2: 661-72.

Photocure, (2011). Visonac™ for treatment of acne. Available at: http://www.photocure.com/RD/Dermatology/Visonac-for-treatment-of--acne/ Accessed on June 2011.

Photopharmica website, (2007). Photopharmica targets infected wounds with its photodynamic therapy. Available at: http://www.photopharmica.com/news/01_07_07b.htm Accessed on July 2007.

Pinheiro SL, Donega JM, Seabra LM, Adabo MD, Lopes T, do Carmo TH, Ribeiro MC, Bertolini PF. (2010). Capacity of photodynamic therapy for microbial reduction in periodontal pockets. *Lasers Med Sci,* 25: 87-91.

Poirel L, Lagrutta E, Taylor P, Pham J, Nordmann P. (2010). Emergence of metallo-ss-lactamase NDM-1-producing multidrug resistant Escherichia coli in Australia. *Antimicrob Agents Chemother*.

Pudziuvyte B, Bakiene E, Bonnett R, Shatunov PA, Magaraggia M, Jori G. (2011). Alterations of Escherichia coli envelope as a consequence of photosensitization with tetrakis(N-ethylpyridinium-4-yl)porphyrin tetratosylate. *Photochem Photobiol Sci,* 10: 1046-55.

Raab O. (1900). Ueber die Wirkung fluorescirender Stoffe auf Infusorien. *Z Biol,* 39: 524-46.

Ragas X, Dai T, Tegos GP, Agut M, Nonell S, Hamblin MR. (2010). Photodynamic inactivation of Acinetobacter baumannii using phenothiazinium dyes: in vitro and in vivo studies. *Lasers Surg Med,* 42: 384-90.

Raghavendra M, Koregol A, Bhola S. (2009). Photodynamic therapy: a targeted therapy in periodontics. *Aust Dent J,* 54 Suppl 1: S102-9.

Rossi R, Bruscino N, Ricceri F, Grazzini M, Dindelli M, Lotti T. (2009). Photodynamic treatment for viral infections of the skin. *G Ital Dermatol*

6 References

Venereol, 144: 79-83.

Sachetelli S, Khalil H, Chen T, Beaulac C, Senechal S, Lagace J. (2000). Demonstration of a fusion mechanism between a fluid bactericidal liposomal formulation and bacterial cells. *Biochim Biophys Acta,* 1463: 254-66.

Salem, II, Flasher DL, Duzgunes N. (2005). Liposome-encapsulated antibiotics. *Methods Enzymol,* 391: 261-91.

Schafer M, Schmitz C, Horneck G. (1998). High sensitivity of Deinococcus radiodurans to photodynamically-produced singlet oxygen. *Int J Radiat Biol,* 74: 249-53.

Schastak S, Ziganshyna S, Gitter B, Wiedemann P, Claudepierre T. (2010). Efficient Photodynamic Therapy against Gram-Positive and Gram-Negative Bacteria Using THPTS, a Cationic Photosensitizer Excited by Infrared Wavelength. *PLoS One,* 5: e11674.

Shih MH, Huang FC. (2011). Effects of photodynamic therapy on rapidly growing nontuberculous mycobacteria keratitis. *Invest Ophthalmol Vis Sci,* 52: 223-9.

Singh GS, Pandeya SN. (2011). Natural products in discovery of potential and safer antibacterial agents. *Opportunity, Challenge and Scope of Natural Products in Medicinal Chemistry*: 63-101.

Sizemore RK, Caldwell JJ, Kendrick AS. (1990). Alternate gram staining technique using a fluorescent lectin. *Appl Environ Microbiol,* 56: 2245-7.

Smijs TG, Pavel S. (2011). The susceptibility of dermatophytes to photodynamic treatment with special focus on Trichophyton rubrum. *Photochem Photobiol,* 87: 2-13.

Smistad G, Jacobsen J, Sande SA. (2007). Multivariate toxicity screening of liposomal formulations on a human buccal cell line. *Int J Pharm,* 330: 14-22.

Smistad G, Nguyen NB, Hegna IK, Sande SA. (2011). Influence of liposomal formulation variables on the interaction with Candida albicans in biofilm; a multivariate approach. *J Liposome Res,* 21: 9-16.

Spikes JD. (1997). Photodynamic Action: From Paramecium to Photochemotherapy*. *Photochem Photobiol,* 65: 142S-7S.

Dental Tribune International, (2011). Antibakterielle Photodynamische Therapie-Standpunkt und Ausblick. Available at: http://www.dental-tribune.com/articles/content/id/4939/scope/specialities/secti

6 References

on/dental_hygiene Accessed on 2011-5-13.

Strathmann M, Wingender J, Flemming HC. (2002). Application of fluorescently labelled lectins for the visualization and biochemical characterization of polysaccharides in biofilms of Pseudomonas aeruginosa. *J Microbiol Methods,* 50: 237-48.

Touitou E, (1996). Compositions for applying active substances to or through the skin. United States Patent and Trademark Office: (Patent No.) 5540934.

Touitou E, (1998). Composition for applying active substances to or through the skin. (Patent No.) 5716638.

Valduga G, Breda B, Giacometti GM, Jori G, Reddi E. (1999). Photosensitization of wild and mutant strains of Escherichia coli by meso-tetra (N-methyl-4-pyridyl)porphine. *Biochem Biophys Res Commun,* 256: 84-8.

von Tappeiner H, Jodlbauer A. (1904). Ueber die wirkung der photodynamischen (fluorescierenden) stoffe auf protozoen und enzyme. *Dtsch Arch Klin Med,* 80: 427-87.

Wainwright M. (2010). 'Safe' photoantimicrobials for skin and soft-tissue infections. *Int J Antimicrob Agents,* 36: 14-8.

Wainwright M, Mohr H, Walker WH. (2007). Phenothiazinium derivatives for pathogen inactivation in blood products. *J Photochem Photobiol B,* 86: 45-58.

The Science Creative Quarterly, (2004). CATIONIC PEPTIDES: A NEW HOPE. Available at: http://www.scq.ubc.ca/cationic-peptides-a-new-hope/ Accessed on August 2004.

Wilson BC, Patterson MS. (2008). The physics, biophysics and technology of photodynamic therapy. *Phys Med Biol,* 53: R61-109.

Zeina B, Greenman J, Corry D, Purcell WM. (2003). Antimicrobial photodynamic therapy: assessment of genotoxic effects on keratinocytes in vitro. *Br J Dermatol,* 148: 229-32.

Zolfaghari PS, Packer S, Singer M, Nair SP, Bennett J, Street C, Wilson M. (2009). In vivo killing of Staphylococcus aureus using a light-activated antimicrobial agent. *BMC Microbiol,* 9: 27.

7 Abbreviations

ALA	5-Aminolevulinic acid
AMP	Antimicrobial peptide
APDT	Antimicrobial photodynamic therapy
C. albicans	*Candida albicans*
CFU	Colony forming unit
Cryo-TEM	Cryogenic transmission electron microscopy
DOTAP	*N*-[1-(2,3-dioleoyloxy)propyl]-*N,N,N*-trimethylammonium methylsulfate
DPPC	1,2-Dipalmitoyl-*sn*-glycero-3-phosphocholin
DPPG	1,2-Dipalmitoyl-*sn*-glycero-3-[phospho-*rac*-(1-glycerol)]
EPC	Egg phosphatidylcholine
ISC	Intersystem crossing
Liposome-EPC	Liposomes composed of egg phosphatidylcholine
Liposome-S100	Liposomes composed of Lipoid S100
Liposome-S75	Liposomes composed of Lipoid S75
LPS	Lipopolysaccharide
MFI	Mean fluorescence intensity
mPEG$_{2000}$-DSPE	1,2-Distearoyl-*sn*-glycero-3-phosphoethanolamine-*N*-[methoxy (polyethylene glycol)-2000]
MRSA	Methicillin-resistant *Staphylococcus aureus*
NADH	Nicotinamide adenine dinucleotide
NDM-1	New Delhi metallo-β-lactamases 1
NHS-liposomes	NHS-PEG$_{2000}$-DSPE containing liposomes without incubation with ligands

7 Abbreviations

NHS-PEG$_{2000}$-DSPE	1,2-Distearoyl-*sn*-glycero-3-phosphoethanolamine-*N*-[3-(*N*-succinimidyloxyglutaryl)aminopropyl(polyethyleneglycol)-2000-carbamyl]
P. aeruginosa	*Pseudomonas aeruginosa*
PACT	Photodynamic antimicrobial chemotherapy
PBS	Phosphate buffered saline
PCS	Photon correlation spectroscopy
PDI	Photodynamic inactivation or polydispersity index
PDT	Photodynamic therapy
PS	Photosensitizer
ROS	Reactive oxygen species
S. aureus	*Staphylococcus aureus*
VISA	Vancomycin-intermediate resistant *S. aureus*
VRSA	Vancomycin-resistant *S. aureus*
WGA	Wheat germ agglutinin
WGA-liposomes	WGA modified liposomes
WLBU2-liposomes	WLBU2 modified liposomes

8 Acknowledgements

CURRICULUM VITAE

Personal Information
Name: Kewei Yang
Date of Birth: Oct. 28, 1982
Place of Birth: Heilongjiang Province, P.R. China
Nationality: Chinese
E-mail: kewei.yang@uni-jena.de

Education

1) **Jul.2007-Aug.2011**
   PhD candidate in Friedrich-Schiller-University Jena (Germany), Institute of Pharmacy, Dept. of Pharmaceutical Technology.
   Supervisor: Professor Dr. Alfred Fahr

2) **Mar. 2005—July.2007**
   Master degree of science in Pharmaceutics in Peking University (China), School of Pharmaceutical Sciences.

3) **Sep. 2001—Mar. 2005**
   Bachelor degree of science in Pharmaceutical sciences in Peking University (China), School of Pharmaceutical Sciences.

Research Experience

➢ ***Thesis for doctor degree***: Bacteria-targeting liposomal formulations for antimicrobial photodynamic therapy (2007~2010, in corporation with biolitec AG, Germany), including preparation and characterization of liposomes, different techniques of coupling ligands (peptides, lectins and antibodies) to liposomes, bacteria culture, *in vitro* binding experiment using flow cytometry, and *in vitro* photoinactivation test.

➢ High-throughput screening of liposomal formulations (2010~2011) using ethanol injection method and automated devices for incorporation of photosensitizers, antibiotics and steroids.

➢ ***Thesis for master degree***: Application of macromolecular micelles as novel drug delivery system (2004~2007), including synthesis of mPEG grafted chitosan and lactose-PEG grafted chitosan to prepare novel micelles for liver-targeted delivery of glycyrrhizinate, formulation optimization and characterization, drug release study, hemocompatibility test, stability and pharmacokinetics.

➢ R&D of a new transdermal patch of sinomenine (2005): formulation optimization and *in vivo* transdermal study.

➢ Study of the pharmacokinetics of different oral formulations of silybin in rats. (2006)

Publications, Posters and Presentations

1. **YANG Ke-wei**, YANG Zhuo-li, SUN Yu-feng, LIU Yan. Application of macromolecular micelles as drug carriers. Chinese journal of new drugs, 2006, 15(19):16-20.

2. Zhuo Li Yang, **Ke Wei Yang**, Xin Ru Li, Yan Liu. Preparation and in vitro release kinetics of Amphotericin B-loaded poly(ethyleneglycol)-poly(dl-lactide) block copolymer micelles. Chinese pharmaceutical journal. 2007, 42(7): 519-523.

3. **YANG Ke-wei,** LI Xin-ru, YANG Zhuo-li, LIU Yan Diammonium glycyrrhizinate loaded mPEG-grafted-chitosan polyion complex micelles: preparation and in vitro characterization. Chinese journal of new drugs, 2007, 16(13):1030-1034.

4. Zhuo Li Yang, Xin Ru Li, **Ke Wei Yang**, Yan Liu. Amphotericin B-loaded poly(ethylene glycol)-poly(lactide) micelles: Preparation, freeze-drying and in vitro release. Journal of Biomedical Materials Research: Part A, 2008, 85A(2): p. 539-546.

5. **Ke Wei Yang**, Xin Ru Li, Zhuo Li Yang, Ping Zhu Li, Fei Wang, Yan Liu. Novel polyion complex micelles for liver-targeted delivery of Diammonium glycyrrhizinate: *in vitro* and *in vivo* characterization. Journal of Biomedical Materials Research: Part A, 2009, 88A(1): p. 140-148.

6. Li, Xinru; Yang, Zhuoli; **Yang, Kewei;** Zhou, Yanxia; Chen, Xingwei; Zhang, Yanhui; Wang, Fei; Liu, Yan and Ren, Lijun. Self-Assembled Polymeric Micellar Nanoparticles as Nanocarriers for Poorly Soluble Anticancer Drug Ethaselen. Nanoscale Research Letters, 2009. 4(12): p. 1502-1511.

7. Chen M, Li XR, Zhou YX, **Yang KW**, Chen XW, Deng Q, Liu Y, Ren LJ. Chen, M., et al., Improved absorption of salmon calcitonin by ultraflexible liposomes through intranasal delivery. Peptides, 2009. 30(7): p. 1288-1295.

8. **Kewei Yang**, Joseph T. Delaney, Ulrich S. Schubert, Alfred Fahr. Fast high throughput screening of temoporfin loaded liposomal formulations prepared by ethanol injection method. (Journal of Liposome Research, 2011, early online)

9. **Kewei Yang**, Burkhard Gitter, Ronny Rüger, Gerhard D. Wieland, Ming Chen, Xiangli Liu, Volker Albrecht, Alfred Fahr. Antimicrobial peptide modified liposomes for bacteria targeted delivery of temoporfin in photodynamic antimicrobial chemotherapy. Photochemical & Photobiological Science, 2011, 10, 1593-1601.

10. **Kewei Yang**, Burkhard Gitter, Ronny Rüger, Volker Albrecht, Gerhard D. Wieland, Alfred Fahr. Wheat Germ Agglutinin Modified Liposomes for the Photodynamic Inactivation of Bacteria. (Photochemistry and Photobiology, 2011, early online)

11. **Poster**: Lectin modified liposomes for improvement of antibacterial photodynamic therapy. Annual meeting of German Pharmaceutical Association (DPhG), 2009.

12. **Poster**: Wheat germ agglutinin modified liposomes for improvement of photodynamic antibacterial chemotherapy. Annual meeting of German Pharmaceutical Association (DPhG), 2010.

13. **Poster and short oral presentation**: High-throughput screening of liposomal formulations: preparation, characterization and surface modification. Controlled Release Society German Chapter Annual Meeting, 2011.

14. **Oral presentation**: Surface modification of liposomes for bacterial-targeting. 19th Mountain/ Sea liposome workshop, Oberjoch, Germany, 2008.

15. **Oral presentation**: Bacteria-targeting liposomes for antimicrobial photodynamic therapy. 20th Mountain/Sea liposome workshop, Ameland, the Netherlands, 2009.

16. **Oral presentation**: High-throughput screening of liposomal formulations: preparation, characterization and surface modification. 21th Mountain/ Sea liposome workshop, Oberjoch, Germany, 2011.

Statement

I am clear about the Promotionsordnung of the Faculty of Biology and Pharmacy at the Friedrich-Schiller-University Jena. All parts of the dissertation were produced by myself. Hereby I declare that this dissertation does not contain any material previously submitted for a degree or diploma at another university or any material previously written or published by any other person, except where due acknowledgment or reference is made in the text. I also declare that I did not obtain the assistance of a dissertation counseling agent and that I did not provide any direct or indirect financial remuneration to any third party in connection with the content of my dissertation.

Jena, 07.07.2011 ………………………….
Kewei Yang